

TU Delft

# Passive Suction under Mud Mats

Model – Testing - Validating

Christiaan den Hertog  
3-6-2017

# *Administrative Data*

## **Author:**

Christiaan den Hertog, Bsc  
1509969  
christiaandenhertog@gmail.com

## **Committee**

Prof. Dr. Ir. C van Rhee  
c.vanrhee@tudelft.nl  
Faculty of Mechanical Materials and Maritime Engineering

Dr. Ir. S.A. Miedema  
s.a.miedema@tudelft.nl  
Faculty of Mechanical Materials and Maritime Engineering

Dr. Ir. A.M. Talmon  
a.m.talmon@tudelft.nl  
Faculty of Mechanical Materials and Maritime Engineering

Dr. Ir. M. van Damme  
m.vandamme@tudelft.nl  
Faculty of Civil Engineering

## Abstract

The subject of this master thesis is related to the passive suction under mud mats. Mud mats are used in the offshore industry to prevent structures from sinking in the soil after installation. If for some reason a structure has to be lifted, on the one side due to an installation error, on the other side due to removal the force needed to lift the structure sometimes exceeds the total submerged weight. This report contains a Literature survey conducted regarding the above subjects. This report also shows the design of a test setup and procedure for lifting a plate from a sand bed. In the end the report follows the modelling of an analytical model which is validated using the test data

The focus of this report lies with finding out what basic parameters dominate this force and what the influence of these parameters are during lifting in sand. Experiments will be conducted to test these parameters. In the end these parameters will be used to develop a simple analytical model to predict the order of the breakout force. The model will then be validated with the experiments. The main research question is:

*How are the breakout force and breakout time influenced by the permeability of the sand and the lifting force? Can an analytical model, that uses these parameters, predict the lifting force within a certain margin?*

Literature states that no breakout forces are to be expected due to the large permeability of sand but from cutting theories it is known that under pressures exist around the blade tip, especially for the smaller grain sizes. A test setup was built to study the lifting process and measure the pressure under the plate and its displacement for a given load. The tests were performed in two different sands (Silverbond and Geba Weiss) for a range of different loads with two different plates: A 2-Dimensional setup and a 3-Dimensional setup. An analytical model was created to predict the lifting force for a given permeability and upward velocity of the plate. In the end the model was validated with the test data.

The test data showed that for the 2-Dimensional case the pressure profile was of a rectangular shape. A factor 10 in breakout time between the sands can be observed. The 2-Dimensional model gives a good estimation of the lifting load in Silverbond sand when using velocities from the beginning of the lifting process. For the Geba sand, after adjusting the length of the flow paths, the model also gives a good fit.

The experiments with the 3-Dimensional plate showed that the pressure profile under the plate is of a rectangular shape with steep slopes towards the edge of the plate. Nothing can be concluded about a relation between the breakout time and the permeability for the same load between the two different sands due to an inertia dominated process.

The 3-Dimensional model predicts the lifting force accurately for the Silverbond sand using the velocities from the beginning of the lifting process. For the Geba sand the permeability had to be scaled to give a good fit. This is because of model assumptions and using flow paths. Adjusting the tune factor did not give satisfactory results.

# Contents

Nomenclature.....	
List of Figures.....	
List of Tables.....	
1 Introduction.....	1
1.1 Problem Description.....	1
1.2 Purpose of Research.....	2
2 Theory.....	4
2.1 Earlier Research.....	4
2.2 Parallel Resistor method.....	5
2.3 Conclusions.....	8
3 Testing.....	9
3.1 Introduction.....	9
3.2 Test setup.....	9
3.3 Test Parameters.....	12
3.4 Test Procedure.....	14
4 General Test Results.....	16
4.1 Introduction.....	16
4.2 Net loads.....	16
4.3 Measurement Analysis.....	17
4.4 Conclusions.....	21
5 2 Dimensional Results.....	22
5.1 Expectations.....	22
5.2 Time of breakout.....	22
5.3 Mean Displacement.....	24
5.4 Mean Pressures.....	26
5.5 Comparing the Two Sands.....	28
5.6 Conclusions.....	29
6 3 Dimensional Results.....	30
6.1 Expectations.....	30
6.2 Mean time of breakout.....	30
6.3 Mean Displacement.....	32
6.4 Mean Pressure.....	34

6.5	Comparing the Two Sands.....	37
6.6	Consolidation.....	38
6.7	Conclusion .....	40
7	Analytical Model.....	41
7.1	2D Analytical Model .....	41
7.2	3D Analytical Model .....	43
7.3	Expectations .....	47
8	Validation .....	50
8.1	Introduction.....	50
8.2	2-Dimensional Comparisons.....	50
8.3	3-Dimensional Comparisons.....	54
8.4	Scaling.....	58
8.5	Conclusions.....	60
9	Conclusions and Recommendations .....	62
9.1	2-Dimensional Conclusions .....	62
9.2	3-Dimensional Conclusions .....	62
	Bibliography.....	64
Appendix A	Sensor Data .....	66
Appendix B	Permeability Tests .....	67
Appendix C	Sieve Analysis. ....	69
Appendix D	Layer Thickness.....	70
Appendix E	2-Dimensional Test Results .....	71
Appendix F	3-Dimensional Test Results .....	85

## Nomenclature

$q$	Specific Flow	m/s
$\Delta p$	Pressure Difference	Pa
$k$	Permeability	m/s
$k_{max}$	Maximum permeability	m/s
$k_{min}$	Minimum Permeability	m/s
$\Delta s$	Flow path length	m
$dh$	Hydraulic head	m
$dl$	Length	m
$\rho_w$	Density Water	kg/m <sup>3</sup>
$g$	Gravitational Constant	m/s <sup>2</sup>
$\epsilon$	Dilatation	–
$v_c$	Cutting Velocity	m/s
$\beta$	Shear Angle	Radians
$R_x$	Resistance of flow line $x$	s
$R_t$	Total resistance of all flow lines	s
$p$	Average pressure over shear zone	Pa
$dn$	Step size over shear zone	–
$p_i$	Integrated pressure over shear zone	Pa
$D_{50}$	50% particle size distribution	–
$D_{15}$	15% particle size distribution	–
$dZ$	Height in vertical direction under plate	m
$dt$	time	s
$dL$	Step size pie slice	–
$dR1$	Width of Pie slice on the plate	m
$dR2$	Width of Pie slice outside the plate	m
$r$	radius	m
$Q$	Volumetric flow rate	m <sup>3</sup> /s
$v_p$	Upward velocity plate	m/s
$S$	Surface beneath plate at $dR1$	m
$a$	Arclength flow line	m
$n$	Number of flow line steps	–
$n_{slices}$	Number of slices	–
$dP_{slice}$	Pressure drop over slice	Pa
$d_p$	Displacement during breakout	m
$E_v$	volume created under plate by lifting	m <sup>3</sup>
$S_p$	surface area of the plate	m <sup>2</sup>
$N_{max}$	Maximum porosity of the sand	–
$N_{min}$	Minimum porosity of the sand	–
$I_v$	Initial volume influenced zone	m <sup>3</sup>
$L$	Layer thickness of influenced zone	m

# List of Figures

- Figure 1.1 – Model of the Under pressures versus the lifting loads ..... 1
- Figure 2.1 – The Equipotential lines and the flowlines for a cutting case..... 6
- Figure 2.2 – The Water flow towards the cutting zone..... 7
- Figure 3.1 – Diagram of the test setup..... 10
- Figure 3.2 – Layout of the location of the pressure sensors on the 2-Dimensional plate ..... 11
- Figure 3.3 – Layout of the location of the pressure sensors on the 3-Dimensional plate ..... 11
- Figure 3.4 – Photos of the test setup and equipment..... 12
- Figure 4.1 – An example of the unfiltered velocity ..... 18
- Figure 4.2 – The load and the displacement versus the time for a 3-Dimensional test in Silverbond sand, (3D-S-70N-1). ..... 18
- Figure 4.3 – The pressure and the velocity versus the time for a 3-Dimensional test in Silverbond sand, (3D-S-70N-1). Note the filtered velocity ..... 19
- Figure 4.4 – A failed 2-Dimensional test, as can be seen the breakout time is very short, (2D-S-150N-3)..... 20
- Figure 4.5 – A failed 2-Dimensional test, the pressure sensors registered a lot of dynamic results, (2D-S-150N-3)..... 20
- Figure 5.1 – The time of breakout for the Silverbond sand, the spread of the different tests is visible. Note that it looks like the trend is having an Asymptotic value, beware that it is only a trend line. ... 23
- Figure 5.2 – The time of breakout for the Geba sand. Here the trend is going to zero, again it is only a trend line and it is not suspected to cross the Net load axis. .... 24
- Figure 5.3 - The mean displacement of for the tests performed with the Silverbond sand. .... 25
- Figure 5.4 - The mean displacement of for the tests performed with the Geba sand..... 25
- Figure 5.5 – The mean plate pressure versus the measured pressure for the Silverbond sand. Especially for the 124 Newton load the difference is big..... 26
- Figure 5.6 The mean plate pressure versus the measured pressure for the Geba sand. Here the differences occur with almost every test. .... 27
- Figure 5.7 – The Measured Pressure versus the mean plate Pressure. .... 27
- Figure 5.8 – The results of DP4 versus the mean plate pressure, DP4 carries the information about the pressure profile under the plate. .... 28
- Figure 5.9 – The differences in breakout for the different sands ..... 29
- Figure 6.1 – The mean time of breakout for the Silverbond sand, notice the descending trend..... 31
- Figure 6.2 – The mean time of breakout for the Geba sand, notice that the difference between the 5 Newton load and the 13N load is large. .... 32
- Figure 6.3 - The mean displacement of for the tests performed with the Silverbond sand. .... 33
- Figure 6.4 - The mean displacement of for the tests performed with the Geba sand..... 33
- Figure 6.5 – The mean plate pressure versus the measured pressure from DP1 for the Silverbond sand. Notice again the difference in measured pressure and the mean plate pressure. .... 34
- Figure 6.6 – For all the test the mean pressure of DP1 is higher than the other 2 sensors. .... 35
- Figure 6.7 – The mean plate pressure versus the measured pressure for the Geba sand. .... 35
- Figure 6.8 – For all the test the mean pressure of DP1 is higher than the other 2 sensors. .... 36
- Figure 6.9 – Comparison between the mean plate pressures and the measured pressures. .... 36
- Figure 6.10 – Time of breakout for the 2 sands. Notice the huge difference. .... 37

Figure 6.11 – Underwater pre-loading.....	38
Figure 6.12 – Consolidation test 1.....	39
Figure 6.13 – Consolidation test 2.....	40
Figure 7.1 – Flow lines underneath the plate.....	41
Figure 7.2 – The plate seen from above, now the pie slice model becomes clear. ....	44
Figure 7.3 - Flow paths. ....	45
Figure 7.4 – The tuning factor of the flow paths.....	46
Figure 7.5 – The limitation of the model.....	47
Figure 7.6 – Linear pressure development under the plate.....	47
Figure 7.7 – The force development under half the plate. ....	48
Figure 7.8 – The pressure development under the total plate .....	48
Figure 7.9 – Corrected pressure development under the plate.....	49
Figure 8.1 – 2D - Model comparison for the Silverbond sand, the trend is visible but the model over estimates. ....	50
Figure 8.2 – First predictions of the model, a large over estimation. ....	51
Figure 8.3 – The point where the velocity is derived from the test data.....	52
Figure 8.4 – The model versus the test data with the new velocities for the Silverbond sand. ....	52
Figure 8.5 – The model versus the test data with the new velocities for the Geba sand.....	53
Figure 8.6 – The model versus the test data using a tune factor for the flow path length. ....	54
Figure 8.7 – The measured data set out versus the model data for the Silverbond sand with the mean velocities over the complete process.....	55
Figure 8.8 - The model versus the test data with the velocities from the beginning of the process for the Silverbond sand. Note that the permeability stays the same.....	56
Figure 8.9 – The predictions of the model for the Geba sand using the mean velocities over the complete lifting process. ....	57
Figure 8.10 – - The model versus the test data with the velocities from the beginning of the process for the Geba sand.....	57

**List of Tables**

Table 3.1 – Load Parameters for the Silverbond sand. .... 13

Table 3.2 – Load Parameters for the Geba Sand..... 14

Table 3.3 – Test matrix for the 2-Dimensional test in the Silverbond sand. .... 14

Table 3.4 – Test matrix for the 2-Dimensional test in the Geba sand..... 15

Table 3.5 – Test matrix for the 3-Dimensional test in the Silverbond sand. .... 15

Table 3.6 – Test matrix for the 3-Dimensional test in the Geba sand..... 15

Table 4.1 – The net load values for the Silverbond sand in the 2D situation..... 16

Table 4.2 – The net load values for the Geba sand in the 2D situation. .... 17

Table 4.3 – The net load values for the Silverbond sand in the 3D situation..... 17

Table 4.4 – The net load values for the Geba sand in the 3D situation. .... 17

Table 8.1 – The mean layer thickness per test setup and sand type. In the right column, the layer thickness is defined as a percentage of the 2-D plate width and the 3-D plate diameter..... 59

# 1 Introduction

## 1.1 Problem Description

As a big part of the extracted oil comes from offshore areas, large structures are needed to create a horizontal, safe, working space above the water level for oil drilling. One of the structures is the so-called jacket which consist of several hollow pipes welded together. A commonly used method for attaching big structures to the sea floor is the use of long piles which are driven into the soil. In the case of a jacket the piles are driven through pile sleeves which provide guidance.

When jackets are installed on the sea bottom several problems can occur. Apart from installation errors such as for instance lifting errors, one of these problems is related to the situation below the water surface. Most offshore areas are formed of soft, unconsolidated soil on which it is difficult to perform the pile driving operations. The jacket has the tendency to sink in the soil on the side where piles are driven into the bottom.

To prevent the jacket from falling over mud mats are used. These mats support and distribute the weight of offshore structures on the soft soil. In this way, the structure is able to stand on the sea floor.

When the structure is finally standing on the sea floor the weight of the structure pushes the water out of the soil which creates a more consolidated soil state at the interface between the mud mat and the soil. Lifting of the structure after it has been lowered now means that not only the weight but also the (passive) suction of the soil has to be overcome. According to (Liam Finn, 1972): If the object is embedded and an attempt is made to lift it adhesion will develop under the base of the object. The difference between the force now required to lift the object and the submerged weight is the breakout force ( $F_{Lift}$ ), see Figure 1.1. With breakout defined as the moment the plate comes loose from the bottom.

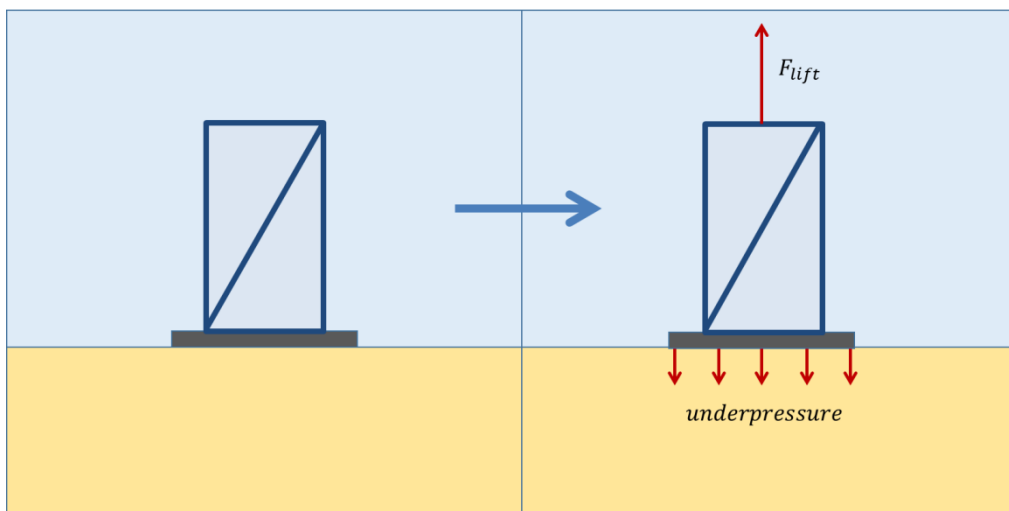


Figure 1.1 – Model of the Under pressures versus the lifting loads

The passive suction occurs as water has to flow into the pores under the mat during lifting and encounters a certain resistance by doing so.

Passive suction can occur in the following situations:

- Decommissioning of the structure: When for example a jacket is removed by lifting it from the bottom a certain force is needed to overcome the suction of the soil on the mud mat.
- Installation of the structure: During an installation error when for example the orientation is wrong or the structure is not levelled correctly.

This thesis is focused on the modelling of the under pressures under a mud mat using an analytical approach. The model is supported by using a test setup to generate data to validate the model.

## 1.2 Purpose of Research

This research is aimed on to the prediction of the force needed to overcome the passive suction between soil and the mud mat using an analytical approach and to get insight in the physical parameters behind this process. During the literature survey a lot of information regarding the topic was found but most of it is focused on other subjects of the breakout phenomena. As a dredging student, an analytical model used for sand cutting was found and the question arose if this model could be modified to predict the breakout force and time. Afterwards this model could be validated with test data.

During the research the following objectives are encountered:

- Literature study: Previous research regarding this subject has been done. However, on different subjects and structures.
- Modelling: the formulation of an analytical model. Use a proven model from dredging cutting theory and adapt this to model the under pressures under mud mats.
- Testing: Using a self-developed test setup to get insight in the governing variables and procedures of lifting a plate from a sand bed.
- Validation: Use the test data for validating the analytical model. Compare the test data with the analytical model.

The research itself is dependent on time and budget therefore the research itself has boundaries:

- Only breakout phenomena in sand will be investigated. Breakout phenomena in clay have been extensively researched. Sand however not, early researchers (Liu, 1969) even stated that lifting in sand does not lead to a breakout force. But, from cutting theory (Miedema, 2014) it is known that small grained sand can lead to under pressures. Therefore, it is interesting to investigate the suction problem for sand.
- The test structures are simplified; this is done to give easy insight in the governing parameters.
- Testing will be done with two different sands, Silverbond of 50  $\mu$  and Geba Weis of 125  $\mu$ m
- Only vertical upright testing will be done, lifting under an angle is a totally different subject involving other parameters.

The main research question to be answered is as follows:

*How are the breakout force and breakout time influenced by the permeability of the sand and the lifting force? Can an analytical model, that uses these parameters, predicts the lifting force within a certain margin?*

To help answering the main research question the following sub questions have been composed:

- Can the Parallel Resistor model from cutting theory (Miedema, 2014) be adapted to use in Breakout Phenomena?
- How does the permeability scale over different sorts of sand using the same breakout load?
- Does pre-loading the plate result in a difference in breakout time in Sand? (Liu, 1969) states that for clay the longer the settlement time the longer the breakout time. For clay soils the situation is different, pore water pressures do not dissipate that easy as in sand. To help investigating the following sub question can be proposed:
  - o Can pre-loading the structure change the permeability of the soil when placed onto the sand bottom?
- How does the breakout time scale when increasing the load, and thus the weight of the structure?
- What is the displacement a plate needs before breakout?

## 2 Theory

### 2.1 Earlier Research

Earlier research concerning the so-called break out forces has been done. The first to do some testing is (Muga, 1968) with the NCEL, Naval Civil Engineering Laboratory. Muga conducted theoretical and experimental studies in order to derive an empirical formula to estimate the force required to lift an object of a certain size from the sea bottom. His formula is dependent on the contact area of the structure, a time allowed for the breakout and a supporting pressure of the soil (recognized as the soil bearing capacity by Terzaghi).

(Vesic, 1969) studied the factors affecting the magnitude of the breakout force, he gave some good recommendations for further research.

(Liu, 1969) also in a NCEL study stated that the breakout force is more dependent on the embedded depth of the object. He was able to specify the breakout force within a certain time frame but could not accurately predict the time of breakout. He also stated that the magnitude of the breakout force is dominated by the soil cohesion, area of structure time of breakout and the permeability of the soil. (Lee, 1973) continued with research for the NCEL, he divided the breakout of partially embedded objects from cohesive seafloors into immediate and long term breakout problems. The conclusion was the breakout will eventually occur under any net uplift force, however much time may be involved. No existing theoretical models were applicable; the estimations of the breakout force gave a range of plus or minus one hundred percent.

(Liam Finn, 1972) used in the basis the same formula as Muga and added some factors for the submerged weight of the base and soil. Also, he added the bearing capacity factor which is a function of the shape of the base.

(Rapoport V, Young A.G, 1983) stated that the empirical relations found before are easy to use but limited to a certain soil type. they derived analytical equations for one dimensional cases. Also, their approach assumed general soil failure and is therefore an upper limit of the breakout force. (Foda, 1982) used a boundary layer formulation, he stated that when an object is lifted from the seafloor a gap will arise between the structure and bottom. Using mathematics, he describes all the governing effects for gap flow and eventually gives a prediction of the breakout force based on this flow.

(Das, 1991) further proposed modifications for the formulas regarding the breakout force using the contact bearing pressure, a relation between the object area and the object weight and he stated that the time an object rests on the sea bottom affects the breakout force. (Al-Shamrani, 1995) did a finite element analysis on the break out phenomena. His analyses were in agreement with the empirical formulas stated by earlier research. However, limited field information is available for confirmation of his model.

(Mei, C.C., Yeung, R.W., Liu, K.F., 1985) investigated based on the assumptions from (Foda, 1982) the breakout phenomena and showed that breakout also occurs without the assumptions of an elastic soil skeleton.

(Craig, 1987) and (Chen, 2012) both did a series of centrifugal test to investigate the breakout phenomena. (Craig, 1987) did this to investigate the installation of a jacket. (Chen, 2012) to investigate the uplift capacity of the mud mats in slightly over consolidated clay.

For tilted lifting (Huang, H.M., Lin, M.Y., Huang, L.H., 2010) investigated the flow field under the structure induced by the tilted lifting and the lift force using an analytical approach.

What can be observed from the literature is that few to no research in to breakout phenomena in sand have been carried out. Also, no modelling is done into this subject. From cutting theory it is known that cutting in sand develops under pressures around the blade tip. An analytical model exists where these under pressures are calculated. Therefore, it is interesting to investigate the breakout phenomena in sand.

To model the lifting process in sand the first idea was to use Plaxis as a program. After a couple of weeks using Plaxis it was decided that Plaxis was too complex to give easy insight in the governing parameters.

For modeling the lifting process an Analytical model will be used and modified. (Miedema, 2014) published a book about cutting theories used in Sand, clay and Rock. For this report the analytical sand pore pressure calculation model will be used that describes water flow in the sand bed but does not take the stresses in the grain skeleton of the soil in to account. The pressure calculation is useful for prediction of the lifting force.

## **2.2 Parallel Resistor method**

As an analytical model an adaption of the Parallel Resistor model for water under pressures in the sand on and round a blade during saturated sand cutting will be used. This model will be adapted for the under pressures under the mud mat.

Miedema uses his model as a method to use the basics of the sand cutting theory in a very practical and pragmatic way. The model is primarily used to give some fast and easy insight in the pressure development around the blade. From the theory and comparisons with FEM calculations it is known that the model has an accuracy of 10% (Zhao, 2001). The model itself is calibrated with measurement data. For such a model, given the accuracy of the input parameters, this is a good result. The problem with FEM calculations is that they are time consuming to make and therefore expensive. Also, they are most of the time case dependent and therefore non-universal in use.

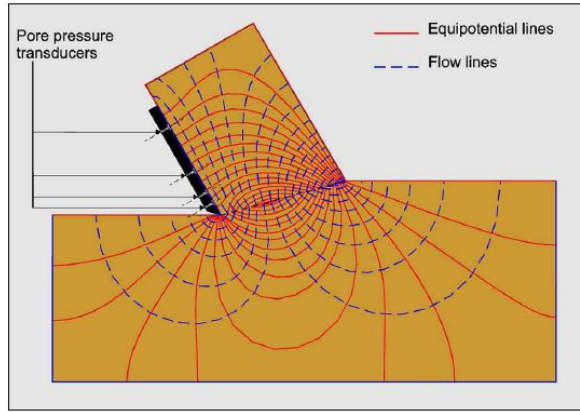


Figure 2.1 – The Equipotential lines and the flowlines for a cutting case

The model of Miedema is based on the flow lines in the sand bed. Miedema reasons that following the flow lines through the bed to the shear zone the water flow will encounter a certain resistance. This resistance is proportional to the distance the water has to travel and dependent on the permeability of the soil, see Figure 2.1.

The longer the flow line, the bigger the resistance and the smaller the permeability the more difficult it is for the water to flow through the soil.

Dilatation is described as an increase in volume due to shear deformations. During cutting dilatation takes place with as result an increase in pore under pressures (Miedema, 2014).

Now the law of Darcy describes a relation between the specific flow  $q$  (m/s) and the pressure difference  $\Delta p$  (Pa):

$$q = k * i = k * \frac{\Delta p}{\rho_w * g * \Delta s} \quad (2.1)$$

Where:

$\Delta s$  = Flow length

$k$  = Permeability

$i = dh/dl$

$\rho_w$  = Density water

$g$  = gravitational constant

The total specific flow for the cutting case originates from the flow caused by the dilatation, in the cutting case this is defined as follows:

$$q = \epsilon * v_c * \sin(\beta) \quad (2.2)$$

Where:

- $\epsilon$  = Dilatation
- $v_c$  = Cutting Velocity
- $\beta$  = Shear Angle

Therefore, one can state:

$$\epsilon * v_c * \sin(\beta) = k * \frac{\Delta p}{\rho_w * g * \Delta s} \quad (2.3)$$

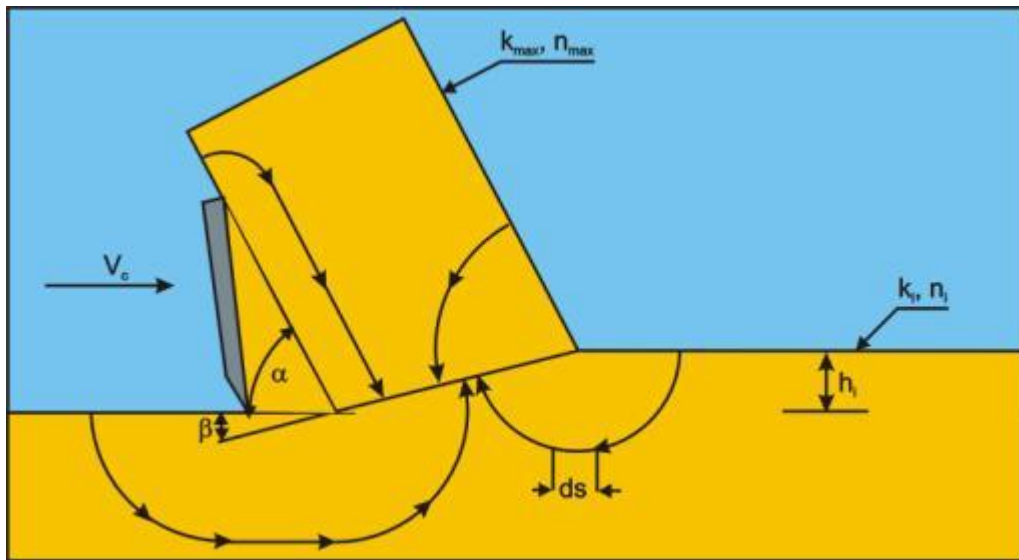


Figure 2.2 – The Water flow towards the cutting zone.

Now the length of the four flow lines can be calculated, see Figure 2.2. Using the corresponding permeability in combination with shifting some variables the following relation is found:

$$\rho_w * g * \epsilon * v_c * \sin(\beta) = \frac{\Delta p}{\left(\frac{\Delta s}{k}\right)} \quad (2.4)$$

For the different lengths and permeability's:

$$\rho_w * g * \epsilon * v_c * \sin(\beta) = \frac{\Delta p}{\left(\frac{\Delta s_1}{k_{max}}\right)} + \frac{\Delta p}{\left(\frac{\Delta s_2}{k_{max}}\right)} + \frac{\Delta p}{\left(\frac{\Delta s_3}{k_i}\right)} + \frac{\Delta p}{\left(\frac{\Delta s_4}{k_i}\right)} \quad (2.5)$$

As the length of a flow line divided by the permeability can be seen as a resistance the following applies:

$$\rho_w * g * \epsilon * v_c * \sin(\beta) = \frac{\Delta p}{(R_1)} + \frac{\Delta p}{(R_2)} + \frac{\Delta p}{(R_3)} + \frac{\Delta p}{(R_4)} \quad (2.6)$$

Following the rule of parallel resistors and using the resistance values found above the following equation is found:

$$\frac{1}{R_t} = \frac{1}{R_1} + \frac{1}{R_2} + \frac{1}{R_3} + \frac{1}{R_4} \quad (2.7)$$

Combining equation 2.6 and 2.7 results in an equation describing the pressure difference in the shear zone on a certain point:

$$\Delta p = \rho_w * g * \epsilon * v_c * \sin(\beta) * R_t \quad (2.8)$$

Integrating over the shear zone gives the average pressure over the shear zone, With  $dn$  the step size over the shear zone.

$$p = \frac{1}{dn} \sum_{i=0}^{dn} \Delta p_i \quad (2.9)$$

## 2.3 Conclusions

Early publications showed that already in the sixties a lot of attention was put in the research on breakout phenomena. A lot of this research was aimed at testing in the field using for example ships and submarines. Also, a lot of publications were dependent on the location of the test site. As specific soil conditions are present at these sites it is not evident to draw general conclusions. A lot of the earlier research is indirectly or directly based on the research done in the sixties primarily by Muga. In the eighties Foda looked on the breakout phenomena from another angle proposing new formulas to predict the breakout force. (Das, 1991) performed some experiments in soft clay with cylindrical objects.

It can be concluded that no real tests on scale are performed in fine grained sand. As clay behaves different than sand it is not evident to use the same formulas found in the early days for soils based on sand. To get some understanding of the basic physical parameters an analytical model is created to predict the breakout force in sand. The model used is based on the parallel resistor method used in (Miedema, 2014). This model has some similarities with the lifting case, for example, in cutting cases under pressures are present under and around the cutting blade. This gave the inspiration to adapt this model for the lifting case. To validate this model laboratory test will be performed.

## 3 Testing

### 3.1 Introduction

In many scientific researches testing with a certain setup is done. In this case testing is done to give the analytical model some fundamental backup. Also in comparison with field testing the small-scale laboratory setup has some advantages:

- More parameters are easier to control.
- Good visibility on the setup.
- Costs are low compared to field tests.
- Tests are easier to reproduce, faster and under same conditions.

The test results will be used to validate the model outcome. As mentioned before the testing will only be done using fine grained sand as soil.

At first it was important to check whether some results can be derived from the test setup at all. Therefore, a preliminary test setup was build according to some expectations.

Expectations:

- Suction can be measured using differential pressure meters.
- With a transparent acrylic plate the water flow might be observed during the lifting process.
- After lifting a hole in the sand bed can be observed, under pressures stick the sand to the plate during lifting.

After careful testing, some improvements were made to the test setup, in the early stages a strong nylon rope was used for lifting but this proved to be too elastic generating unrealistic results and too much fluctuation in the load. Also, it proved to be difficult to level the sand bed correctly resulting most of the time in immediate breakout of the plate. The visibility in the reservoir was unfortunately very bad. Especially the fine-grained sand carried some dust with it.

Suction under the plate was eventually registered by the Differential Pressure sensors after making sure the right sequence of venting was used. At first it was questionable to use the DP sensors as it was suspected the pressure was small. Testing showed that the sensors could be used. After every test a gap in the sand bed was present so it seemed that the plate was taking a portion of sand with it during the lifting process.

After fine-tuning the test and learning from the preliminary testing the final test setup was in operation.

### 3.2 Test setup

The tests are performed in the Dredging Laboratory of the technical university in Delft. The test setup is built around an existing acrylic reservoir with the following dimensions: 80x80x80 cm. Around the reservoir a rigid frame is placed which holds the pulleys. A simple diagram of the test setup is shown in Figure 3.1

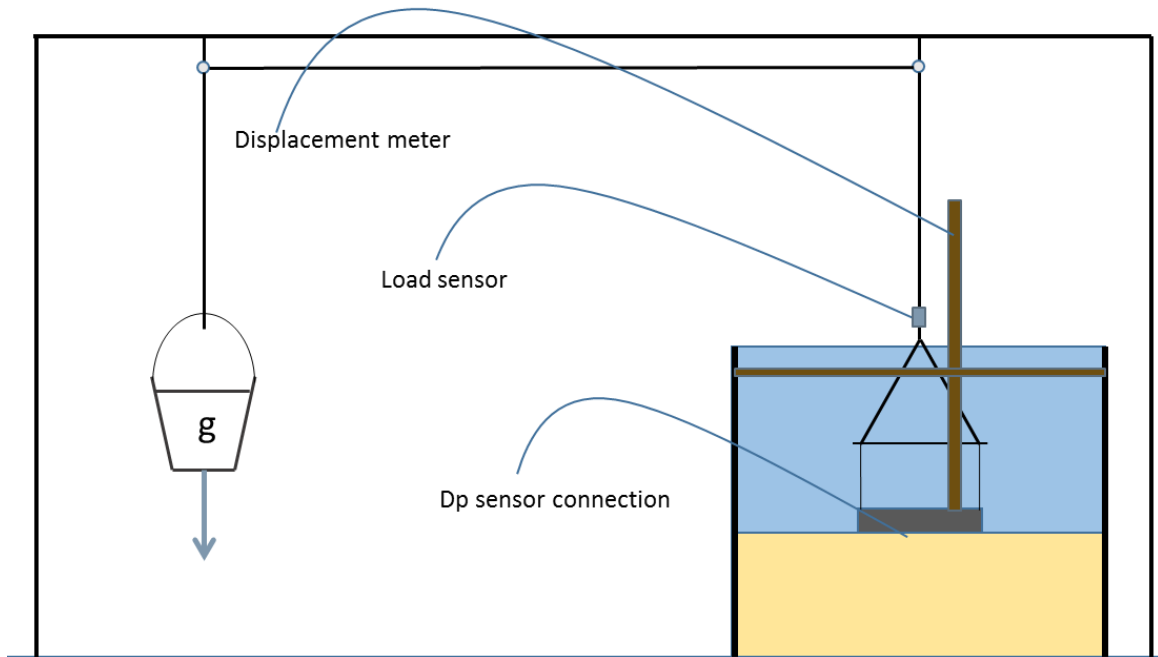


Figure 3.1 – Diagram of the test setup

In the reservoir, an acrylic plate is placed with a thickness of 30mm. This is done to make sure the deformations due to bending can only occur with a very high, unrealistic, loading. It was expected that only small displacements are needed to lead to breakout of the plate, therefore only minimal deformations due to bending can be allowed. Testing will be done with 2 types of acrylic plate, a *rectangular* and a *round* version. The rectangular plate is sealed off against two sides of the reservoir with thin rubber gaskets with low friction, this is done to create a pure 2-Dimensional case. The round plate is modeled to use for the 3-Dimensional case.

In the plates, several 3 mm holes are drilled to make connections for the Differential Pressure sensors, DP sensors. These are connected via rigid poly flow hoses; the holes are divided over the 2-Dimensional (Rectangular) and 3-Dimensional (Round) plate according to Figure 3.2 and Figure 3.3 respectively. The plate will rest on the sand bed, the sand bed is always of the same thickness, namely 700 millimeters.

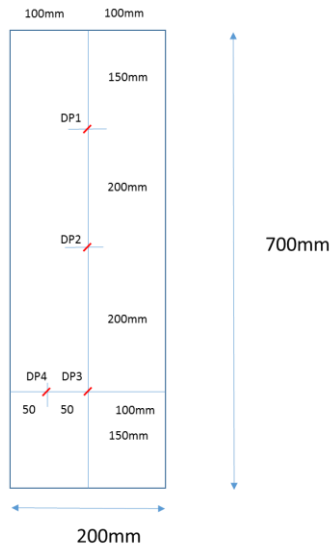


Figure 3.2 – Layout of the location of the pressure sensors on the 2-Dimensional plate

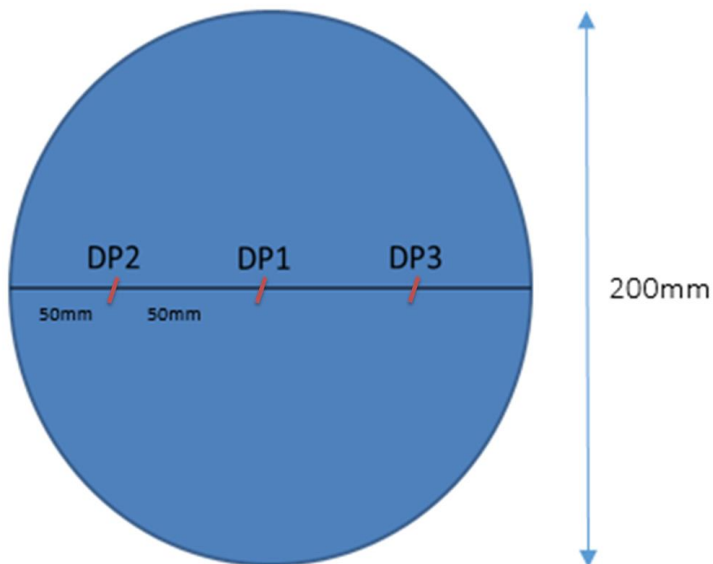


Figure 3.3 – Layout of the location of the pressure sensors on the 3-Dimensional plate

The plates are lifted via a flexible steel rope which runs over two frictionless pulleys. At the other end of the cable a bucket is placed to hold weights needed to create the specified load.

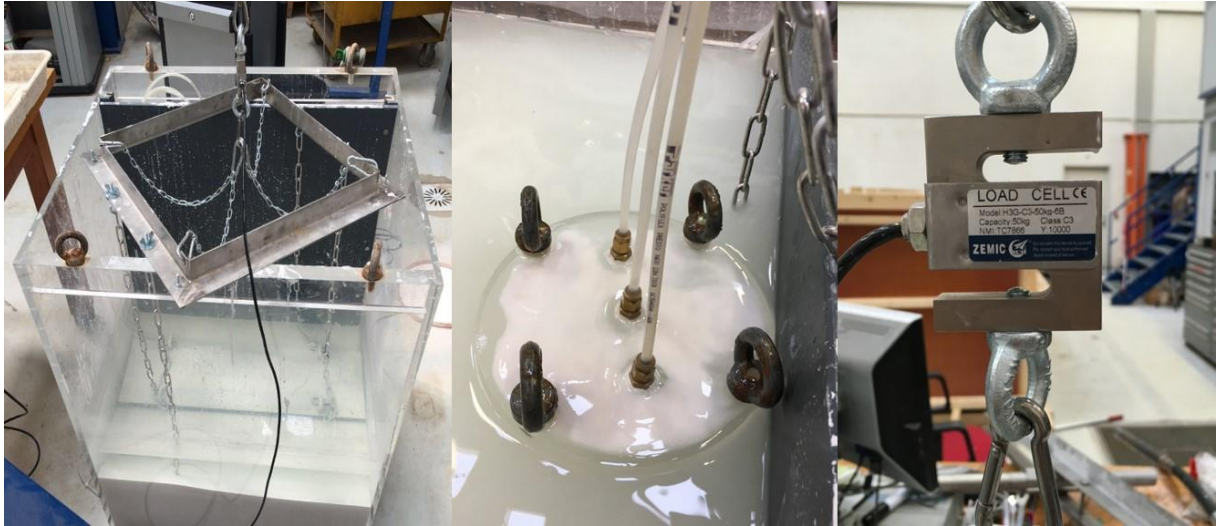


Figure 3.4 – Photos of the test setup and equipment

The load is transferred to the plate by a rigid stainless steel lifting frame which is connected via four chains to the plate, see Figure 3.4

Between the lifting frame and the steel cable a load cell is placed to measure the load exerted by the bucket on the plate. During the lifting the displacement is measured via a displacement sensor placed onto the plate, the sensor is calibrated for every test.

As mentioned before there are connections in the plate for hoses leading to DP sensors. The sensors measure the under pressure beneath the plate and are therefore negatively calibrated.

### 3.3 Test Parameters

To get some insight in the physical processes it is important to define the test parameters correctly. Different parameters are to be tested.

#### 3.3.1 Sand types

The pressure difference predicted by the parallel resistor model is dependent on the permeability of sand. Therefore, to check the validity of the model different types of sand will be used, however the permeability cannot be too large otherwise no sufficient under pressure can build up. The two sands used are the Silverbond D6 and Geba 0.06-0.25 due to availability in the laboratory.

These two sands are tested in the laboratory of civil engineering. An earlier sieve analysis has been done by Ir. Rik Bisschop. Test data showed that the  $D_{50}$  of Silverbond and Geba is  $51 \mu\text{m}$  and  $125 \mu\text{m}$  respectively.

Both sand have endured a falling head test to check the maximum value of the permeability. Silverbond got a value of  $5\text{e-}6 \text{ m/s}$ . Geba, having a larger grain size, had a value of  $7\text{e-}5 \text{ m/s}$ . This is the smallest permeability for this type of sand as it was make sure the sand was packed as tight as possible during the test. The values of the porosity are tested at the civil engineering laboratory. The values for the Geba sand tested as:

$$N_{max} = 0.47$$

$$N_{min} = 0.40$$

And for the Silverbond sand:

$$N_{max} = 0.54$$

$$N_{min} = 0.39$$

### 3.3.2 Consolidation

Another factor that defines permeability in soil is the consolidation. One can reason that if a weight is placed on the sea bottom for a certain amount of time the water will flow out of the soil bed underneath the mat. How much water and how fast is dependent on the weight above the mat, duration, compressibility of the soil and the permeability of the soil. This variable is not of great interest for structures who have been placed on the sea bottom a long time ago as the soil underneath the mats has reached its maximum consolidation given its weight. The results will be of interest for modelling the installation process of such a structure. This variable will be tested by placing a big weight onto the 3-Dimensional plate and let the plate rest for a certain amount of time. Afterwards it can be checked if different weights placed onto the plate will result in different breakout times.

### 3.3.3 Lifting loads

The lifting loads are an important variable, actually they are of influence on two other variables namely the velocity and the breakout time. Lifting with a bigger load means that the upward velocity of the plate will be larger which means that the expected under pressures increase. Lifting with a larger velocity means that the breakout time is shorter. The question is how these variables relate with the use of different sands. Lifting with the same load on Geba should give an overall faster process than lifting on Silverbond.

The lifting loads are chosen according to the dry weight of the lifting frame added by the submerged weight of the plates. As mentioned before breakout can only occur if there is a net upward force, therefore the minimum load needs to be larger than the combined weight.

Silverbond sand	Load 1	Load 2	Load 3	Load 4
2D	130N	150N	170N	
3D	65N	70N	90N	110N

Table 3.1 – Load Parameters for the Silverbond sand.

Geba sand	Load 1	Load 2	Load 3
2D	90N	110N	130N
3D	50N	60N	70N

Table 3.2 – Load Parameters for the Geba Sand

Table 3.1 and Table 3.2 give the total load imposed on the complete structure. These loads can be verified by the use of the load cell. When comparing the under pressures with the loads it is important to note that the loads should be corrected for the weight of the frame and the underwater weight of the plate. When correcting for this weight the net pulling load under the plate is known.

### 3.4 Test Procedure

The sand is placed into the reservoir with water and mixed thoroughly to exclude possible trapped air bubbles. The mixture is vibrated to speed up the settling and left resting for a week. This creates a solid sand bed onto which the plates can be placed. This has to be done for the two sand types ensuring equal sand – water distribution.

Before placing a plate onto the surface the sand is smoothed with a steel ruler and left for setting. The plate is hanging in the water so that the DP-sensors can be vented. The plate is then placed on the smooth sand surface and vibrated around the plate to ensure no air is trapped under the plate and to create a homogeneous sand bed. After settling for an hour (water is clear again) the test can begin. Weights are carefully placed into the bucket in such a way no dynamic peak load is exerted onto the frame.

Every test is run three or more times with the same weights to get some good average values. The testing find place according to the test matrices shown in tables below. The red colored tests shown in the tables below are the test that are discarded due to reasons specified in chapter 4.

2-D Tests	Silverbond		
	Testname		
Load (N)	Test 1	Test 2	Test 3
130N	2D-S-130N -1	2D-S-130N -2	2D-S-130N -3
150N	2D-S-150N -1	2D-S-150N -2	2D-S-150N -3
170N	2D-S-170N -1	2D-S-170N -2	2D-S-170N -3

Table 3.3 – Test matrix for the 2-Dimensional test in the Silverbond sand.

2-D Tests		Geba		
	Testname			
Load (N)	Test 1	Test 2	Test 3	
90N	2D-G-90N -1	2D-G-90N -2	2D-G-90N -3	
110N	2D-G-110N -1	2D-G-110N -2	2D-G-110N -3	
130N	2D-G-130N -1	2D-G-130N -2	2D-G-130N -3	

Table 3.4 – Test matrix for the 2-Dimensional test in the Geba sand.

3-D Tests		Silverbond			
	Testname				
Load (N)	Test 1	Test 2	Test 3	Test 4	
65N	3D-S-65N -1	3D-S-65N -2	3D-S-65N -3		
70N	3D-S-70N -1	3D-S-70N -2	3D-S-70N -3	3D-S-70N -4	
90N	3D-S-90N -1	3D-S-90N -2	3D-S-90N -3		
110N	3D-S-110N -1	3D-S-110N -2	3D-S-110N -3	3D-S-110N -4	

Table 3.5 – Test matrix for the 3-Dimensional test in the Silverbond sand.

3-D Tests		Geba			
	Testname				
Load (N)	Test 1	Test 2	Test 3	Test 4	
50N	3D-G-50N -1	3D-G-50N -2	3D-G-50N -3	3D-G-50N -4	
60N	3D-G-60N -1	3D-G-60N -2	3D-G-60N -3		
70N	3D-G-70N -1	3D-G-70N -2	3D-G-70N -3		

Table 3.6 – Test matrix for the 3-Dimensional test in the Geba sand.

## 4 General Test Results

### 4.1 Introduction

The data from the test setup was recorded with Labview and further processed by Matlab. The data was recorded with a sample frequency of 100hz. The results are then corrected for offset values, this means that the test setup will run idle for a minute every test to record the idle values of the sensors. The values are then later subtracted from the complete data set.

As there were in fact two different tests performed, namely the 2-dimensional and the 3-dimensional test, these will be treated separately.

In advance of testing a test plan was written to check how many tests were to be performed. Unfortunately, not every test came out as a reliable result. Some test results are therefore discarded. This is done after carefully examining the results. Most of the time unrealistic short breakout times led to removing of the test results, this is probably due to the fact the plate did not made good contact with the sand bed, air was trapped beneath it or the sand itself had air in it. In other cases there was a clear problem with air in the polyflow hoses to the DP sensors so no correct pressure registration took place. The specific test results are reported in Chapter 5 and 6

### 4.2 Net loads

For analyzing the measurements, it is important to reason how the load is interpreted. The load imposed onto the lifting frame is not equal to the load under the plate, this is because when lifting the structure first the dry and submerged part of the frame have to be overcome, after that the under pressure is created. For analyzing the net load is of more importance, therefore in the tables below the load is converted to a net load. The factor used is, as mentioned, dependent on the dry weight and the submerged part (e.g. the plate) of the structure. For the 2-Dimensional situation the difference between the load and the net load is 52 Newtons., for the 3-Dimensional the difference is calculated as 45 Newtons

2-D Tests	Silverbond
Load (N)	Net load (N)
130N	78N
150N	98N
170N	118N

Table 4.1 – The net load values for the Silverbond sand in the 2D situation.

2-D Tests		Geba
Load (N)		Net load (N)
90N		<b>38N</b>
110N		<b>58N</b>
130N		<b>78N</b>

Table 4.2 – The net load values for the Geba sand in the 2D situation.

3-D Tests		Silverbond
Load (N)		Net load (N)
65N		<b>20N</b>
70N		<b>25N</b>
90N		<b>45N</b>
110N		<b>65N</b>

Table 4.3 – The net load values for the Silverbond sand in the 3D situation.

3-D Tests		Geba
Load (N)		Net load (N)
50N		<b>5N</b>
60N		<b>15N</b>
70N		<b>25N</b>

Table 4.4 – The net load values for the Geba sand in the 3D situation.

### 4.3 Measurement Analysis

The test data was recorded with Labview at a sample rate of 100hz per second. This generates a lot of raw data which need to be filtered, see Figure 4.1 . Using Matlab to filter the signals with a moving average filter the resulting signals are used to generate plots like those in Figure 4.2 and Figure 4.3. Figure 4.2 shows the Load and Displacement versus the Time for the 3-Dimensional plate. What can be seen is that the load is located around the 26 Newton as the Displacement increases steadily. The Load has a short interruption in the signal at around 20 seconds. This is because all the weight used in the test setup are placed into the bucket carefully one at a time to make sure no dynamics are disturbing the data. The Peak load is derived from the values at roughly 26 seconds, the maximum displacement is the displacement taken just before the breakout.

In Figure 4.3 the pressure and velocity versus the time is plotted. The velocity is derived from the displacement. After filtering the trend is visible. The velocity is used to determine the time of breakout. Looking closer at the velocity at around 90 seconds it can be seen that the slope of the velocity signal increases rapidly, this means that the plate including the lift frame are accelerating.

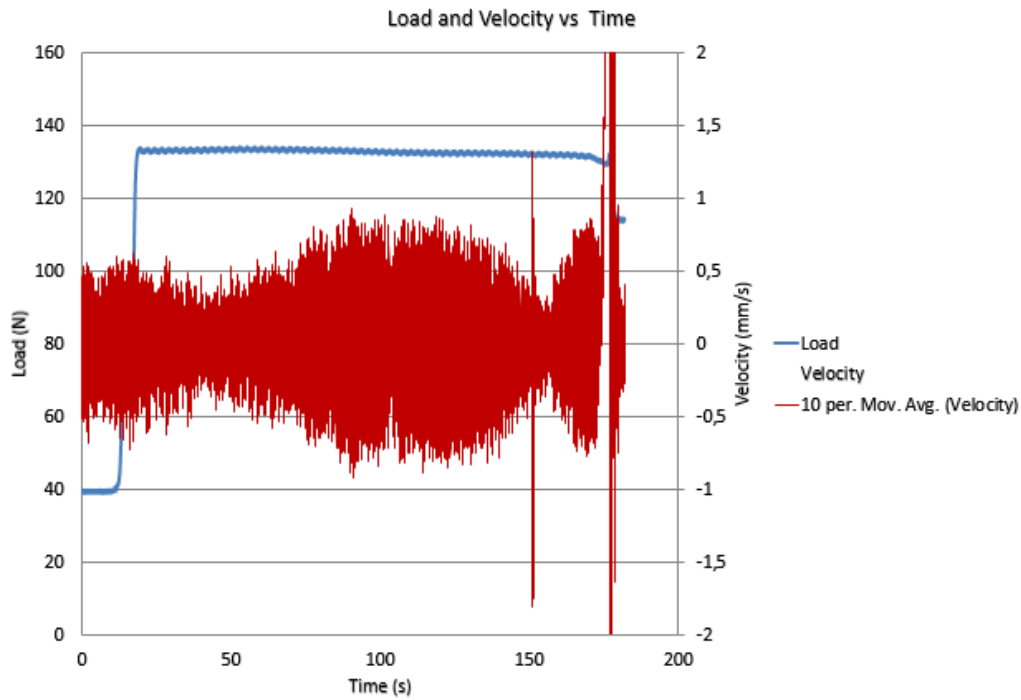


Figure 4.1 – An example of the unfiltered velocity.

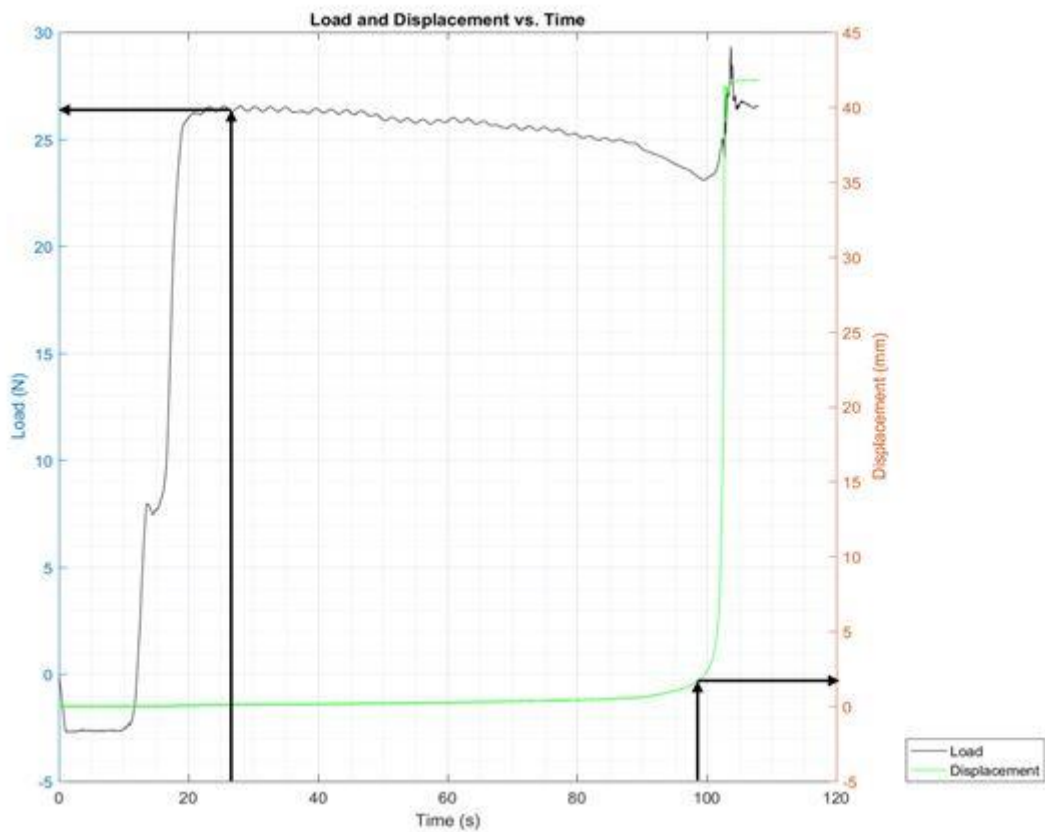


Figure 4.2 – The load and the displacement versus the time for a 3-Dimensional test in Silverbond sand, (3D-S-70N-1).

From these data plots the peak values are used for further analysis in Chapter 5 and 6. The reason for using the peak values can be understood if one looks at the signal for the pressure. At around 15

seconds the Load in Figure 4.2 starts to increase like a ramp function. The pressure signals in Figure 4.3 response different. They increase more like a first order system. The reason for this is to be answered later on. At the point the velocity was increasing rapidly also the pressure signals begin to act different. Large jumps in the signals can be spotted. This is due to the dynamics affects taking place when the plate begins his journey to the surface with a sudden increase in lift velocity. The peak values to be used for the pressure signals are in this case taken right before breakout.

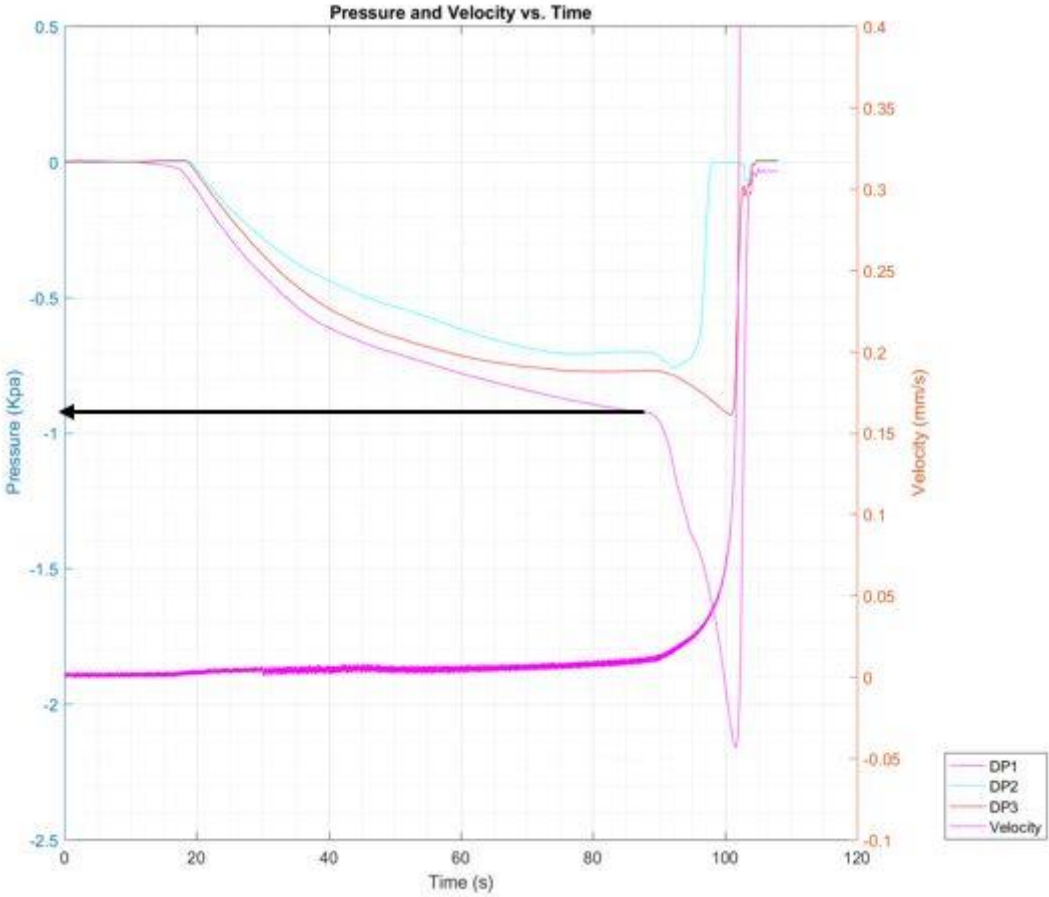


Figure 4.3 – The pressure and the velocity versus the time for a 3-Dimensional test in Silverbond sand, (3D-S-70N-1). Note the filtered velocity

Unfortunately, not all test performed were usable. Sometimes imposing the load on the plate and lifting frame initiated immediate breakout as by other test the breakout time was normal but little or no pressure registration happened. These situations can be linked to trapped air underneath the plate or the sand bed proved not to be perfectly smooth. In Figure 4.4 and Figure 4.5 the results of a 2-Dimensional test that went wrong are plotted. What can be seen is that the load was increasing. During the increase the velocity also started to increase rapidly leading to a breakout time of under 5 seconds. These kind of test results are excluded from further analysis.

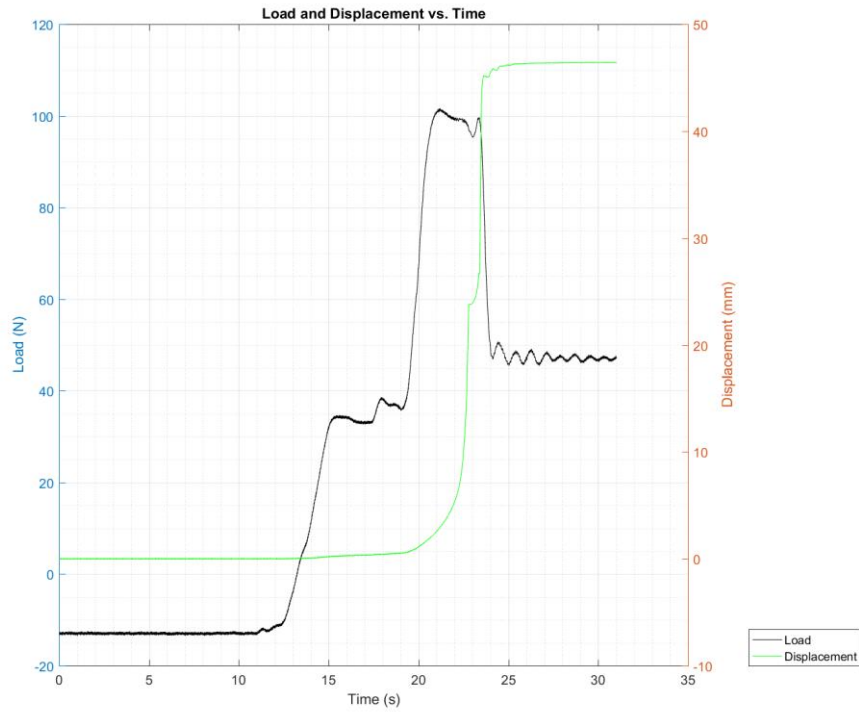


Figure 4.4 – A failed 2-Dimensional test, as can be seen the breakout time is very short, (2D-S-150N-3)

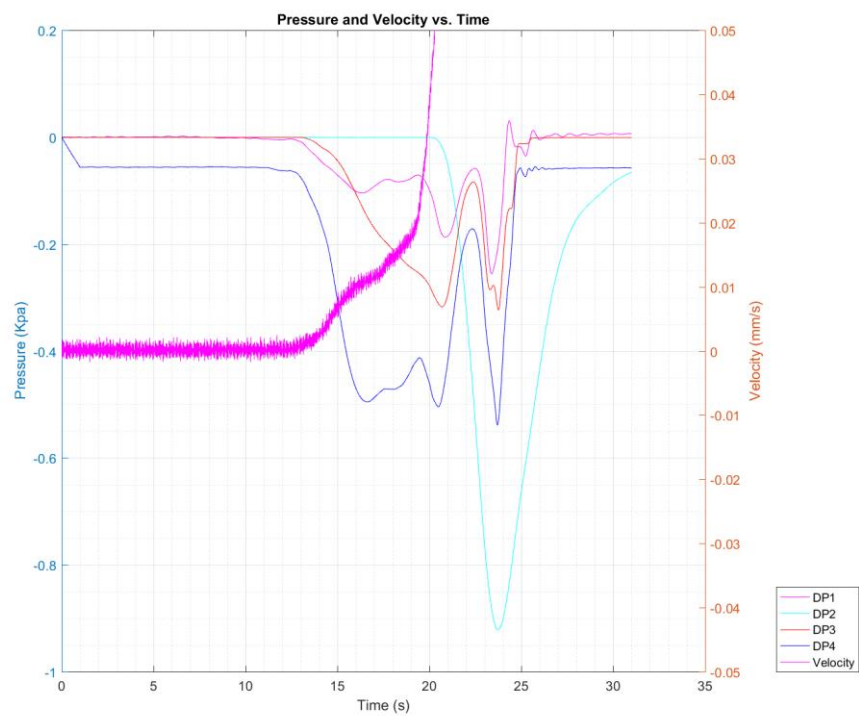


Figure 4.5 – A failed 2-Dimensional test, the pressure sensors registered a lot of dynamic results, (2D-S-150N-3).

#### **4.4 Conclusions**

What can be concluded from analyzing the test data is that pressure registration is difficult. A lot of tests are dealing with delays in pressure registration. This is probably due to the pressure mounting points on the plate. Some damping can occur if these holes are getting constipated with sand. A method for avoiding this kind of results in future testing would be the use of more pressure sensors linked to each other so that the mean value of a couple of mounting points is used. Also, equipping the mounting points on the plate with little filter stones could be a solution. Another reason for bad pressure registration can be air in the hoses. Before every test the sensors are getting vented for a couple of seconds. However, air inside the sand bed could influence the pressure measurement.

## 5 2 Dimensional Results

The first tests to be performed were done with the 2-Dimensional plate. The plate has connections for up to five DP sensors. Four of them were used and distributed over the plate according to Figure 3.3. The sand types used to build up the sand bed were the Silverbond and Geba sand mentioned before. The magnitude of the different loads that were applied on the plate are according to Table 3.1. This chapter will show the results of the 2-Dimensional test and show some of the relations found.

### 5.1 Expectations

As with every laboratory test there are some, theoretical, expectations. As for the 2 dimensional plate these were as following:

- Breakout time is directly related to the permeability of the sand. The permeability of the sand is linked to the  $D_{15}$  quadratic (Den Adel, 1989), this holds that if the grain size doubles the permeability becomes 4 times as big. As the permeability increases roughly with a factor 8 it was estimated that the breakout time also decreases roughly a factor 8.
- According to the model outcome (See chapter 7) the pressure development for the 2-Dimensional case is expected to be linear given any input over the width of the plate. By all means the under pressure measured on a point closer to the plate edge is expected to be lower than a point on the center line of the plate, furthest away from the plate edge. In this case DP1, DP2 and DP3 should give similar results as DP4 should give a lower output. As the 2-dimensional model is linear and DP4 is located on a quarter of the plate the under pressure is expected to be half of the under pressure measured by the other sensors.
- The average time of breakout is supposed to decrease as the load increases. One can expect that doubling the load should give half the breakout time as the model itself is linear.

### 5.2 Time of breakout

#### 5.2.1 Introduction

The time of breakout is defined as the time the plate needs for breakout over the different tests under the same conditions. Expected was that for the Silverbond sand the breakout time is noticeable larger than for the Geba sand. This, as mentioned before, has to do with the difference in permeability for the both sands which leads to a higher resistance for water to flow along the flowlines and thus a larger breakout time.

#### 5.2.2 Silverbond 51 $\mu$ m Sand

The average breakout time for the Silverbond sand is plotted in Figure 5.1. What can be seen is that the breakout time for the net load of roughly 80 newtons has a range around 120 seconds. For the 100 and 125N net load the breakout times are in the range of 90 and 80 seconds respectively. The trendline is added to help visualize the descending trend. Notice that the Load values plotted are the Net load values under the plate. This means that the submerged weight is subtracted.

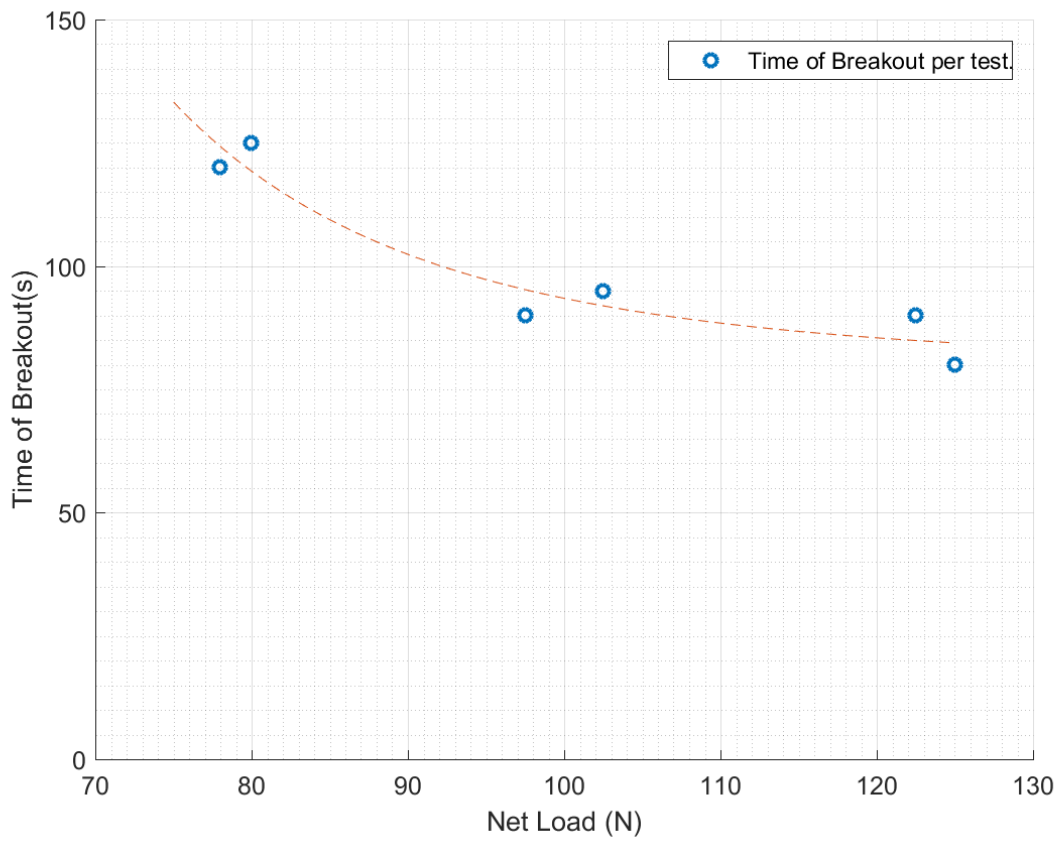


Figure 5.1 – The time of breakout for the Silverbond sand, the spread of the different tests is visible. Note that it looks like the trend is having an Asymptotic value, beware that it is only a trend line.

### 5.2.3 Geba 125 $\mu$ m Sand

The average breakout time for the Geba sand is plotted in Figure 5.2. Again, a descending trend is visible

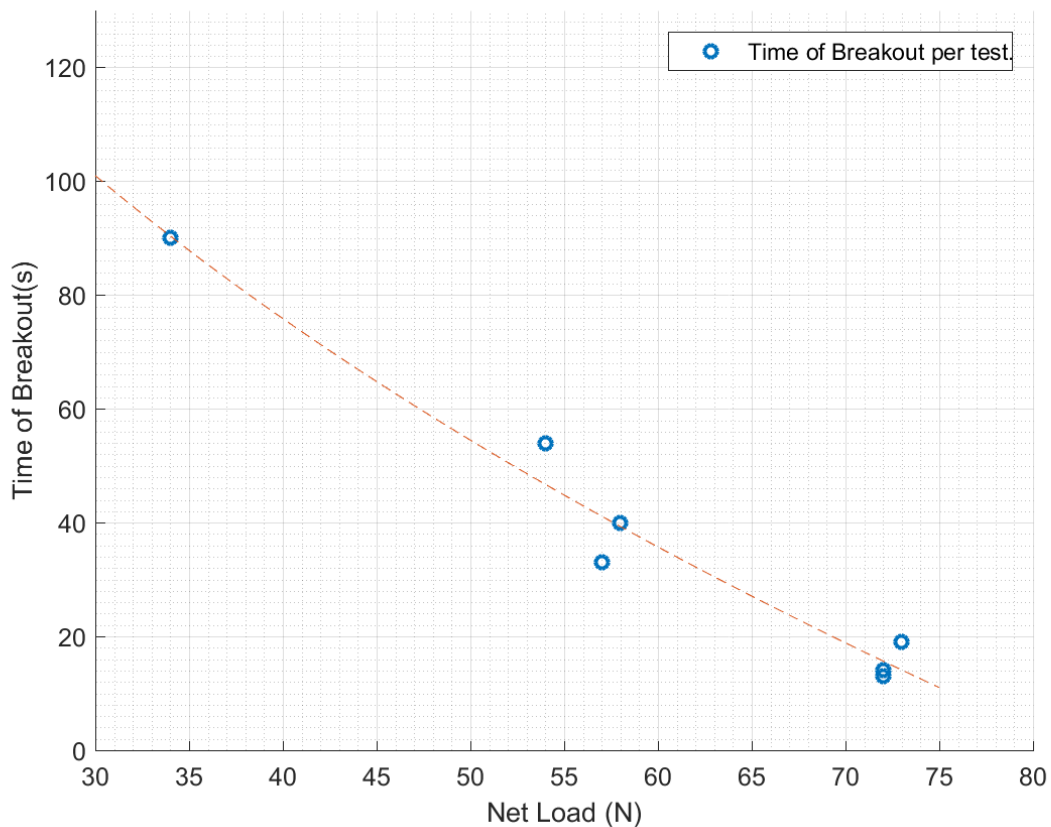


Figure 5.2 – The time of breakout for the Geba sand. Here the trend is going to zero, again it is only a trend line and it is not suspected to cross the Net load axis.

#### 5.2.4 Conclusion

From analyzing the breakout time of the 2-Dimensional plate it can be concluded that the breakout time does not scale linearly with the force. For the Silverbond sand an increase of around 25N decreases the breakout time by almost a factor 2, further increase of the same load gives a marginal decrease in breakout time. For the Geba sand however the breakout time follows a more linear slope, see Figure 5.2

### 5.3 Mean Displacement

#### 5.3.1 Introduction

The mean displacement is defined as the displacement the plate travels before breakout. This displacement can easily be extracted from the test data as the displacement follows a relatively horizontal line before breakout, after breakout the plate accelerates fast so an increasing slope can be spotted in the line of displacement. Again, the displacement is an average value over the different tests under same conditions.

#### 5.3.2 Silverbond 51 $\mu$ m Sand

In Figure 5.3 the mean displacement for the different loads is plotted. As can be observed the mean displacement does have a quite constant trend. They are all located around the 2 millimeters of

displacement needed before breakout. Notice that the loads are the imposed loads on the structure, not the net loads

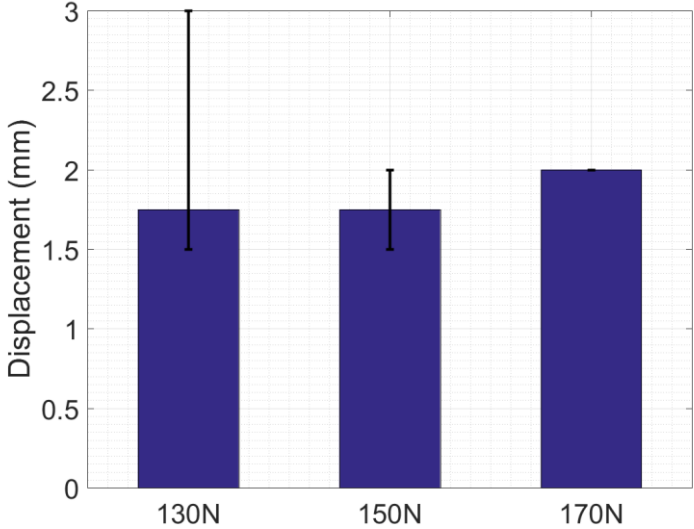


Figure 5.3 - The mean displacement of for the tests performed with the Silverbond sand.

### 5.3.3 Geba 125µm Sand

For the Geba sand the mean displacement has some more variation, the displacement for the 90 Newton load is twice the displacement than that of the 130 Newton load.

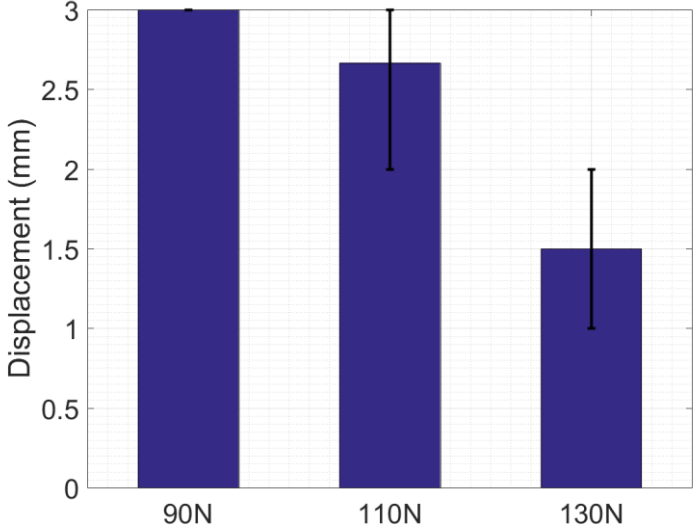


Figure 5.4 - The mean displacement of for the tests performed with the Geba sand.

### 5.3.4 Conclusions

The mean displacements of both the Silverbond and the Geba sand are all of the same order. The difference between the points is small, only the Geba sand had some deviation. What can be concluded is that this displacement is needed before breakout can happen, the displacement is

related to a certain amount of water needed before breakout can occur. The differences in the mean displacement are small between the two sand, therefore nothing can be concluded about this.

## 5.4 Mean Pressures

### 5.4.1 Introduction

The mean under pressures are the pressures derived from results measured by DP1, DP2 and DP3. This means that the mean under pressures are the peak under pressures found in the center line of the plate, see Chapter 4. The under pressures are corrected for offset values as mentioned before. Together with the measured under pressures the expected under pressures are shown. These are the peak under pressured derived from the imposed load by dividing the load by the surface of the plate.

### 5.4.2 Results

A good verification of the readings of the DP sensors is to compare the measured pressure with the load. After all the pressure underneath the plate should be equal to the load. In other words, there should be an equilibrium if the setup is static. The mean plate pressure is derived by dividing the load over the surface of the plate, this means that the mean plate pressure is a mean pressure over the plate. For the three different loads the pressure is averaged and compared to the mean plate pressure. The result for the Silverbond sand is shown in Figure 5.5, the Geba sand results are shown in Figure 5.6

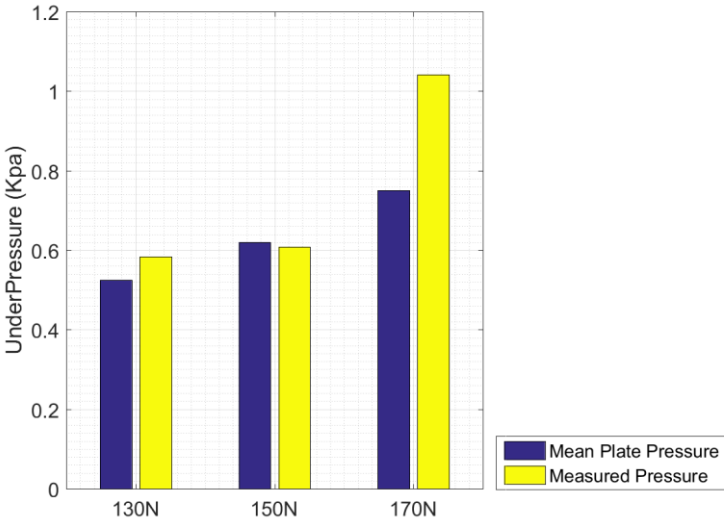


Figure 5.5 – The mean plate pressure versus the measured pressure for the Silverbond sand. Especially for the 124 Newton load the difference is big.

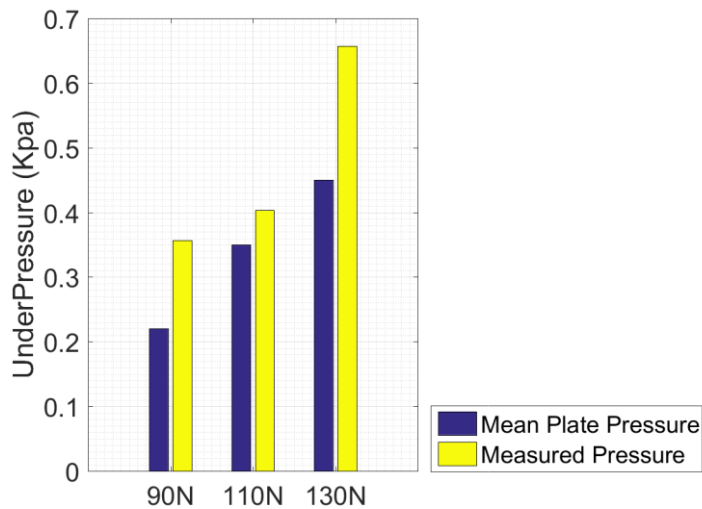


Figure 5.6 The mean plate pressure versus the measured pressure for the Geba sand. Here the differences occur with almost every test.

As can be seen there is a difference in measured pressure and the expected plate pressure. To get some better understanding of what is happening all data points are plotted and the measured pressure is plotted against the mean plate load. The plot in Figure 5.7 shows the mean plate pressure versus the measured pressure. However, the measured points do not represent the mean pressure but show the local pressure. The trend shows that the measured pressure is for most points higher than mean plate pressure which is to be expected as the flow lines are longer.

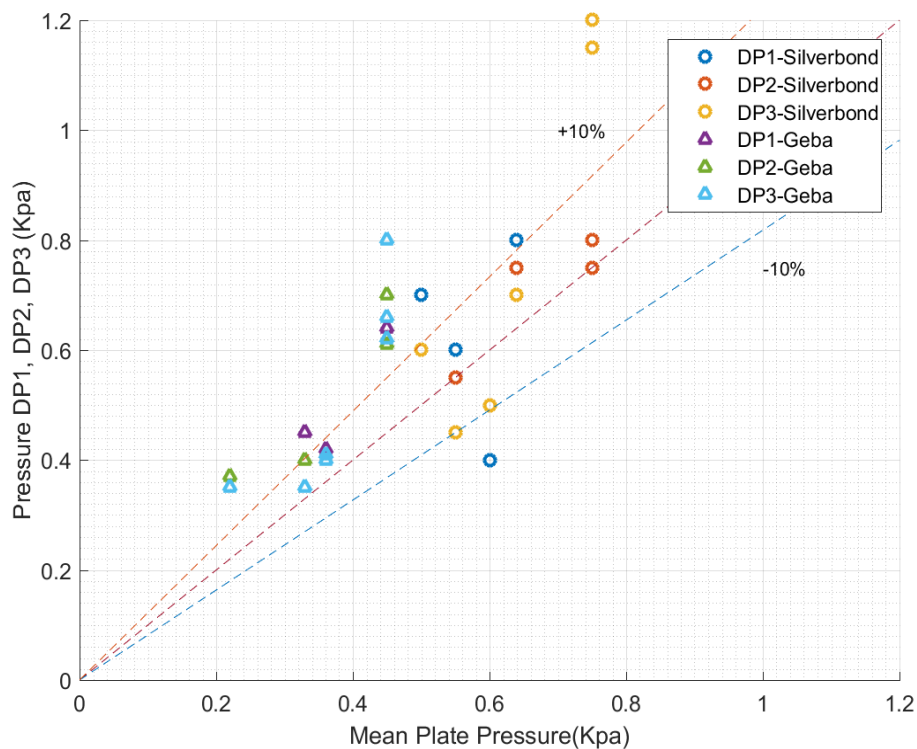


Figure 5.7 – The Measured Pressure versus the mean plate Pressure.

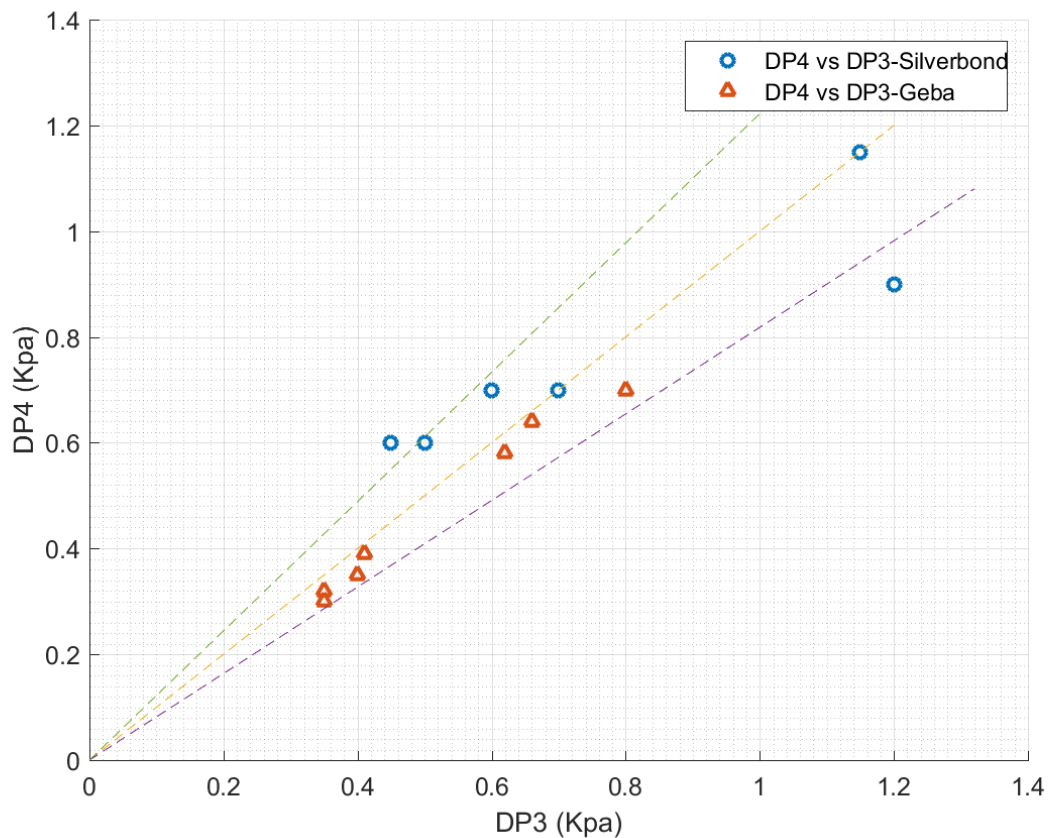


Figure 5.8 – The results of DP4 versus the mean plate pressure, DP4 carries the information about the pressure profile under the plate.

A reason for this is that one only measures at one point and the real pressure profile underneath the plate is not homogeneous as with the mean plate pressure. At the edge of the plate a strong pressure gradient is present, as the pressure at the edge is zero. Therefore, the pressure in the middle is obviously higher than the mean pressure.

The first three DP sensors are all located in one line. DP sensor 4 is located more to the edge of the plate and therefore has some more information. In Figure 5.8 the results of DP4 are plotted against the mean plate pressure. What can be seen is that they mostly fall within the 10% margin. This means that they are roughly equal. Thus, at the location of DP4 the pressure is almost the same as in the center of the plate. This says that the pressure profile is nonlinear and has steep slopes towards the edge of the plate. More cannot be concluded as more sensors are needed.

### 5.4.3 Conclusion

Taking a closer look at both sands the only thing of notice is that the absolute pressure of the Silverbond sand is higher than the pressure measured of the Geba sand. This makes sense as the Silverbond sand creates a higher under pressure than the Geba sand. This is of course the result of a different load range.

## 5.5 Comparing the Two Sands

To see if the difference in permeability between the Silverbond and Geba sands is visible a comparison between the two-different sand with the same imposed load has to be made. One test of

both sands is done with the same load, this load was measured by the load cell and due to friction in the pulleys has some spread. This spread can be observed in Figure 5.1 and Figure 5.2 respectively. From this spread the mean values had been calculated. What can be observed in Figure 5.9 is that even if the load during the test in the Geba sand is lower the breakout time is roughly a factor 8 smaller in the Geba sand than the test in the Silverbond sand. Comparing this result with the two measured permeability values from paragraph 3.3.1 which gave roughly a factor 10 the result seems plausible.

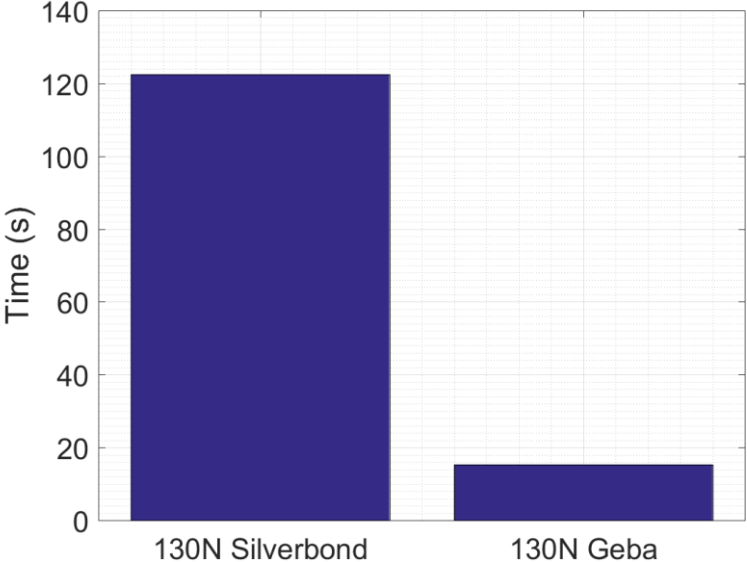


Figure 5.9 – The differences in breakout for the different sands

### 5.6 Conclusions

The 2-Dimensional test setup was not easy to work with, despite that fact the results do not disappoint. The pressure development can partly be reconstructed and for the time of breakout a nice trend between the 2-different sand can be spotted according to the literature (Lee, 1973).

## 6 3 Dimensional Results

The tests to be performed with the 3-Dimensional plate are in basis the same as with the 2-Dimensional plate. The biggest difference is that the plate now is not sealed off against 2 sides making it a 3-Dimensional problem. Also, there is less room for DP sensor connections. The plate has connections for up to three DP sensors. These are distributed across the plate according to Figure 3.3. The sand types used to build up the sand bed were the Silverbond and Geba sand mentioned before. The magnitude of the different loads that were applied on the plate are according to Table 3.2. For the Silverbond sand four different tests have been performed. For the Geba sand again 3 tests. This Chapter will show the results of the 3-Dimensional tests.

### 6.1 Expectations

Again, for the 3-dimensional model some expectations raised before the testing started.

- Breakout time is directly related to the permeability of the sand. The permeability of the sand is linked to the  $D_{15}$  quadratic (Den Adel, 1989); this holds that if the grain size doubles the permeability becomes 4 times as big. As the permeability increases roughly with a factor four it was estimated that the breakout time also decreases roughly a factor four
- The model outcome of the 3-Dimensional model has, as mentioned before, a nonlinear behavior. Due to the assumptions, the pressure development is evened out in the middle. As with the 2 Dimensional plate the pressure towards the edge of the plate is expected to be lower than the pressure in the center of the plate, the question is of the DP2 and DP3 sensor location is far enough from the center of the plate to measure a decrease in pressure.
- The average time of breakout is supposed to decrease as the load increases.

### 6.2 Mean time of breakout

For the mean time of breakout, the principle is the same as with the 2-Dimensional plate. All the tests are plotted against the load. With the help of a dashed line a trend can be visualized.

#### 6.2.1 Silverbond 51 $\mu$ m Sand

The Silverbond sand has been test, as mentioned, with four different loads. What can be seen is that the time of breakout drop hard as the load increases, see Figure 6.1. Notice again that the loads plotted are the net loads under the plate.

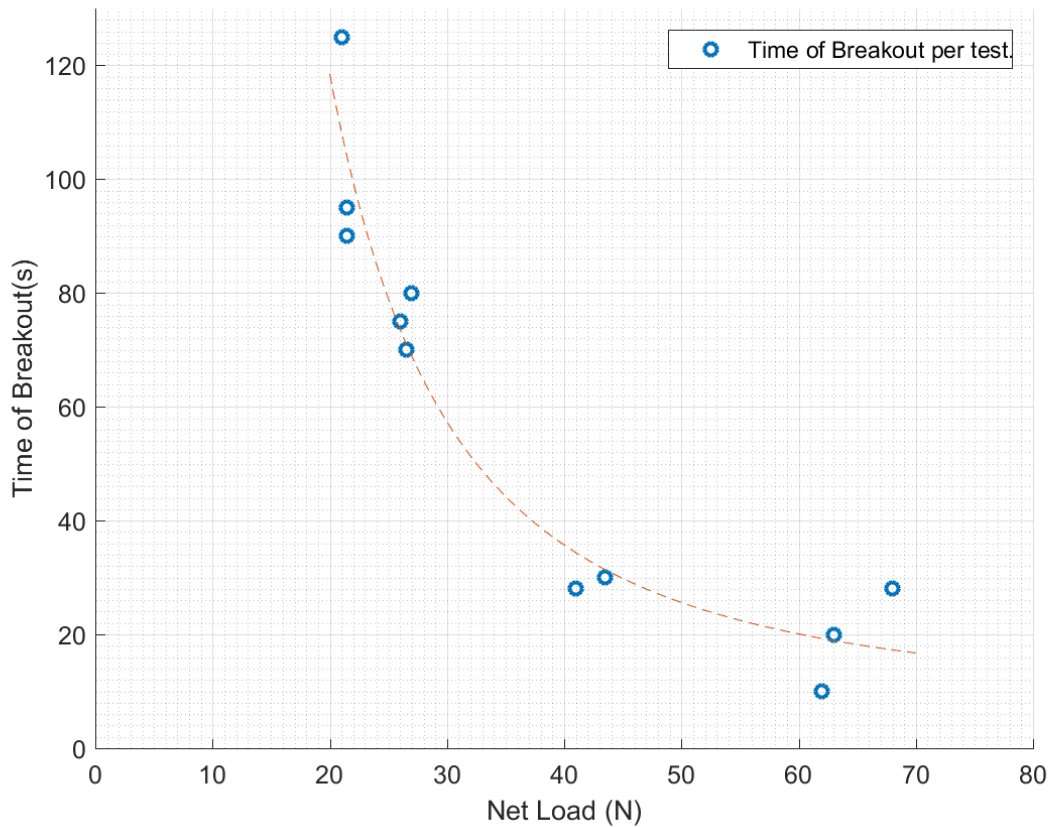


Figure 6.1 – The mean time of breakout for the Silverbond sand, notice the descending trend.

### 6.2.2 Geba 125 $\mu$ m Sand

As for the Geba sand the time of breakout was hard to determine for the bigger loads. The sand is a lot more permeable. In Figure 6.2 it can be seen that at the 2 highest net loads the breakout is almost immediate after applying the load. This fast breakout is directly linked to the large permeability of the sand.

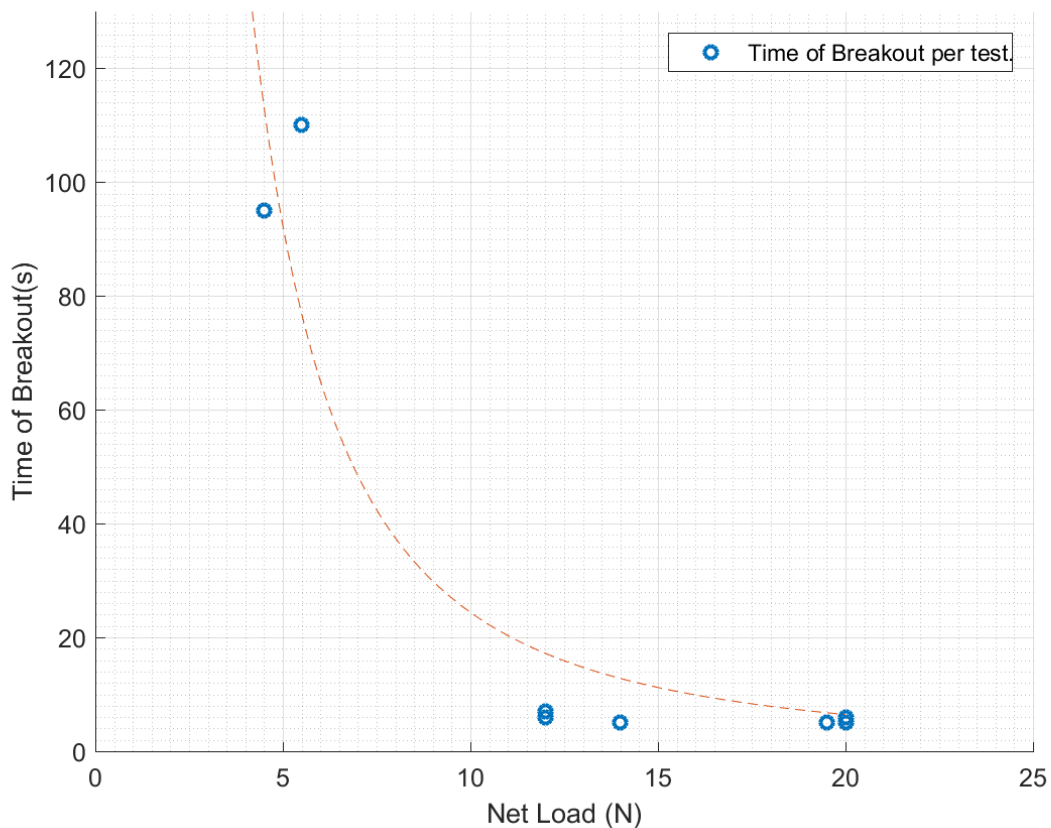


Figure 6.2 – The mean time of breakout for the Geba sand, notice that the difference between the 5 Newton load and the 13N load is large.

### 6.2.3 Conclusions

What can be concluded over the breakout time for the Silverbond sand is that as the load increases the breakout time decreases following a nice slope. Enough tests were performed to see the trend which is plotted in Figure 6.1. For the Geba sand the results are more difficult to read. What probably happened is that the scale of the applied weights was too large leading to test results at the boundaries of the breakout time. When a load of 50 Newton is applied, a net load of 5 newton in the graph, the mean breakout time is just above the 100 seconds. Increasing the net load with 10 Newtons the breakout time is already under the 10 seconds. This means that for the larger load the breakout time is more dominated by the inertia of the setup than the under pressures under the plate. A more refined load scale during the testing had been of better use. However, if one plots the breakout time the same behavior as with the Silverbond sand can be spotted, see Figure 6.2

## 6.3 Mean Displacement

The mean displacement of the 3-Dimensional plate is defined in the same way as the mean displacement for the 2-Dimensional plate.

### 6.3.1 Silverbond 51µm Sand

For the Silverbond sand the mean displacements are shown in Figure 6.3. The displacements before breakout are all in the order of 2-2.5 millimeters, around 400 particle diameters. A descending trend can be observed however nothing can be concluded about this trend.

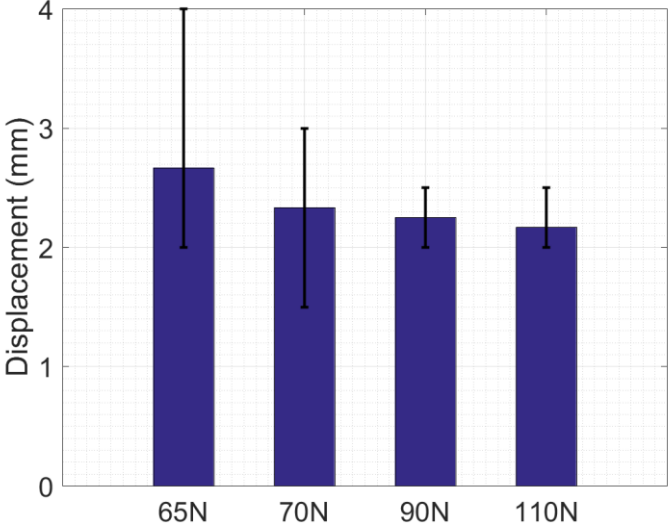


Figure 6.3 - The mean displacement of for the tests performed with the Silverbond sand.

### 6.3.2 Geba 125µm Sand

For the Geba sand the mean displacements are plotted in Figure 6.4. The mean displacements are all in the same order of around 2 millimeters before breakout.

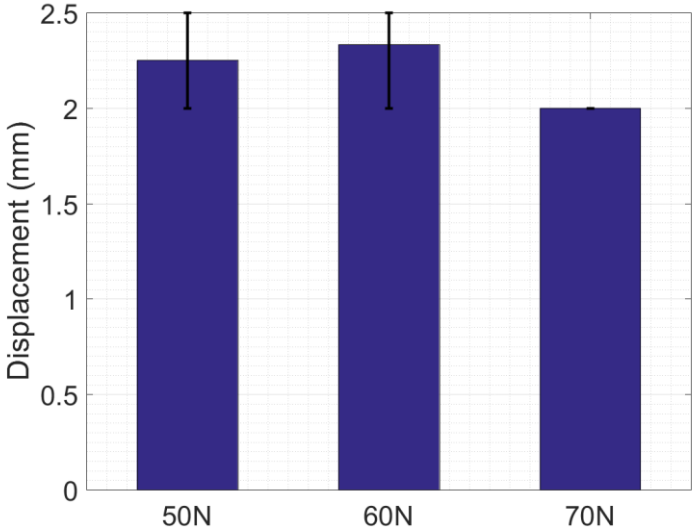


Figure 6.4 - The mean displacement of for the tests performed with the Geba sand.

### 6.3.3 Conclusions

For the Silverbond sand nothing can be concluded regarding the descending trend of the mean displacements. The differences in displacement between the different loads are so small that the displacement can be regarded as equal over the test. Again, no differences can be seen between

both grain sizes. What can be said about the mean displacement is that it does not scale with the particle diameter.

## 6.4 Mean Pressure

### 6.4.1 Introduction

The mean pressure of the plate is the mean pressure in the center of that plate and derived from the result of DP1. The difference with the 2-Dimensional plate is that now only one sensor can be located in the center. DP2 and DP3 are located on the same distance at two sides of the plate. Therefore, the result of these 2 sensors is averaged in the plots below. Again, the mean plate pressure is calculated according to the imposed load.

### 6.4.2 Results

For the Silverbond sand the mean pressure of DP1 versus the mean plate pressure is shown in Figure 6.5. What can be observed is that the measured central plate pressure is higher than the mean plate pressure.

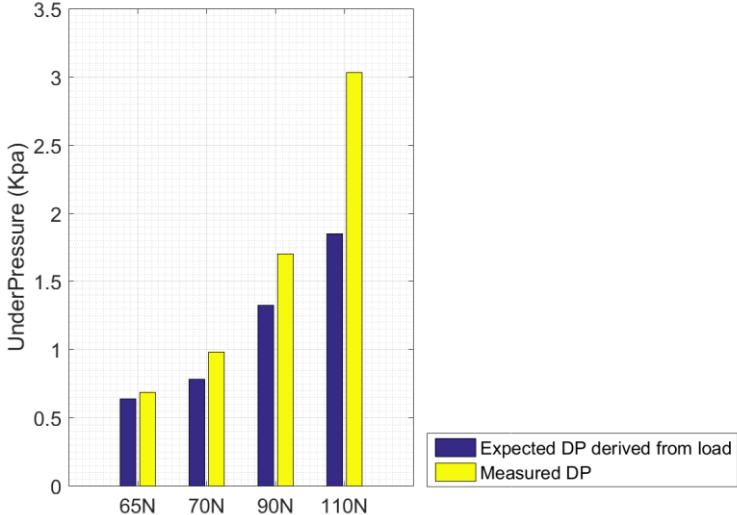


Figure 6.5 – The mean plate pressure versus the measured pressure from DP1 for the Silverbond sand. Notice again the difference in measured pressure and the mean plate pressure.

Comparing DP1 with the mean result of DP2 and DP3 gives results plotted in Figure 6.6. What can be seen is that the result of DP1 in the center is higher than the mean values of DP2 and DP3

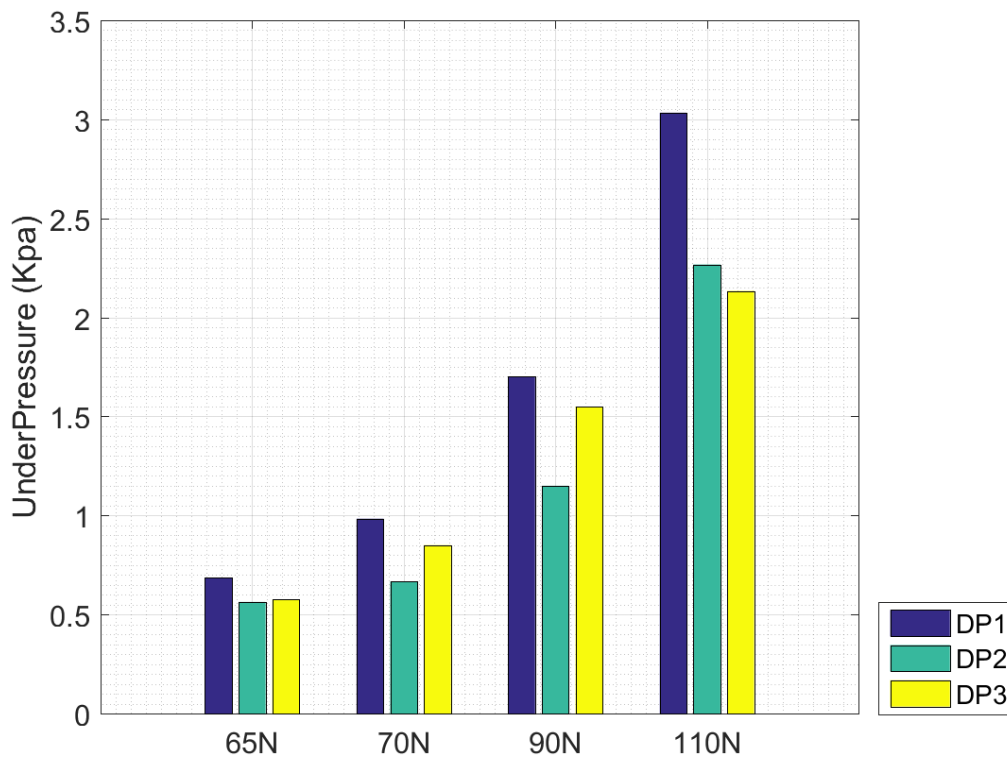


Figure 6.6 – For all the test the mean pressure of DP1 is higher than the other 2 sensors.

For the Geba sand the results are shown in Figure 6.7

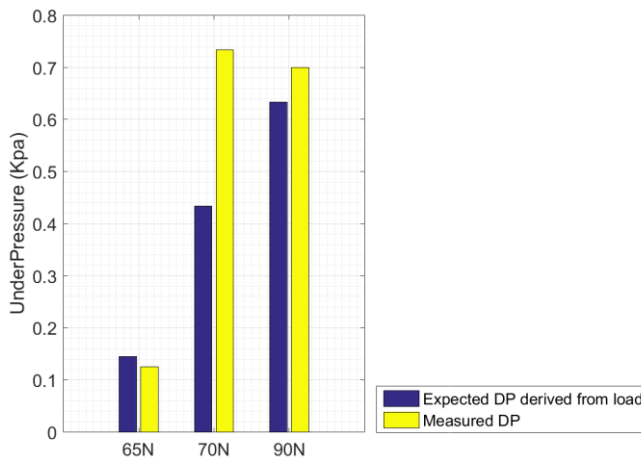


Figure 6.7 – The mean plate pressure versus the measured pressure for the Geba sand.

Again, comparing DP1 with the values of DP2 and DP3 for the Geba sand gives Figure 6.8.

Comparing the Pressures with the mean plate pressures results in Figure 6.9

What can be seen is that DP1 is still higher than DP2 and DP3, though it is not much. This is probably because the permeability of the Geba sand is higher compared to the Silverbond sand. Therefore, the pressure gradient is smaller.

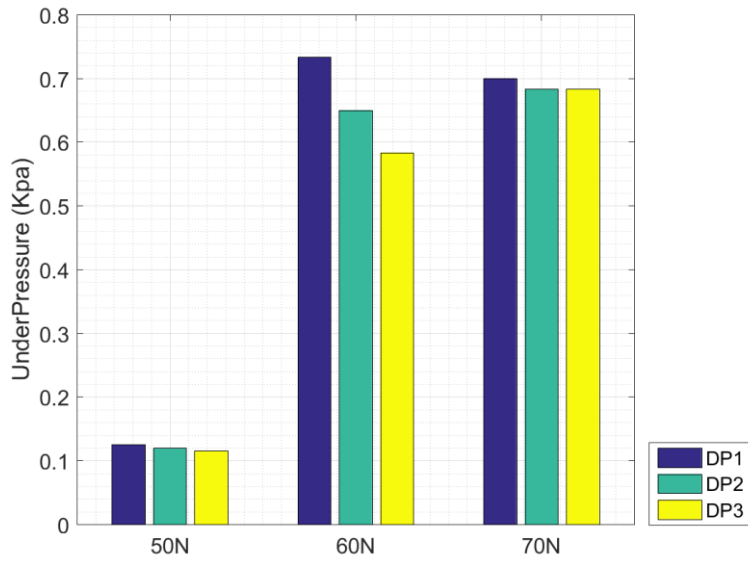


Figure 6.8 – For all the test the mean pressure of DP1 is higher than the other 2 sensors.

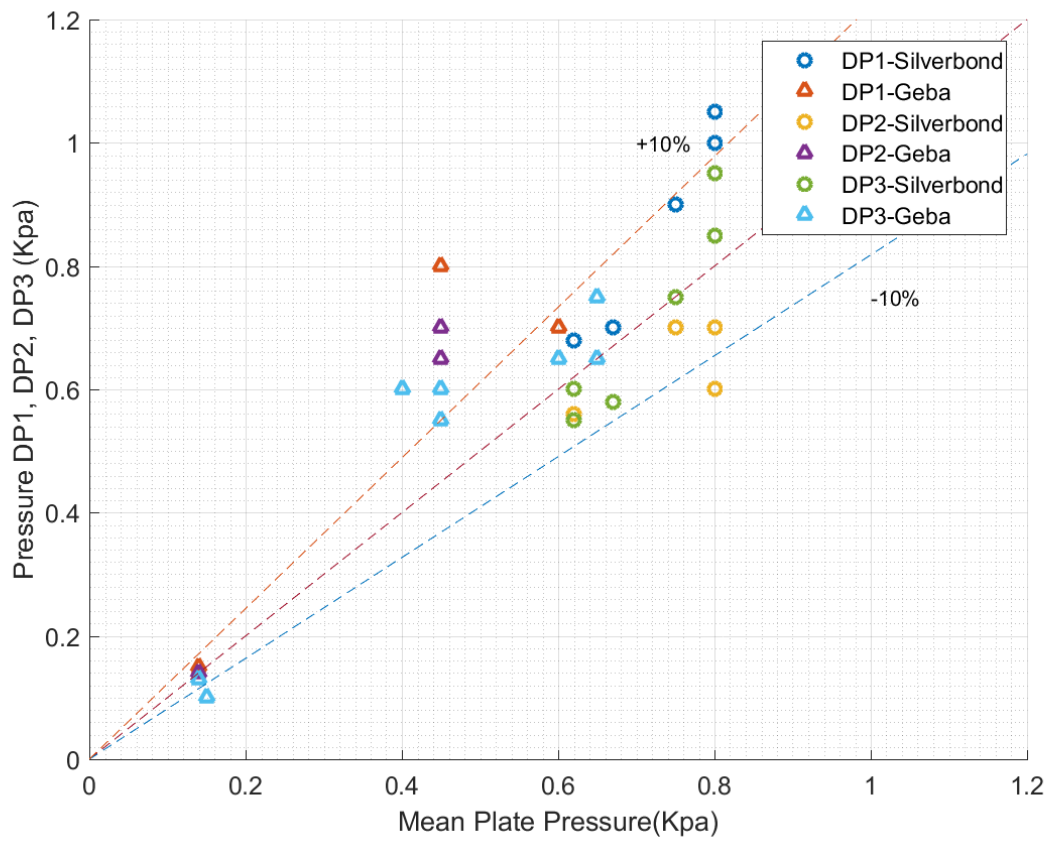


Figure 6.9 – Comparison between the mean plate pressures and the measured pressures.

### 6.4.3 Conclusions

What can be seen is that for the Silverbond sand the results of DP1 are quite a bit higher than the results of the DP2 and DP3 sensors. This makes sense and is a good indication of the pressure profile. To calculate the pressure profile exact more sensors are probably needed. For the Geba sand the results are less different indicating a smoothed pressure profile in the center of the plate. As the packing is different with the Geba sand, leading to differences in the permeability this is possible as the pressure gradient is smaller.

### 6.5 Comparing the Two Sands.

When comparing the Silverbond and the Geba sands for differences in the mean breakout time as with the 2-Dimensional test, the breakout time for the same loads has to be observed. The mean values of the spread in Figure 6.1 and Figure 6.2 have been calculated. Plotting this breakout time for the same loads gives Figure 6.10. What can be observed is that the mean breakout time for the Silverbond sand is 75 seconds, the mean breakout time for the Geba sand is around 5 seconds. This gives roughly a factor 15.

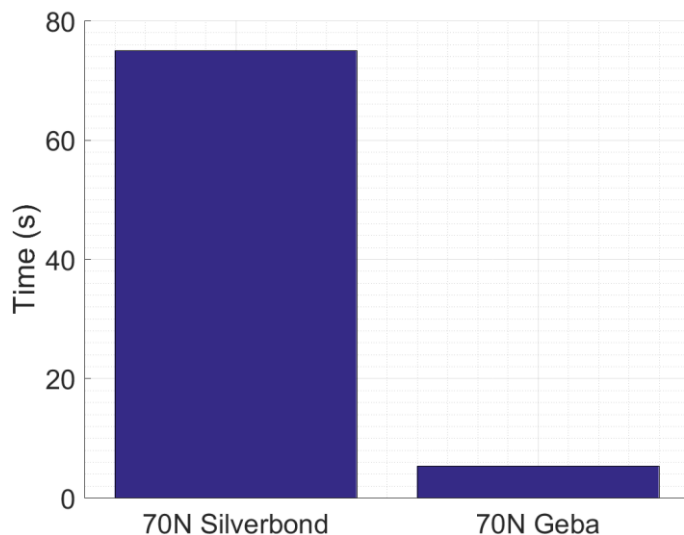


Figure 6.10 – Time of breakout for the 2 sands. Notice the huge difference.

As for comparing the breakout times for the same load and different sands a remark has to be made. Forces slightly larger than the submerged weight plus lifting frame may cause an upward displacement but not enough for breakout. As the force increases the breakout time decreases to almost zero (Liu, 1969). What probably is happening is that the load imposed on the plate is too large for the 3-Dimensional setup in the Geba sand. As can be seen the breakout time of the 70 Newton load is almost the same as the 90 Newton load. An even bigger load will probably give the same time of breakout. The breakout is not dominated anymore by the parameters of the soil but more by the inertia of the setup. For future testing, more research can be done in the area between the 70 Newton and the 90 Newton load.

## 6.6 Consolidation

In earlier research a lot of testing was done regarding the effect if pre-loading a structure has effect on the breakout time. In fact, pre-loading the structure will lead to the consolidation of the soil. The pre-load will load the soil for a certain amount of time, after removal the breakout time is increased with respect to a soil which was not pre-loaded.

For testing the effect of consolidation, the 3-dimensional plate is placed onto a smooth sand bed and loaded for 5 hours with a 20-kg weight using specially designed frame. The setup can be seen in Figure 6.11. Note that this is not the correct Silverbond sand but the Geba instead. This is done due to visibility issued with the Silverbond sand.



*Figure 6.11 – Underwater pre-loading*

Every test has been performed twice, the test with pre-load and the test without pre-load. This gives a total of 4 tests.

The results for the pre-load test are plotted in Figure 6.12 and Figure 6.13 respectively. What can be observed is that the breakout time for both test is practically the same. Actually, the difference is smaller than the mutual difference of normal tests. What can be concluded is that the difference in breakout time is so small that Pre-loading in sand does not make a difference in breakout time. For clay this difference is noticeable. Pre-loading clay gives more plastic deformations. If these deformations will be present in sand it will be in the first couple of minutes, pre-loading for a longer time does not make any difference.

A recommendation for further investigation could be to test on a loosened sand bed instead of a vibrated bed. By vibrating the sand all the stresses are dissipated, looser sand reacts stronger on consolidation. Problem is that testing in loose sand are not easy to reproduce.

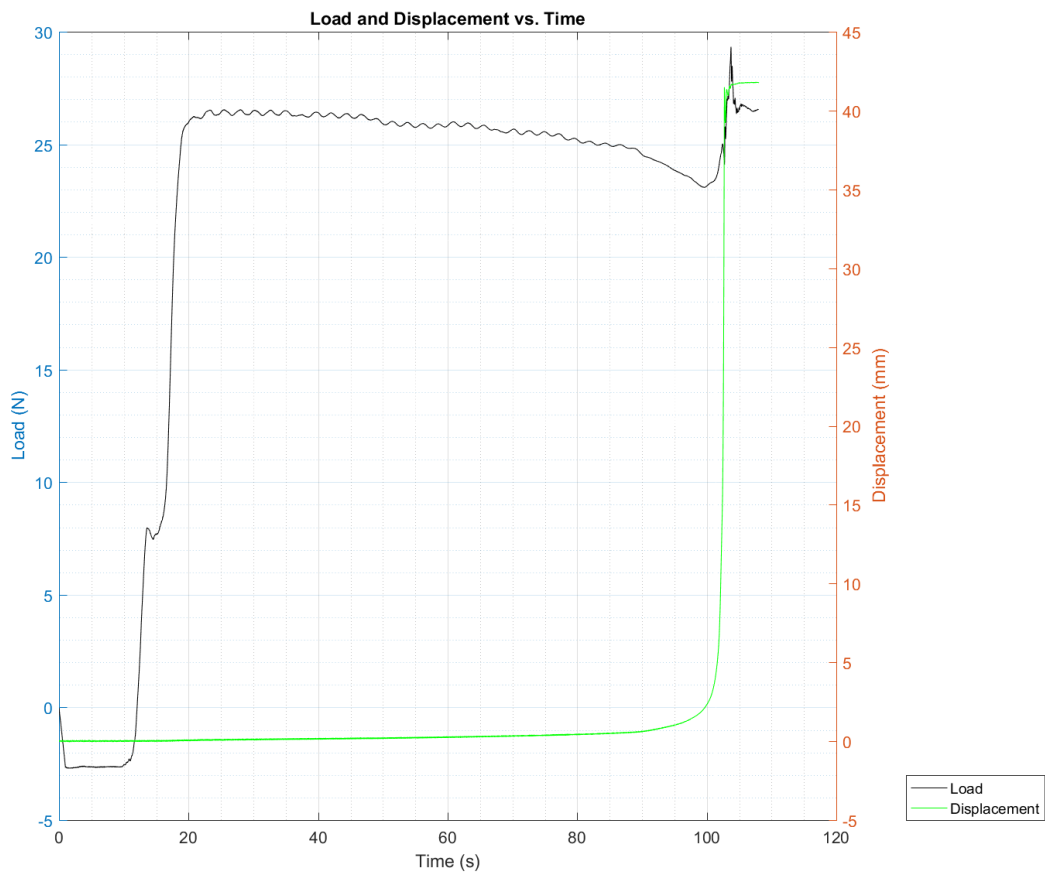


Figure 6.12 – Consolidation test 1

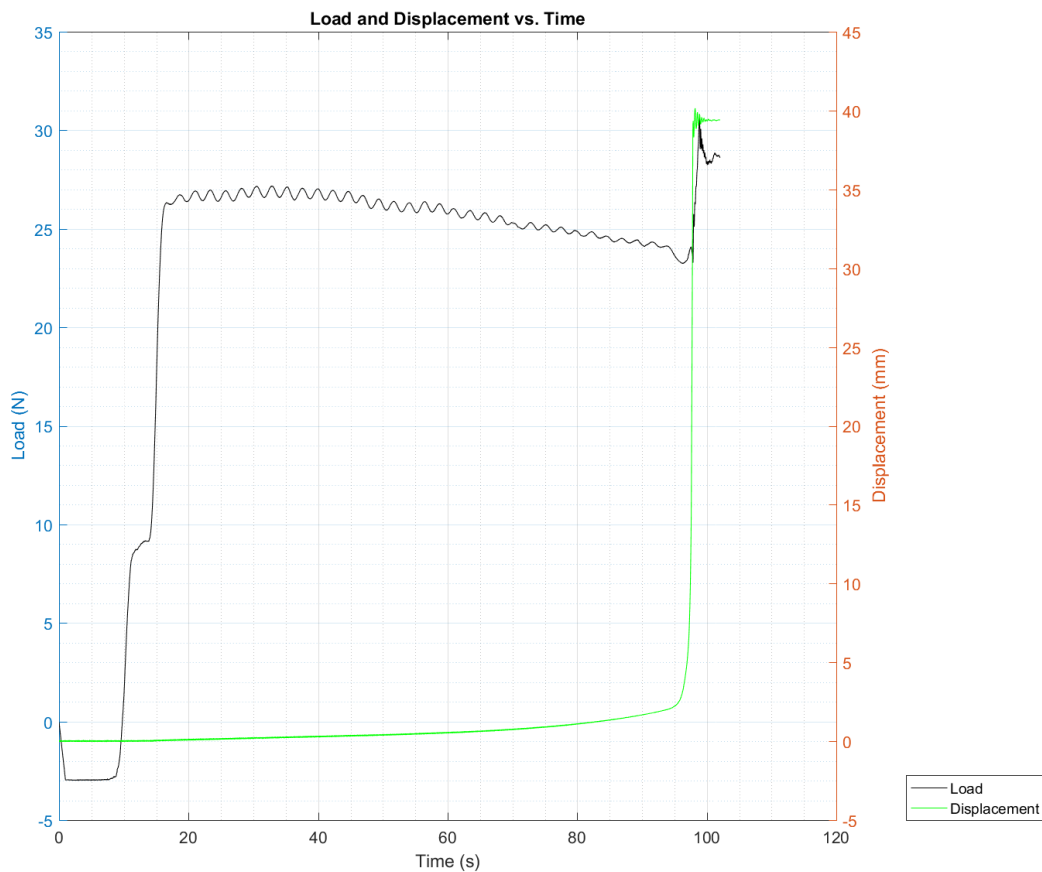


Figure 6.13 – Consolidation test 2

### 6.7 Conclusion

Concluding from the results the 3-Dimensional test can be seen as a success. The test setup functioned well with only the pressure registration as a difficult part. The pressure development can be simulated but more sensors are needed regarding this subject. As for the mean time of breakout between the two sand smaller load steps should be tested for the 3-dimensional setup in the Geba sand. These same loads should be tested in the Silverbond sand to expose the trend. What can be concluded is that the time of breakout follow a nonlinear trend as the load increases.

## 7 Analytical Model

As mentioned before in chapter 3 one can see the Parallel Resistor method is intended for use on 2D cases of sand cutting. Lifting structures, or plates, from the sea bottom is a different case. The model has to be adapted to this case to give a good result. This chapter will explain how the model is adapted for both the 2-Dimensional and the 3-Dimensional case.

### 7.1 2D Analytical Model

First some insight in the situation. The 2D case is, as earlier explained, modelled as a plate on a sand bed. The situation is explained according to Figure 7.1

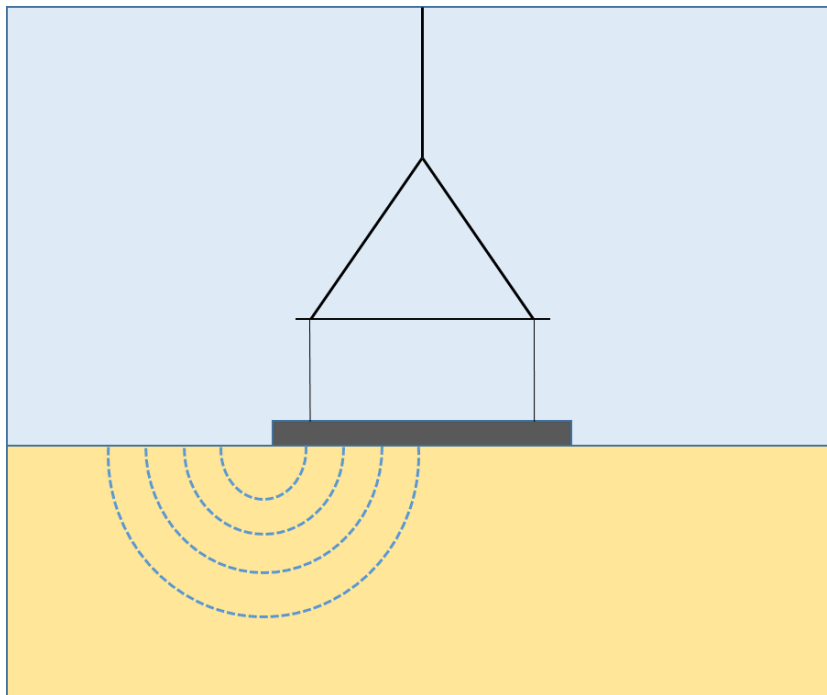


Figure 7.1 – Flow lines underneath the plate

As can be seen the situation is similar to the Miedema setup only no cutting takes place. In this case the force exerted on the lifting frame will try to pull out the plate and by doing so creating an under pressure under the plate. For this under pressure to exist water needs to flow to the area under the plate surface. Assuming circular flow lines, one can make a similar approach as Miedema did for the cutting case. The difference is that now only flow lines from one side are used making the 2D case relatively simple. This is done because if multiple flow lines were used the crossing of the flow lines would have to be analyzed. Mathematically it can be done but the question is if it makes any difference for the breakout force predicted by the model as the influence of this effect can be neglected as the model will predict a force in the same order as the test data. If one want to know the force precisely a finite element model should be used. Analogue to the earlier equations the Law of Darcy is used:

$$q = k * i = k * \frac{\Delta p}{\rho_w * g * \Delta s} \quad (7.1)$$

In this case the change in volume is caused by dilatation and therefore water has to flow in the increased pore volume. Therefore, the total specific flow rate comes from the velocity at which the plate is lifted. So, the specific flow rate is defined as:

$$q = \frac{dz}{dt} \quad (7.2)$$

Where:

$dz$  = Height in vertical direction

$dt$  = time

By combining equation 7.1 and 7.2 the following relation is found:

$$q = \frac{dz}{dt} = k * \frac{\Delta p}{\rho_w * g * \Delta s} \quad (7.3)$$

So, the equation for the pressure difference is found as:

$$\Delta p = \frac{q * \rho_w * g * \Delta s}{k} \quad (7.4)$$

The difference with the parallel resistor method is that the pressure difference is calculated only for half the plate, as the plate is symmetrical it is easy to calculate the force for the complete plate.

Assuming the flowlines are again halve circular they are calculated as following:

$$\Delta s = \pi * r \quad (7.5)$$

With the resistance defined as:

$$R = \frac{\Delta s}{k_i} \quad (7.6)$$

Substituting equation 7.6 in equation 7.4 gives:

$$\rho_w * g * \frac{dz}{dt} = \frac{\Delta p}{(R)} \quad (7.7)$$

Gives the final equation for the pressure difference in the 2D case:

$$\Delta p = \rho_w * g * \frac{dz}{dt} * R \quad (7.8)$$

Integrating over half the plate gives the average pressure:

$$p = \frac{1}{n} \sum_{i=0}^n \Delta p_i \quad (7.9)$$

The average pressure times the surface of the plate now gives the force needed to lift the plate given a certain speed.

## 7.2 3D Analytical Model

The 3D model is based on the same approach. Now a round plate is lifted from the sand bed. This situation cannot be modelled in a 2D model. The problem lies with the form of the plate.

Cutting the plate in half gives the same situation, see Figure 7.1:

However, seen from above it is obvious that using flow lines gives a problem with the total flow. Given a fixed step size, the surface at the edge of the plate is bigger than the surface at the center of the plate. In other words, water from a location outside the plate with a bigger surface flows to a location on the plate with a smaller surface. In fact, this is a geometrical problem. To accommodate for this effect the plate is divided into pie slices. Now the pressure drop over the pie slice can be calculated using flow paths, the slice is divided using a fixed step size which determines the number of flow paths. The paths itself are divided into steps, see Figure 7.2

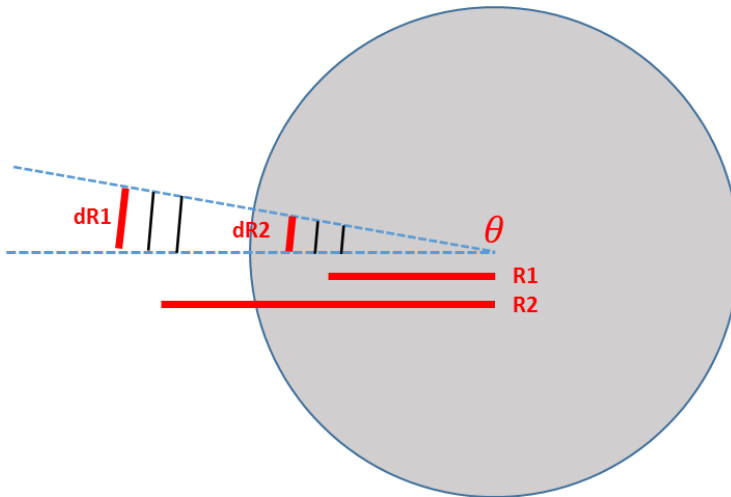


Figure 7.2 – The plate seen from above, now the pie slice model becomes clear.

The surfaces are radius dependent and can be calculated according to:

$$dL * dR \quad (7.10)$$

Where:

$dL$  = Number of flow paths pie slice

$dR$  = width

The width is defined as:

$$dR = 2 * r * \sin\left(\frac{\theta}{2}\right) \quad (7.11)$$

Where:

$r$  = radius

Dividing the flow path in a certain amount of steps the surface at each step can be calculated, see Figure 7.3.

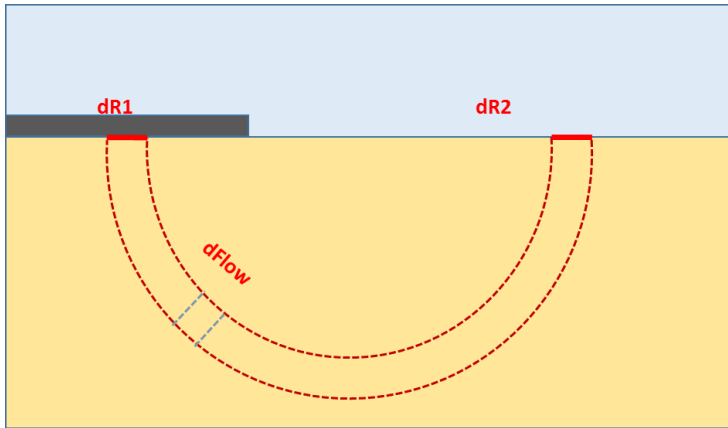


Figure 7.3 - Flow paths.

To calculate the total pressure drop over a flow path the pressure drop over 1 step is calculated and integrated afterwards. The volumetric flow rate right below the plate, at dR1 follows from the upward velocity of the plate which is known as input.

$$Q = Vp * S \quad (7.12)$$

Where:

$Vp$  = Upward velocity of the plate

$S$  = Surface located beneath the plate at dR1

Now the specific flow rate is known as function of the radius

$$q(r) = \frac{Q}{S(r)} \quad (7.12)$$

The pressure drop per step analogue to Darcy:

$$dp(r) = \frac{q(r) * \rho_w * g * ds}{k} \quad (7.13)$$

With:

$$ds = \frac{a}{n} \quad (7.14)$$

Where:

$a$  = arc length

$n$  = number of steps of the flow line

Integrating the pressure over the flow path gives the total pressure drop per flow path. Integrating over the pie slices gives the pressure drop per pie slice. Knowing the surface of a pie slice the force per slice and thus for the plate is known.

$$F = n_{slices} * dp_{slice} \tag{7.15}$$

Where:

- $n_{slices}$  = Number of slices
- $dp_{slice}$  = Pressure drop per slice

In the above scenario, it is assumed that the flow path distance on the plate is the same as outside the plate, in other words the distance is mirrored around the edge of the plate, see the blue path in Figure 7.4. This might not be the case; therefore, the flow path distance can be adjusted using a mirror factor. However, the surface of the flow path also changes, not only the length. The step size of the flow path becomes a variable. This makes sense because the surface outside the plate must be completely covered by the flow paths.

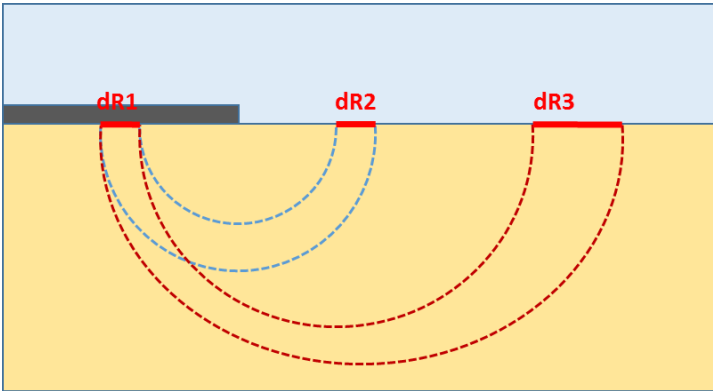


Figure 7.4 – The tuning factor of the flow paths.

It is assumed the during the lifting the plate will extract sand from the bottom, the maximum amount of sand is considered as an upper limit for the analytical model, Finn and Byrne (1972) state that very high suction can develop under embedded object during pullout. When such suction do develop, a general failure can occur. This general failure is set as the upper limit of the model. Initially this is set as the volume of half a sphere times the density of the soil. See Figure 7.5

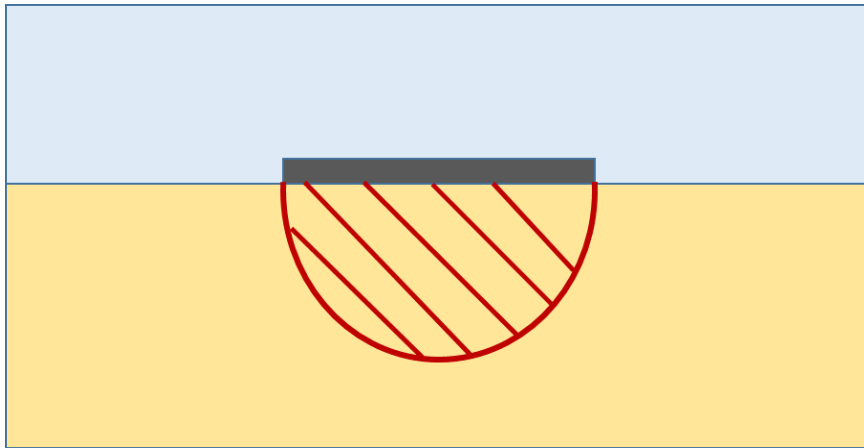


Figure 7.5 – The limitation of the model.

## 7.3 Expectations

### 7.3.1 2-Dimensional model

Both the 2-Dimensional and the 3-Dimensional model can simulate the pressure development under the plates.

The 2-Dimensional Analytical model is directly based on the cutting model of (Miedema, 2014). The plate is simplified in the test setup to force the situation to act like a 2-Dimensional model by closing of the 2 sides of the plate. The outcome of the pressure development of the 2-Dimensional analytical model therefore is linear, see Figure 7.6

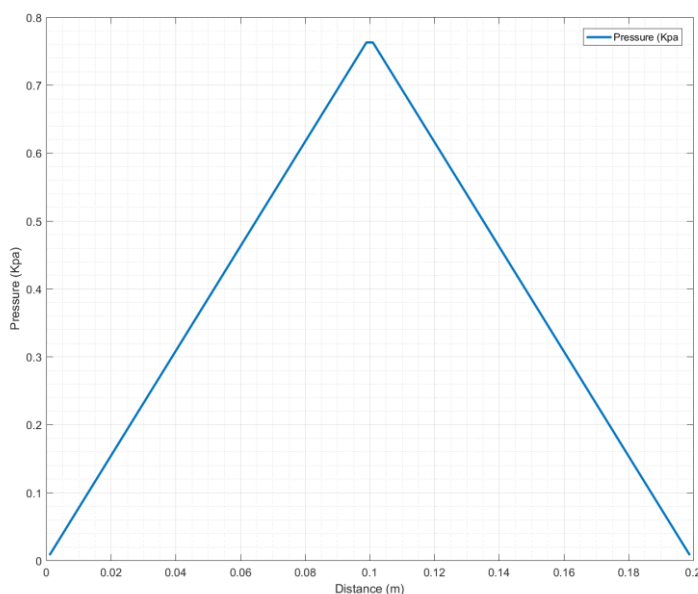


Figure 7.6 – Linear pressure development under the plate.

### 7.3.2 3-Dimensional Model

The 3-Dimensional model uses the pie slice method to accommodate for the effects occurring around the 3-Dimensional round plate. The pressure drop, which eventually gives an estimate for the lifting force, is strongly dependent on the length of the flow path and the surfaced of the flow path. At the

center of the plate the surface of the flow path is very small. This flow path gets its water supply from the largest area outside the circle. In other word, the 1 in the equation drops as it is divided by the surface of the flow line which increase as we move alongside the flow path away from the center. The  $D_s$  in the equation has its maximum for the flow line going to the center. The increase of the length of the flow line cannot match the decrease in surface area of the flow path and therefor in the pressure development under the plate according to the 3-Dimensional analytical model an optimum is present. This optimum, also visible in the force development, lies at about 40 percent from the plate edge, see Figure 7.7

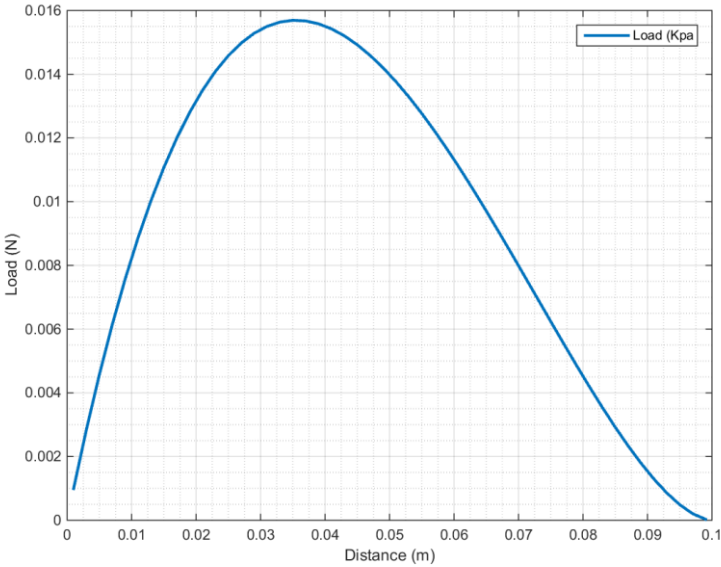


Figure 7.7 – The force development under half the plate.

Combining the development for the total plate gives the results shown in Figure 7.8

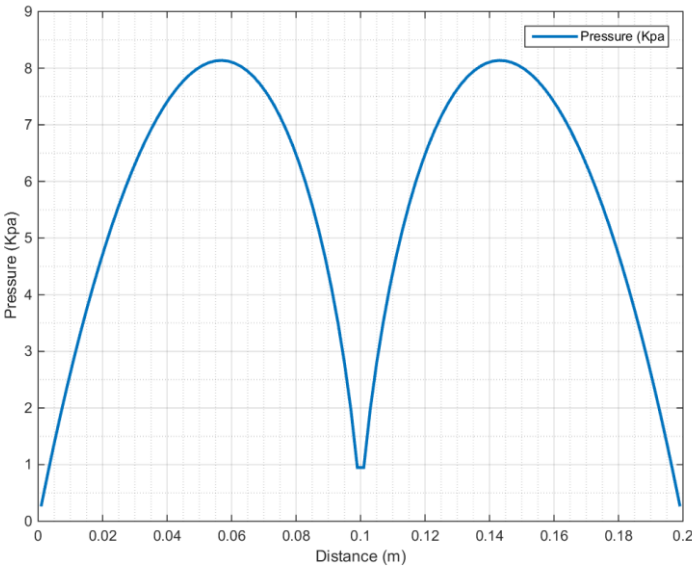


Figure 7.8 – The pressure development under the total plate

The question arises if this is realistic. Based on the measurements this phenomenon is not possible. What is happening?

At first suppose the plate is infinite long pulled at with a certain velocity assuming a stationary situation. Water has the tendency to flow from areas with high pressure to areas with a lower pressure. Flow of water alongside the bottom of the plate is not incorporated in the model.

The second point is that during the calculation there was assumed water in incompressible. In fact, water is for a small part compressible. In real the real situation the pressure will due to these 2 points be evened out. The pressure development will look more like that in Figure 7.9

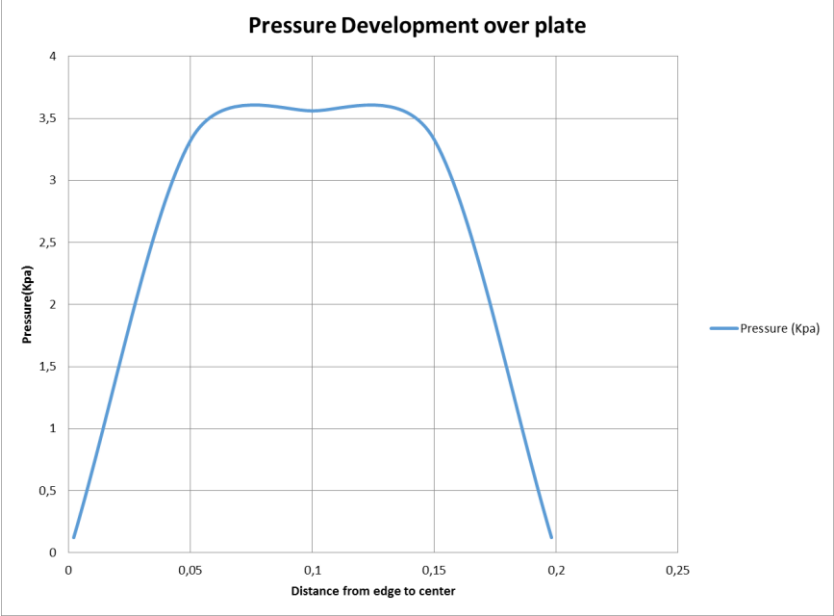


Figure 7.9 – Corrected pressure development under the plate.

# 8 Validation

## 8.1 Introduction

In this chapter the comparison between the model and the measurement data will be investigated, both for the 2-Dimensional model and the 3-Dimensional model. The models itself are explained in Chapter 7.

To validate the model, the force calculated by the model must compared with the test data. If, for example, the test data has a standard deviation from the model the model can be corrected for this. At the beginning of the comparison a certain permeability must be chosen, the velocity is derived from the test data. The point where the velocity is chosen is not obvious. The first approach is to take the mean velocity over the total breakout process.

As mentioned before in paragraph 3.3.1 the permeability of the sand was tested and found at  $5e-6$  m/s for the Silverbond sand and  $7e-5$  m/s for the Geba sand. This are the first input values for the permeability as they will result in the maximum force, no smaller permeability is possible in the sand bed

## 8.2 2-Dimensional Comparisons

For the 2-Dimensional model an input permeability is first chosen at  $5e-6$  m/s. combined with the different velocities from the tests the model gives a prediction for the force. As this (Net) force was also measured it can be compared with the model data. For the Silverbond sand his is done in Figure 8.1. As can be seen the model over estimates the force roughly by a factor 10.

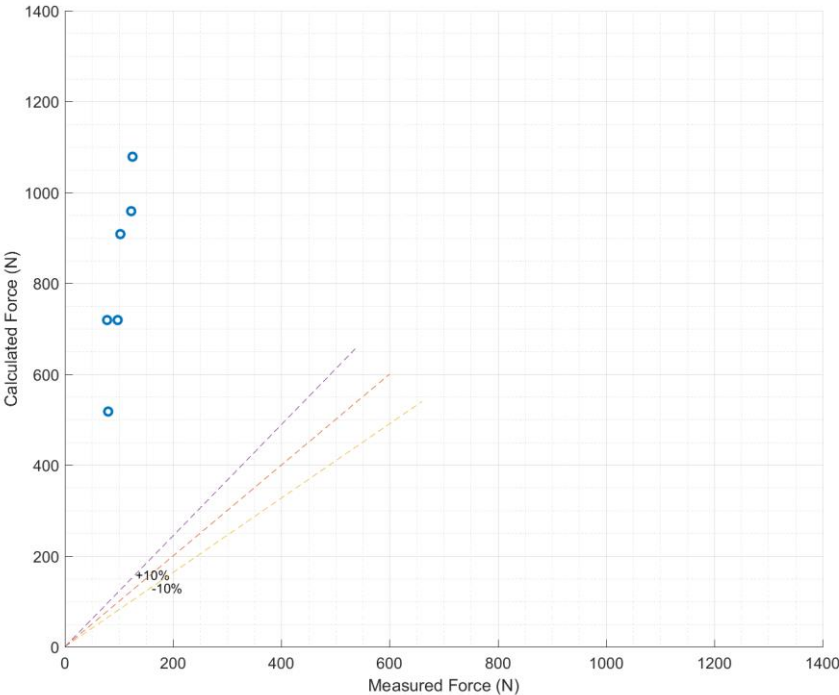


Figure 8.1 – 2D - Model comparison for the Silverbond sand, the trend is visible but the model over estimates.

For the Geba sand the permeability used was  $7e-5$  m/s. Using the velocities from the test data the model outcomes versus the test data can be seen in Figure 8.2. Again, the model over estimates.

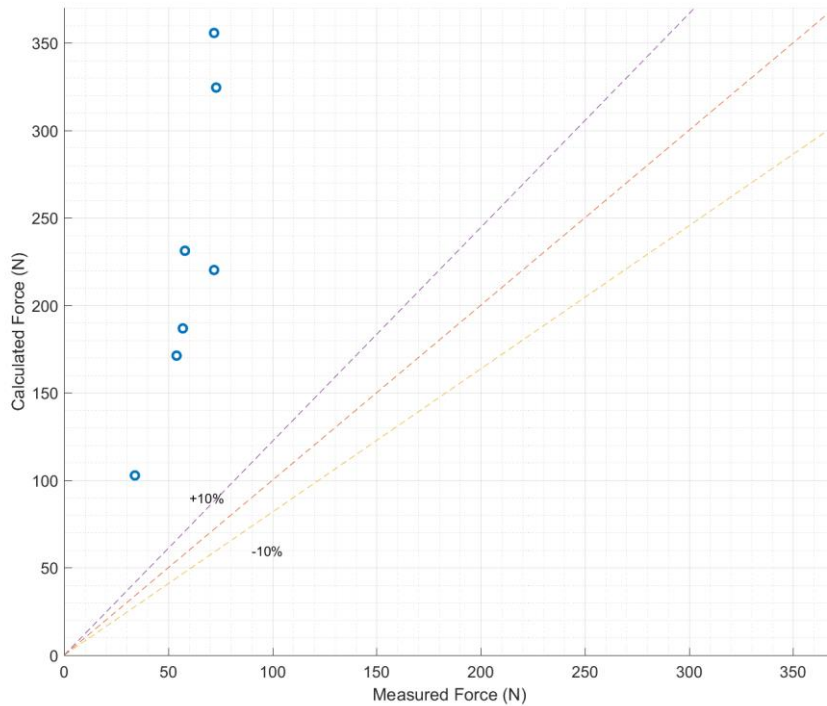


Figure 8.2 – First predictions of the model, a large over estimation.

Scaling back the permeability with a factor 10 is not realistic. The question arises if the right velocity was chosen. If the velocity is the mean velocity over the process it is assumed that the model assumptions are valid during the complete process, but are they?

An important observation of the tests is that after the test almost every time a large gap can be spotted in the sand bed underneath the plate. During the lifting process the sand bed starts to expand with the result that the permeability of the sand increases. The water flows with less resistance through the sand bed.

As an input parameter of the model a constant permeability is taken. If this permeability increases during the process the model will give an over estimation. So maybe the model is not valid during the complete process. To validate this the velocity is analyzed again, now only at the beginning of the process. This makes sense as the sand bed is thoroughly vibrated after every test to ensure maximum packing and thus, in the beginning of the lifting process, the assumptions of the model should be valid.

The velocity follows from the point where the load has reached its maximum, see Figure 8.3.

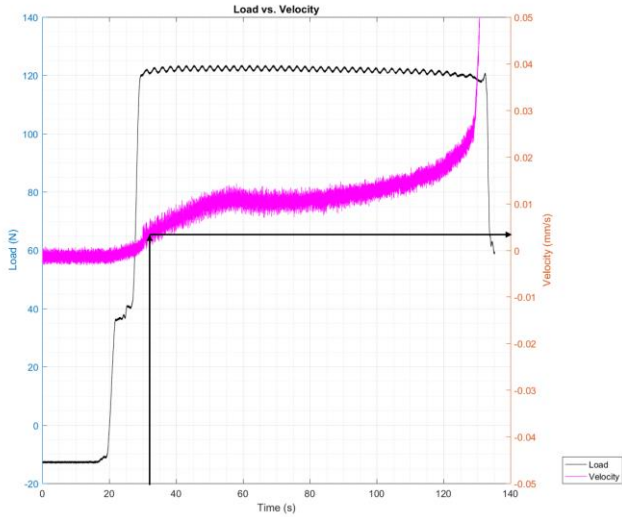


Figure 8.3 – The point where the velocity is derived from the test data.

Using the new velocities, the model predictions seem to give a much better fit to the measured data. Figure 8.4 gives the model predictions for the Silverbond sand. What can be seen is that, using the measured permeability from the laboratory, the model predictions are within the 10% margins. For the Geba sand a factor three has to be used to fit the model predictions with the test data, this can be seen in Figure 8.5

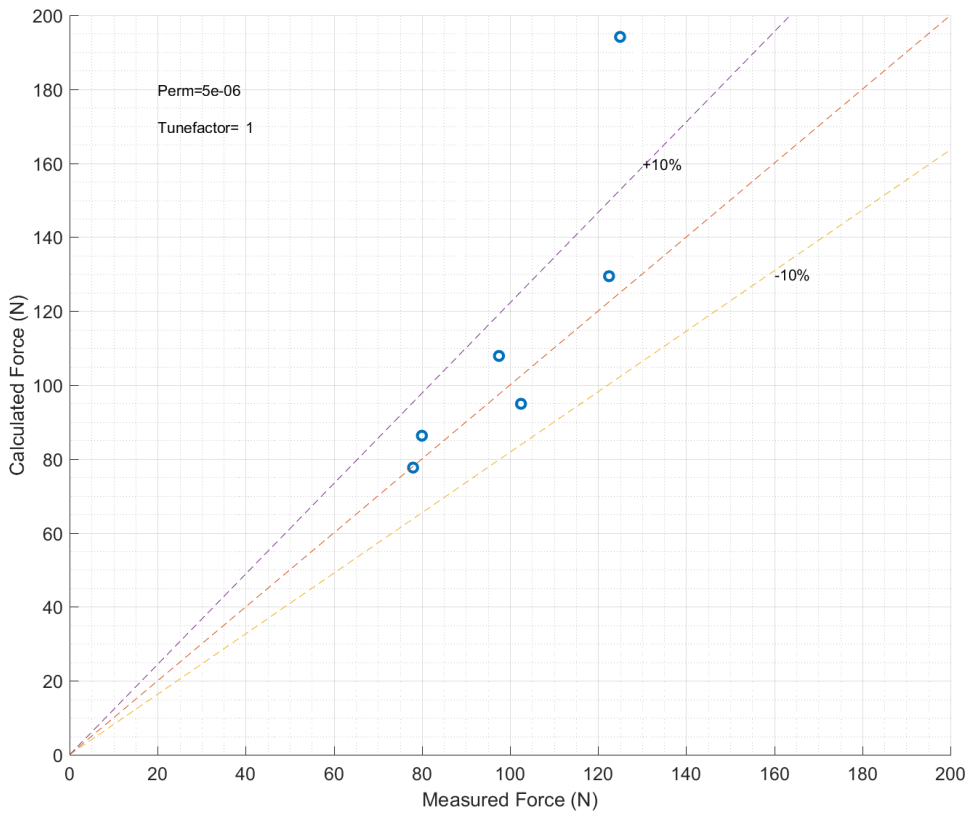


Figure 8.4 – The model versus the test data with the new velocities for the Silverbond sand.

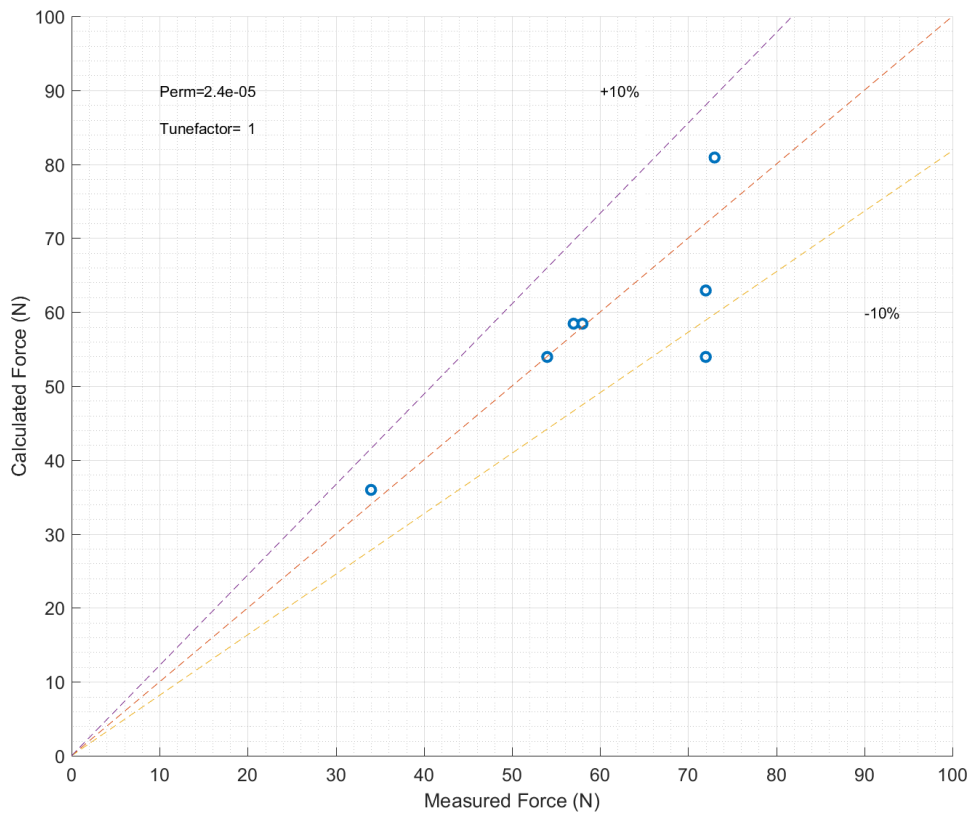


Figure 8.5 – The model versus the test date with the new velocities for the Geba sand.

Still, using a factor three for scaling the permeability is quite large. In the beginning, circular flow paths were assumed and they seem to work for predicting the force using the Silverbond sand. As the Geba sand has a larger porosity it is possible that the water travels a larger distance in the sand bed. To investigate this the tune factor was built into the model. Using a tuning factor of 2 and the initial measured permeability of the Geba sand gives Figure 8.6. What can be observed is that using longer flow path lengths in the model the fit, using the measured permeability and the new velocities, is quite good.

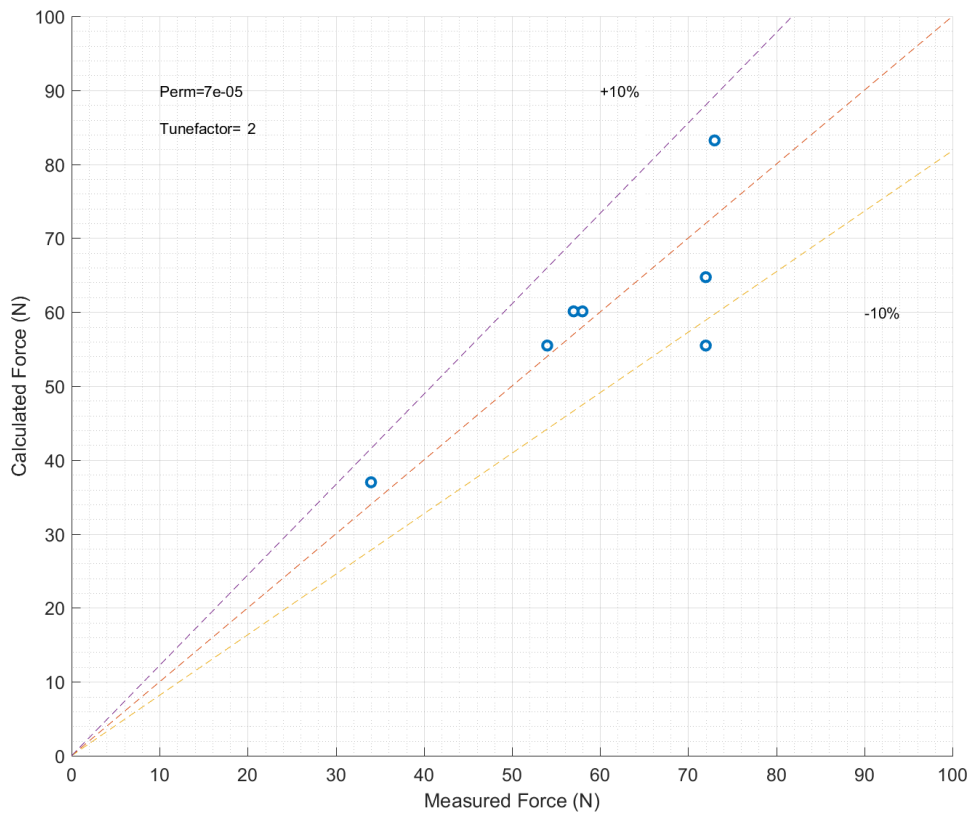


Figure 8.6 – The model versus the test data using a tune factor for the flow path length.

### 8.3 3-Dimensional Comparisons

For the 3-Dimensional model the permeability is initially chosen at the value determined by the soil testing at civil engineering. This value is the maximum value possible and therefore determines the maximum force. The velocities were initially the mean velocities over the complete lifting process.

Setting out the model data for the given permeability and versus the test data for the Silverbond sand gives Figure 8.7.

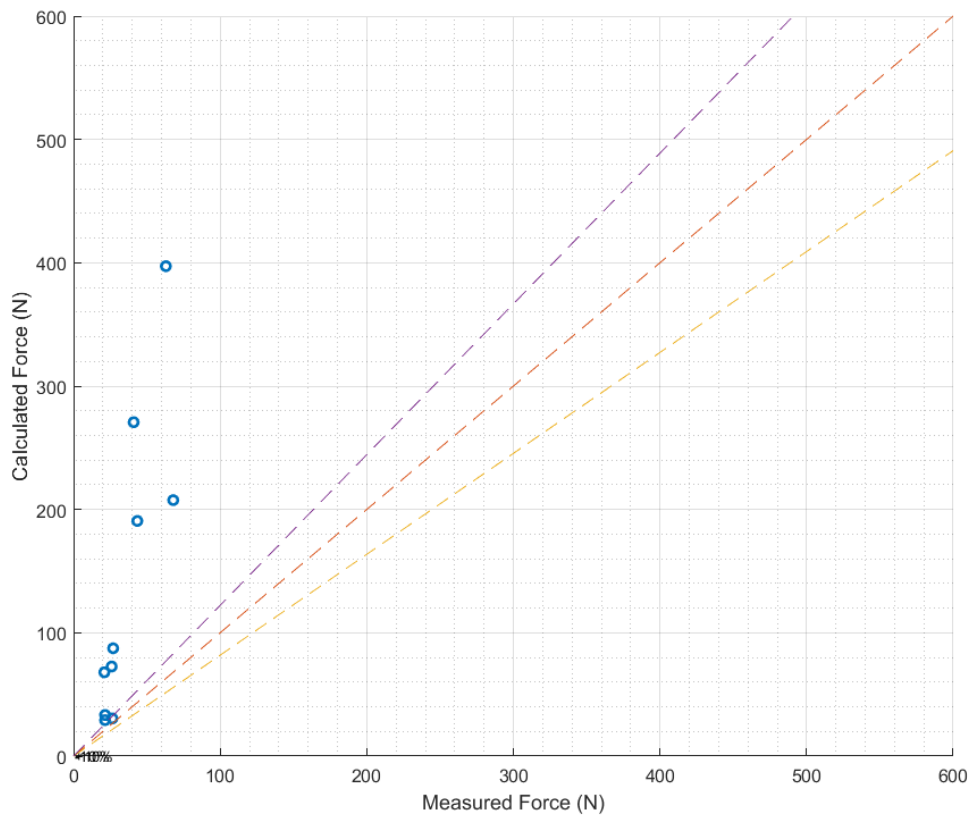


Figure 8.7 – The measured data set out versus the model data for the Silverbond sand with the mean velocities over the complete process.

What can be observed is that the model over estimates the data, just as with the 2-Dimensional model.

Adjusting the velocities in the same way as with the 2-Dimensional model gives Figure 8.8. What can be observed is that the predictions of the model fit the measurement data within a 10% margin. The same as with the 2-Dimensional model.

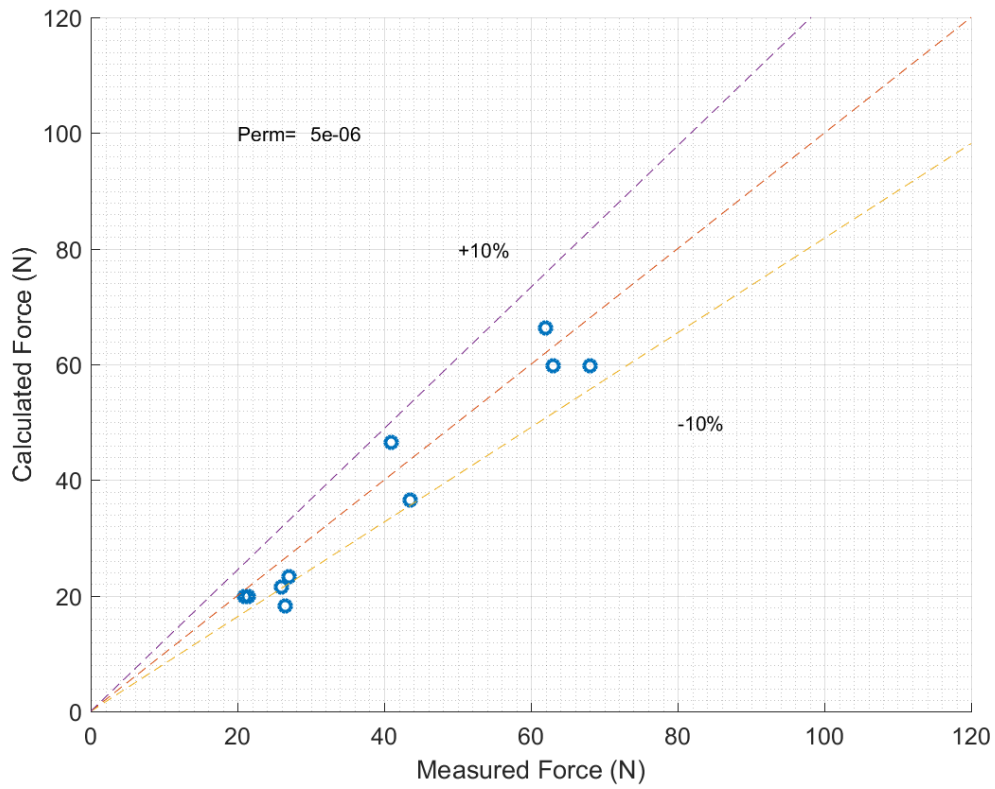


Figure 8.8 - The model versus the test data with the velocities from the beginning of the process for the Silverbond sand. Note that the permeability stays the same.

For the Geba sand the first predictions can be seen in Figure 8.9. As can be seen the model over estimates the force roughly a factor 10. Using the velocities from the beginning of the lifting process the permeability needs a scale down of a factor 4 to give a good fit, see Figure 8.10

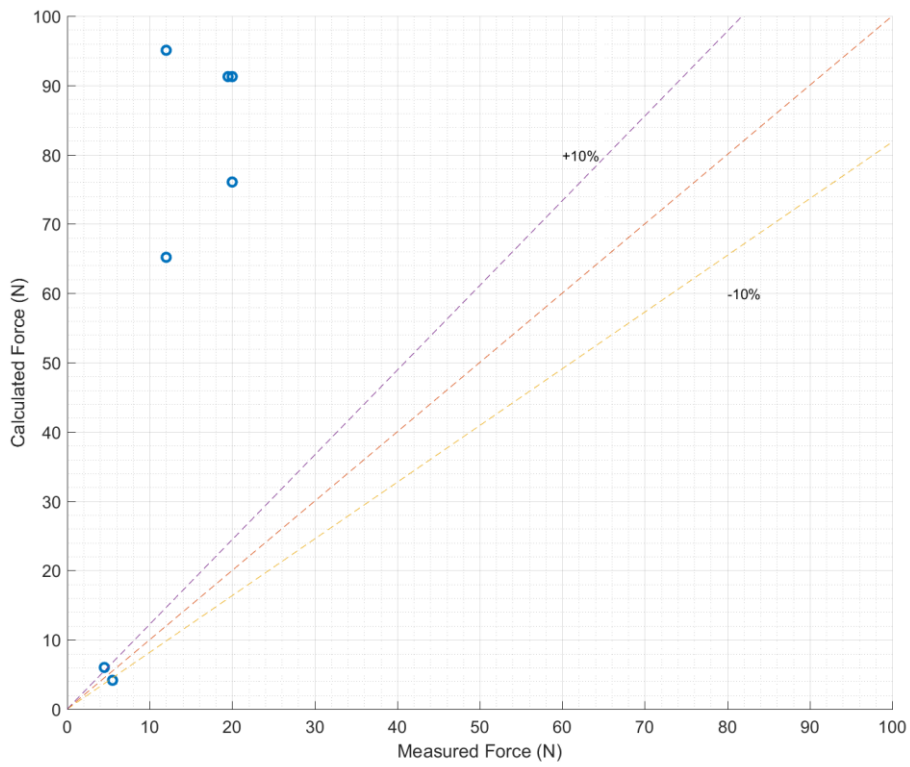


Figure 8.9 – The predictions of the model for the Geba sand using the mean velocities over the complete lifting process.

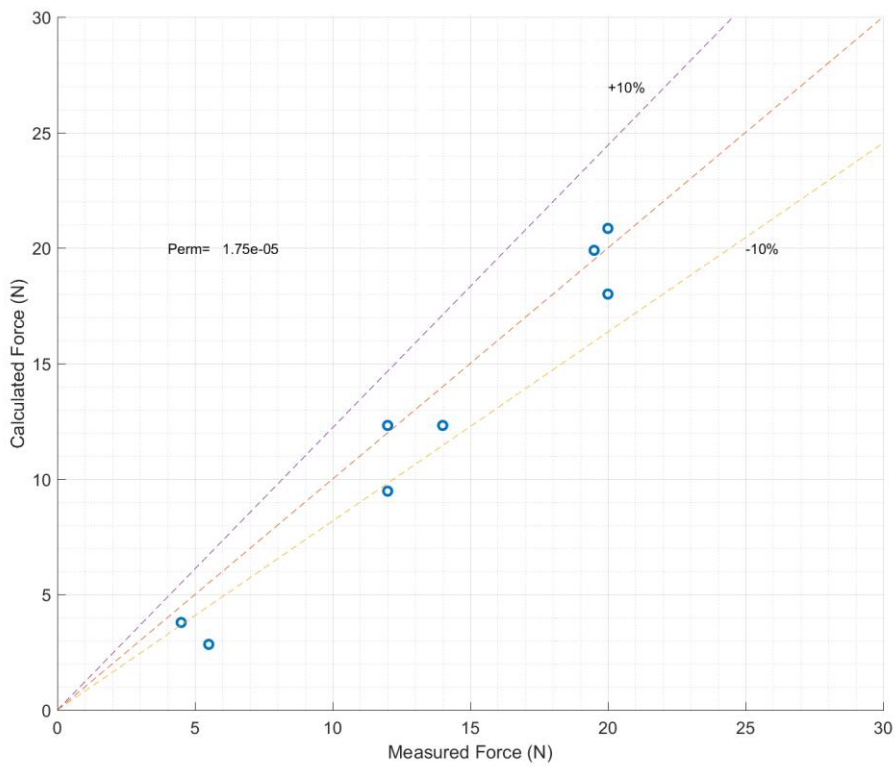


Figure 8.10 – The model versus the test data with the velocities from the beginning of the process for the Geba sand

## 8.4 Scaling

Now the model is validated with the test result the question arises how the results can be scaled to a real-life situation. From the test results the mean displacement of the plate needed for breakout is known. This mean displacement combined with the load which results in under pressures determine the amount of water that is needed during the lifting process.

All tests results showed that the plate was lifted roughly 2 millimeters before breakout. This displacement can be translated into a volume created under the plate which lead to dilatation of the sand. This volume increase has to be filled with water. This volume increase is due to the displacement of the plate.

To scale the results properly it is important to check the thickness of the sand layer under the plate which is influenced by dilatation. In the real-life situation, the sand influenced will probably have a non-rectangular shape but for the sake of simplicity a rectangular shape will be assumed.

The dilatation is defined as

$$\epsilon = \frac{N_{max} - N_{max}}{1 - N_{max}} \quad (8.1)$$

The displacement combined with the plate area determines the added volume due to the lifting process to the influenced zone.

$$E_v = d_p * S_p \quad (8.2)$$

Where:

$E_v$  = Volume created under plate by lifting

$d_p$  = Displacement of the plate during breakout

$S_p$  = Surface area of the plate

Now the extra volume is known the volume of the influenced zone can be calculated by dividing the added volume by the dilatation.

$$I_v = \frac{E_v}{\epsilon} \quad (8.3)$$

Where:

$I_v$  = Initial volume of the influenced zone before the lifting process.

The equivalent layer thickness of the influenced zone is then found by dividing this volume by the surface area of the plate.

$$L = \frac{I_v}{S_p} \quad (8.4)$$

This layer thickness can be calculated for every test with the minimum and maximum porosity as input. These are tested at the civil engineering laboratory. The values for the Geba sand tested as:

$$N_{max} = 0.47$$

$$N_{min} = 0.40$$

And for the Silverbond sand:

$$N_{max} = 0.54$$

$$N_{min} = 0.39$$

The layer thicknesses are then calculated for every test and can be found in Appendix D. For Both the 2-Dimensional and 3-Dimensional test the mean of the layer thickness is calculated per sand type, see Table 8.1. The layer thickness is then defined as a percentage of the plate width in case of the 2-Dimensional setup and the diameter in case of the 3-Dimensional setup.

Test	Mean Layer Thickness (mm)	Percentage of width or diameter
2-D Silverbond	13.9	6,9%
2-D Geba	6.8	3.4%
3-D Silverbond	17.9	9%
3-D Geba	6.7	3.4%

*Table 8.1 – The mean layer thickness per test setup and sand type. In the right column, the layer thickness is defined as a percentage of the 2-D plate width and the 3-D plate diameter*

The influenced zone can now be scaled to a real-life situation and used to determine the size of the real-life mud mat.

No relationship, between the mean layer thickness and the width or the diameter of the plate, other than a linear relationship can be concluded until more tests are conducted.

To do so the right scaling factor has to be found. At first the definition of a scaling factor:

A scaling factor of a quantity is the ratio between the value of the quantity in the prototype and the model:

$$n_x = \frac{x_p}{x_m} \quad (8.5)$$

The time of breakout is dependent on the volume under the plate created by lifting the plate and the flow rate. Therefore:

$$n_T = \frac{n_{E_v}}{n_Q} \quad (8.6)$$

With the volume defined as length to the power three:

$$n_{E_v} = n_L^3 \quad (8.7)$$

The flow rate is defined as:

$$n_Q = n_{area} * n_{velocity} = n_L^2 * n_{v_p} \quad (8.8)$$

The upward velocity of the plate is given by Darcy:

$$n_{v_p} = n_k * n_i \quad (8.9)$$

Where  $i$  is defined as:

$$i = \frac{\Delta h}{L} = \frac{dp}{\rho g L} \quad (8.10)$$

The pressure  $p$  is linked to the imposed load per area:

$$p = \frac{B}{L^2} \quad (8.11)$$

Where  $B$  is the imposed load.

So, with  $\rho$  and  $g$  constant in the model and prototype environment, the scale factor is defined as:

$$n_i = \frac{n_p}{n_L} \quad (8.12)$$

Substituting the above in equation 8.6 gives the final scale factor:

$$n_T = \frac{n_L}{n_k * \left(\frac{n_p}{n_L}\right)} = \frac{n_L^2}{n_k * n_p} \quad (8.13)$$

So, when scaling the time of breakout, the time is dependent on a length scale, pressure and permeability if the soil conditions are not constant. For instance, when the length scale becomes 10 times larger than the breakout time becomes 100 times larger when keeping pressure constant.

It is not certain if this scale rule is valid until full scale test have been conducted.

## 8.5 Conclusions

For the 2-Dimensional model the predictions compared with the measured data lie within the 10 percent margins for the Silverbond sand. Using the model for predictions in the Geba sand the tune factor needs to be adjusted to give a good fit.

Apparently when using the model in Geba sand in a 2-Dimensional situation the flow line length needs to be adjusted. The question is of this factor used to fit the model on to the test data is realistic. The model is built around a number of assumptions and one of the assumptions was that the flow lines are circular. What probably is happening is that the flow from the free surface of the sand next to the plate to the section covered by the plate is more of an ellipse form, in other words more horizontal flow. In this way, the travelled distance of the water in the sand is lower which results in a lower prediction of the force of the 2-Dimensional model with the Geba sand. This is something that adjusting the tune factor proves.

What can be observed is that the model can give reasonable predictions given the velocity is derived from the beginning of the lifting process. The model is valid with a constant permeability.

For the predictions of the 3-Dimensional model the same trend can be spotted. What can be seen with the Silverbond sand is that the fit of the model over the test data is reasonable accurate. For the Geba sand roughly a factor 4 is needed. Using a tune factor in the 3-Dimensional model did not give satisfactory results. A tune factor of 400 was needed to fit the model over the test data with reasonable accuracy. The problem here is that the model uses flow paths instead of flow lines. This was done because of the circular shape of the 3-Dimensional plate as explained in paragraph 7.2. Adjusting the tune factor does not only increase the length of the flow path but also increases the area of the flow path over the length. Adjusting the flow path length does therefore not have such a great impact as with the 2-Dimensional model. This is something that needs further investigation.

## 9 Conclusions and Recommendations

This chapter gives an overview of all the conclusions and recommendations made in this report. First the 2-Dimensional conclusions and recommendations are answered, later the 3-Dimensional case.

### 9.1 2-Dimensional Conclusions

The preliminary experiments already showed that under pressures were present during lifting operations in fine grained sand. The 2-Dimensional experiments show that the breakout time is related to the permeability of the sand. A factor 10 in breakout time given the same load between the Silverbond and Geba sand is the result. For the breakout time it can be seen that doubling the load does not result in dividing the breakout time in halve. The Geba sand seems to have this trend but especially the Silverbond sand differs a lot.

The pressure profile under the 2-Dimensional plate was assumed linear, the testing showed otherwise. A more rectangular pressure profile is present.

The mean displacement before breakout for the two different sands is about the order of 2 millimeters during the testing with different loads. It can be concluded that the grain size of the sand does not influence the mean displacement before breakout.

The 2-dimensional model seems to give reasonable predictions when using velocities from the beginning of the lifting process. The Geba sand needs adjusting of the tune factor to give a good fit.

Further research concerning the 2-Dimensional case would be useful. The model could use some attention. It would be useful if the model could make predictions over the complete lifting process. A variable permeability should be taken into account as the porosity of the sand changes due to the lifting process. If this is done correctly a time prediction could be built in to the model.

To say something about the flow lines in the sand one should consider using pressure sensors in the sand bed. Also, more pressure points are needed to say more about the pressure profile underneath the plate.

### 9.2 3-Dimensional Conclusions

The experiments with the 3-Dimensional setup showed that scaling the breakout time with the permeability of the sand has its limits. During the experiments with the Geba sand a too large load was chosen so that inertia dominated the breakout time. Nothing can be concluded about a relation between the breakout time and the permeability for the same load between the two different sands. What can be concluded is that the breakout time in Silverbond sand follows a nonlinear curve. A same sort of relation can be seen with the experiments in the Geba sand but, as mentioned, the experiments should be conducted with smaller increases in the imposed load.

The pressure sensors of the 3-dimensional plate gave a good indication of the pressure profile beneath the plate. The experiments in the Silverbond sand gave a more or less rectangular shape with steep slopes towards the edge of the plate. The experiments with the Geba sand showed a smoother profile.

For the mean displacement, the conclusion is the same as with the 2-Dimensional plate. No relation of the displacement is found with respect to the grain size of the sand.

Testing for consolidation effects showed that pre-loading the 3-Dimensional plate in sand does not make a difference in breakout time. Pre-loading in the case of thoroughly vibrated sand therefore does not make a noticeable difference in breakout time. Testing on loose sand is a recommendation for future research.

The 3-Dimensional model predicts the lifting force reasonable accurate. For use with the Silverbond sand the fit was within the 10% margins when using the velocities from the beginning of the lifting process. For the Geba sand the permeability had to be scaled to give a good fit. This is because of model assumptions and using flow paths. Adjusting the tune factor did not give satisfactory results.

Further research can be done in to modeling the prediction of the breakout time, this is not incorporated in the model as is the case with the 2-Dimensional model.

## Bibliography

- Al-Shamrani, M. A. (1995). *Finite element analysis of breakout force of objects embedded in sea bottom*. Riyadh, Saudi Arabia: College of Engineering, King Saud University.
- Chen, R. G. (2012). Investigation of the vertical uplift capacity of deep water mudmats in clay. *Canadian Geotechnical Journal* vol. 49, 853-865.
- Craig, W. C. (1987). Extraction forces for offshore foundations under undrained loading. *Journal of Geotechnical Engineering* vol. 116, 868-884.
- Das, B. (1991). Bottom breakout of objects resting on soft clay sediments. *International Journal of Offshore and Polar Engineering* vol. 1, 195-199.
- Den Adel, H. (1989). *Re-analyzing permeability measurements with the Forchheimer relation*. . Geotechnics report CO-272553/56.
- Foda, M. (1982). On the extrication of large objects from the ocean bottom (the breakout phenomenon). *Journal of Fluid Mechanics* vol. 117, 211-231.
- Huang, H.M., Lin, M.Y., Huang, L.H. (2010). Lifting of a large object from a rigid porous seabed. (pp. 106-113). Taipei, China: Department of Civil Engineering, National Taiwan University.
- Lee, H. (1973). Breakout of partially embedded objects from cohesive seafloor soils. *Offshore Technology Conference* (pp. 789-802). Houston, Texas: U.S. Naval Civil Engineering Laboratory.
- Liam Finn, W. B. (1972). The evaluation of the breakout force for a submerged ocean platform. (pp. 863-868). Houston, Texas: Offshore Technology Conference.
- Liu, C. L. (1969). *Ocean sediment holding strength against breakout of embedded objects*. Port Hueneme, California: U.S. Naval Civil Engineering Laboratory.
- Mei, C.C., Yeung, R.W., Liu, K.F. (1985). Lifting of a large object from a rigid porous seabed. *Journal of Fluid Mechanics* vol. 152, 203-215.
- Miedema, S. (2014). *The Delft Sand, Clay & Rock Cutting Model*. Delft.
- Muga, B. (1968). *Ocean bottom breakout forces*. Port Hueneme, California: Naval Civil Engineering Laboratory .
- Rapoport V, Young A.G. (1983). *Prediction for breakout resistance for object embedded into seafloor soil*. Houston.
- Schriek, G.L.M. van der, Rhee, C. van. (2010). Physical scale modeling of dredging processes in sand and gravel. *19th World Dredging Congress*, 859-874.
- Taylor, R. D. (1970). *In place seafloor soil test equipment: a performance evaluation*. Port Hueneme, California: Naval Civil Engineering Laboratory.

Vesic, A. (1969). *Breakout resistance of objects embedded in ocean bottom*. Port Hueneme, California: U.S. Naval Civil Engineering Laboratory.

Zhao, Y. (2001). *The FEM calculation of pore water pressure in sand cutting process by SEPRAN*. Delft.

## Appendix A                      Sensor Data

For further research, it is important to note down the sensors used in the test setup. Four different DP- Sensors were used in combination with a load cell. The manufactures and serial numbers can be found in the tables below.

Sensor from test	Manufacturer and Type	Serial Number
DP1	Rosemount DP3 S22	7466512/0101

Sensor from test	Manufacturer and Type	Serial Number
DP2	Rosemount DP3 S22	10110818

Sensor from test	Manufacturer and Type	Serial Number
DP3	Rosemount DP3	10110817

Sensor from test	Manufacturer and Type	Serial Number
DP4	Rosemount DP3	10110919

Sensor from test	Manufacturer and Type	Serial Number
Loadcell	Zemic H3G-C3-50kg	TC7865

Sensor from test	Manufacturer and Type	Serial Number
Displacement meter	Messotron WT50K	31106

## Appendix B Permeability Tests

The Permeability tests were conducted on the department of civil engineering of the TU delft. The Permeability followed from a falling head test. The tests have been performed several times and the Ks value followed from these tests. The first table gives the test for the Silverbond sand, the second for the Geba sand.

KSAT

Software Version 1.2.0

Firmware Version 1.4

Last setting of the zero point 1-1-0001

Serial Number 0034

PARAMETER

Mode FallingHead

Sample name Test\_50um\_chris6\_001

cross-sectional area of the burette [cm<sup>2</sup>] 4,536

Cross-sectional area of the sample [cm<sup>2</sup>] 50,18

Sample length [cm] 5,0

Plate thickness [cm] 1,0

Crown type SteelMeshCrown

Saturated plate conductivity [cm/d] 20000,000

Start of measurement 8-12-2016 11:16:47

Test duration 00:03:04

RESULT

Use auto offset adjustment True

Fitting Parameter a [cm] 6,15

Fitting Parameter b [s<sup>-1</sup>] -1,09E-03

Fitting Parameter c [cm] -,6

Fitting Parameter r2 [-] 1,0000

Ks Total [cm/d] 51

Ks Total [m/s] 5,94E-06

Ks Soil [cm/d] 43

Ks Soil [m/s] 4,95E-06

Ks Soil normalized at 25,0 Â°C [cm/d] [cm/d] 42

Ks Soil normalized at 25,0 Â°C [cm/d] [m/s] 4,94E-06

KSAT

Software Version 1.2.0

Firmware Version 1.4

Last setting of the zero point 1-1-0001

Serial Number 0034

## PARAMETER

Mode FallingHead

Sample name Gebat2\_001

cross-sectional area of the burette [cm<sup>2</sup>] 4,536

Cross-sectional area of the sample [cm<sup>2</sup>] 50,18

Sample length [cm] 5,0

Plate thickness [cm] 1,0

Crown type FilterPlateCrown

Saturated plate conductivity [cm/d] 20000,000

Start of measurement 17-11-2016 11:54:34

Test duration 00:00:54

## RESULT

Use auto offset adjustment True

Fitting Parameter a [cm] 5,18

Fitting Parameter b [s<sup>-1</sup>] -1,52E-02

Fitting Parameter c [cm]

Fitting Parameter r2 [-] 0,9996

Ks Total [cm/d] 750

Ks Total [m/s] 8,72E-05

Ks Soil [cm/d] 600

Ks Soil [m/s] 6,97E-05

Ks Soil normalized at 25,0 Â°C [cm/d] [cm/d] 595

Ks Soil normalized at 25,0 Â°C [cm/d] [m/s] 6,92E-05

## Appendix C Sieve Analysis.

The sieve analysis has been performed by Ir. Rik Bisschop during his Phd research. two of the sands he used in his research were the Silverbond and the Geba sand. The sieve analysis is shown below:

	D <sub>10</sub>	D <sub>15</sub>	D <sub>50</sub>	D <sub>60</sub>	D <sub>60</sub> /D <sub>10</sub>
Silverbond	0,092	0,098	0,125	0,133	1,45
Geba	0,017	0,021	0,051	0,057	3,35

## Appendix D Layer Thickness

2-Dimensional test, Silverbond	Layer Thickness (mm)
2D-S-130N -2	15.1
2D-S-130N -3	11.4
2D-S-150N -1	11.4
2D-S-150N -2	15.1
2D-S-170N -2	15.1
2D-S-170N -3	15.1

2-Dimensional test, Geba	Layer Thickness (mm)
2D-G-90N -3	9.2
2D-G-110N -1	9.2
2D-G-110N -2	9.2
2D-G-110N -3	6.1
2D-G-130N -1	3
2D-G-130N -2	4.6
2D-G-130N -3	6.1

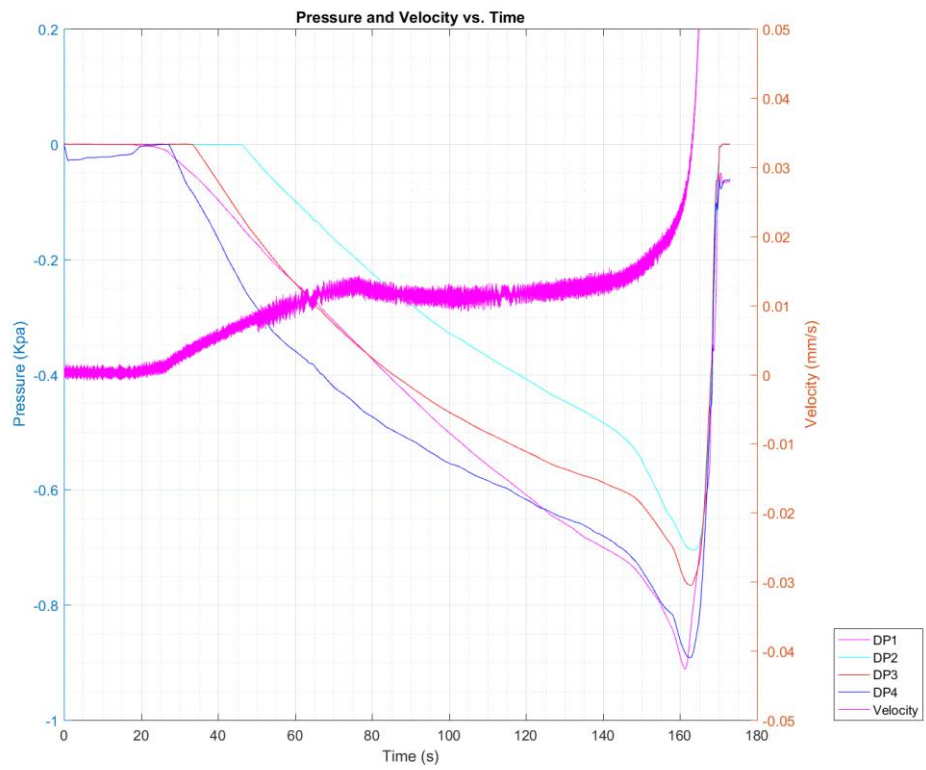
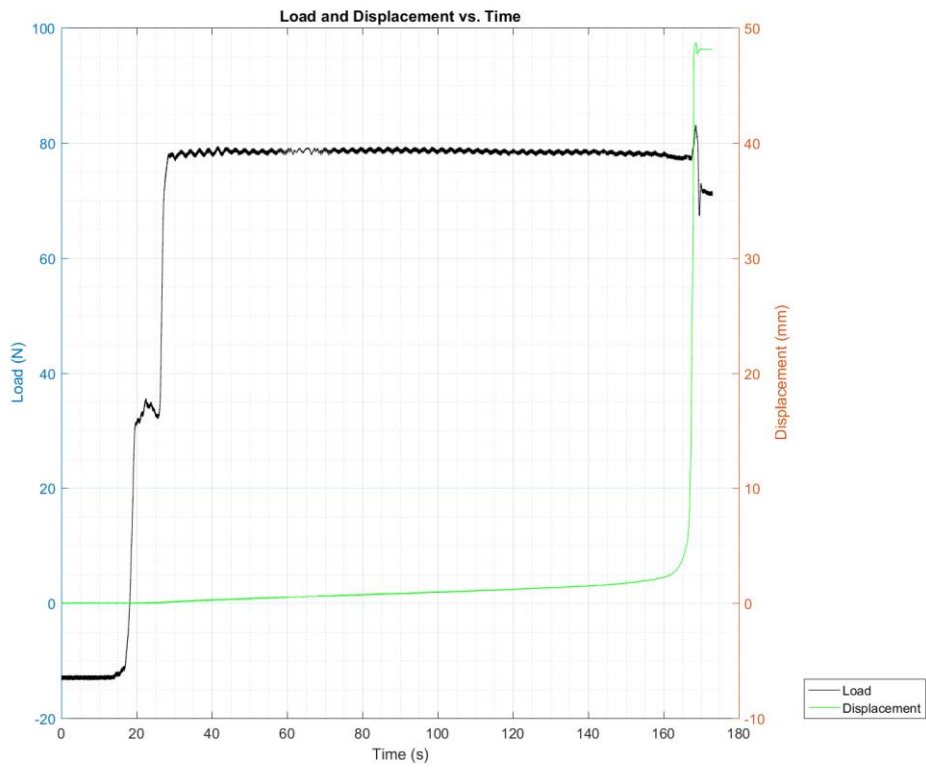
3-Dimensional test, Silverbond	Layer Thickness (mm)
3D-S-65N -1	15.1
3D-S-65N -2	15.1
3D-S-65N -3	30.3
3D-S-70N -1	11.4
3D-S-70N -2	22.7
3D-S-70N -4	18.9
3D-S-90N -1	15.1
3D-S-90N -3	18.9
3D-S-110N -1	18.9
3D-S-110N -2	15.1
3D-S-110N -3	15.1

3-Dimensional test , Geba	Layer Thickness (mm)
3D-G-50N -1	7.7
3D-G-50N -3	6.1
3D-G-60N -1	7.7
3D-G-60N -2	7.7
3D-G-60N -3	6.1
3D-G-70N -1	6.1
3D-G-70N -2	6.1
3D-G-70N -3	6.1

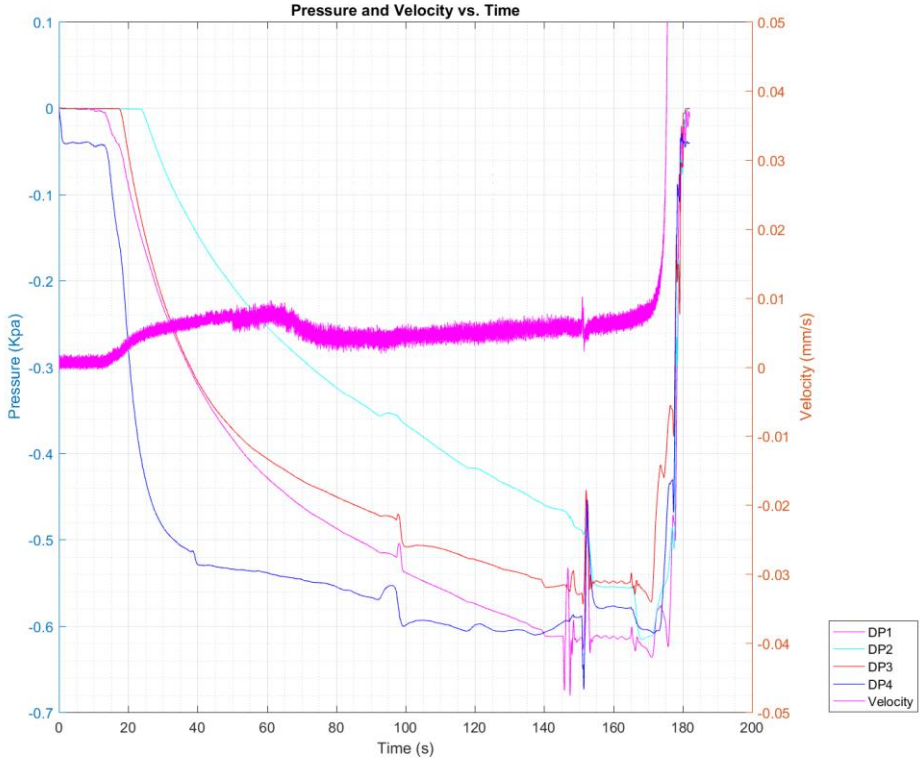
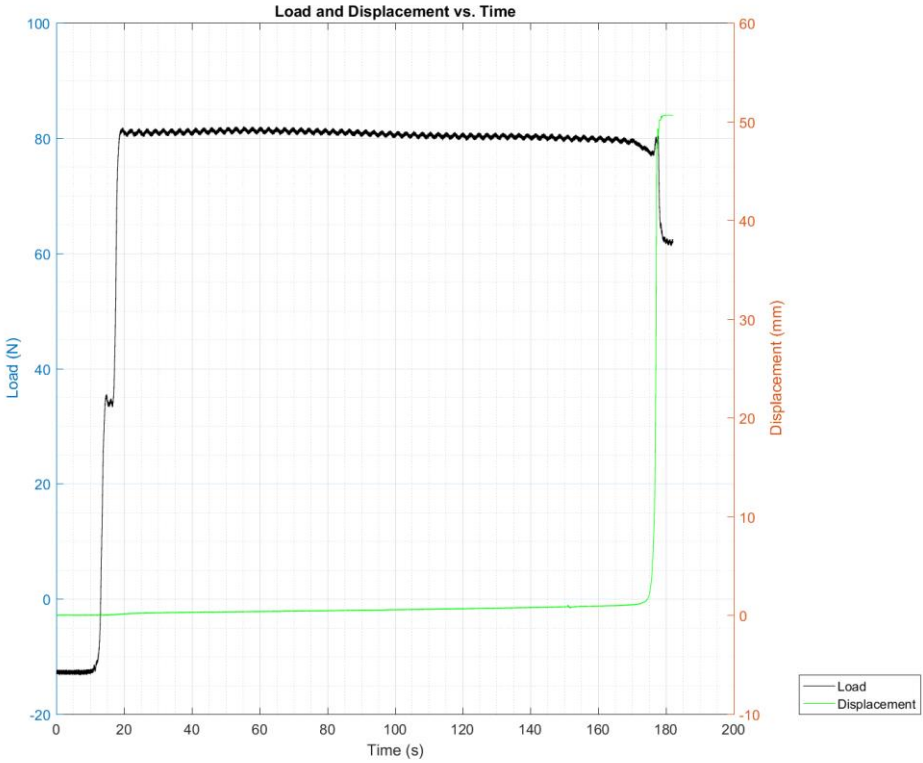
## **Appendix E      2-Dimensional Test Results**

In this appendix, the 2-Dimensional test results are shown. From the many graph produced, there was chosen to show the Load and the displacement versus the time in one graph and the Pressure and the velocity versus the time in the other. All used data can be derived from these 2 graphs. On the start of every page the test number is mentioned.

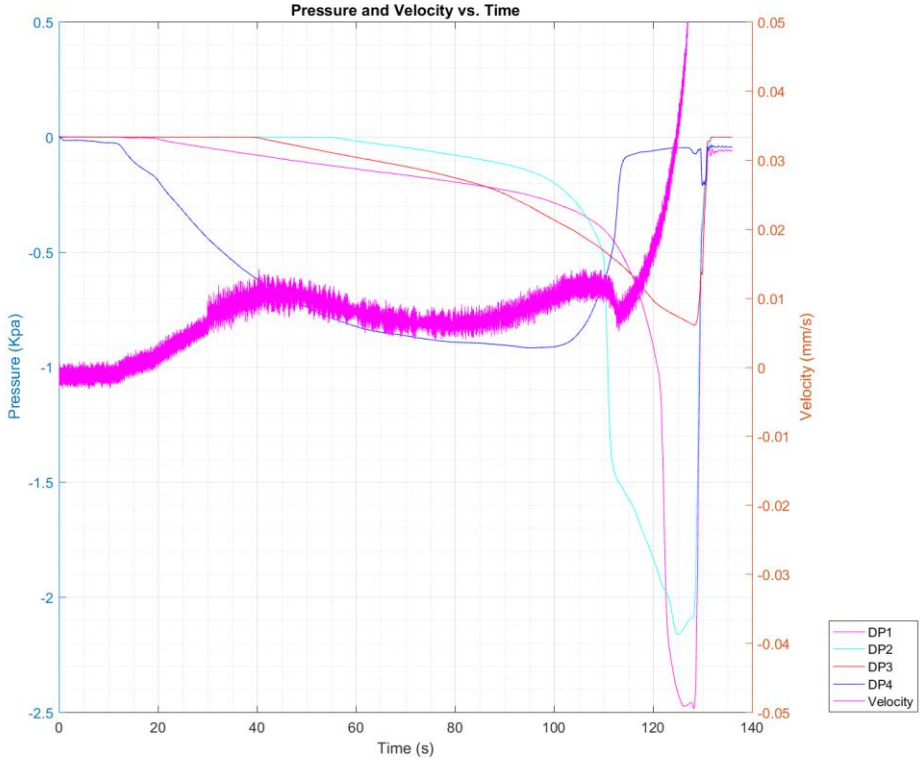
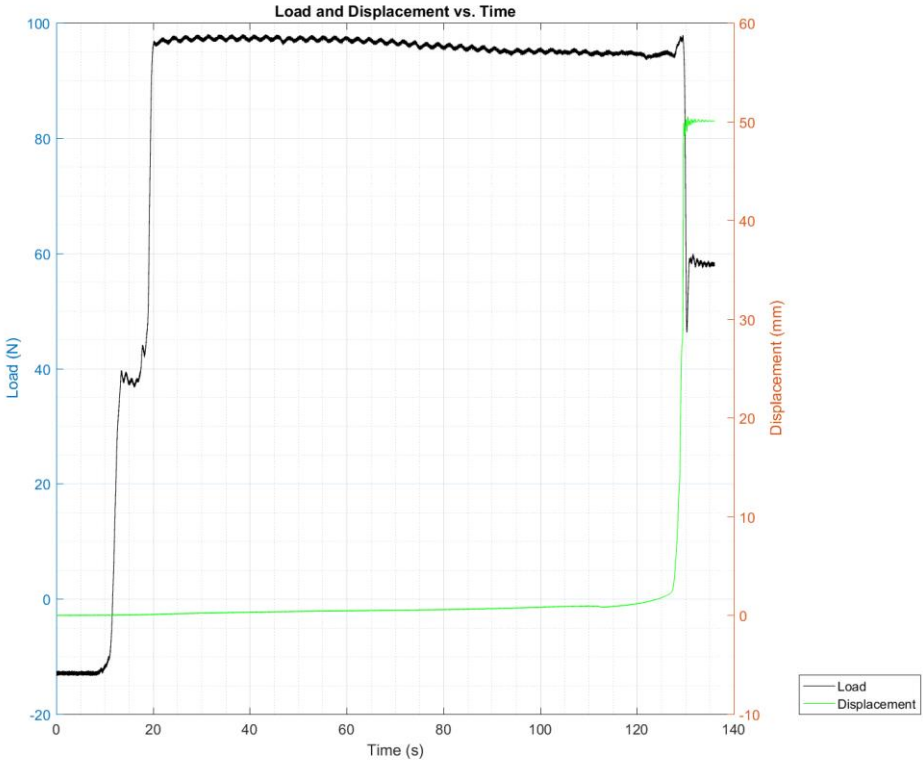
# 2D-S-130N -2



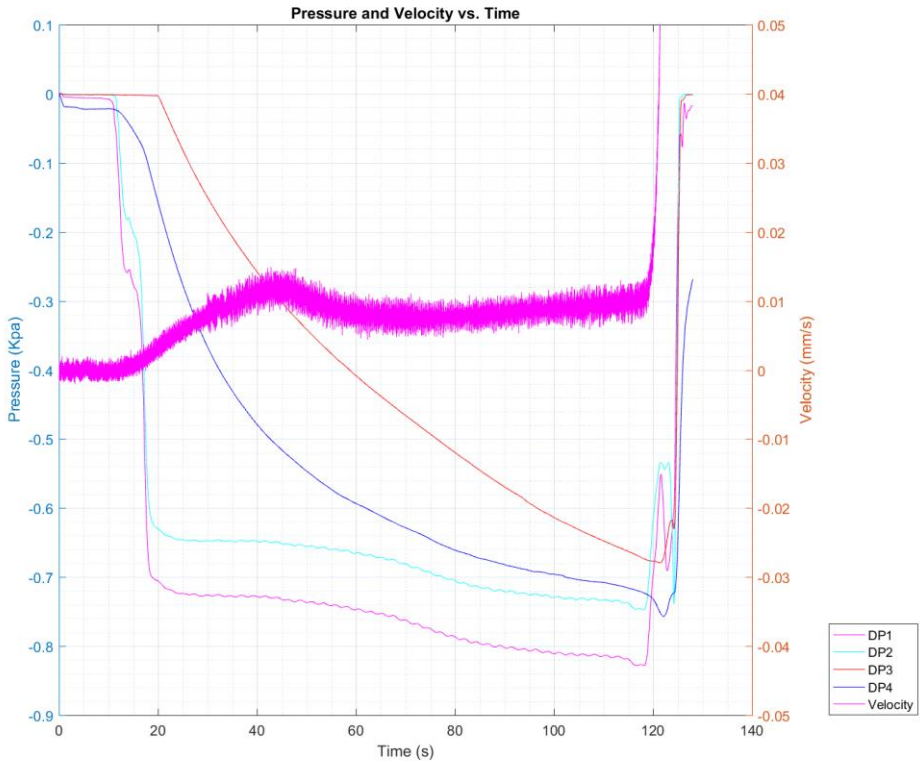
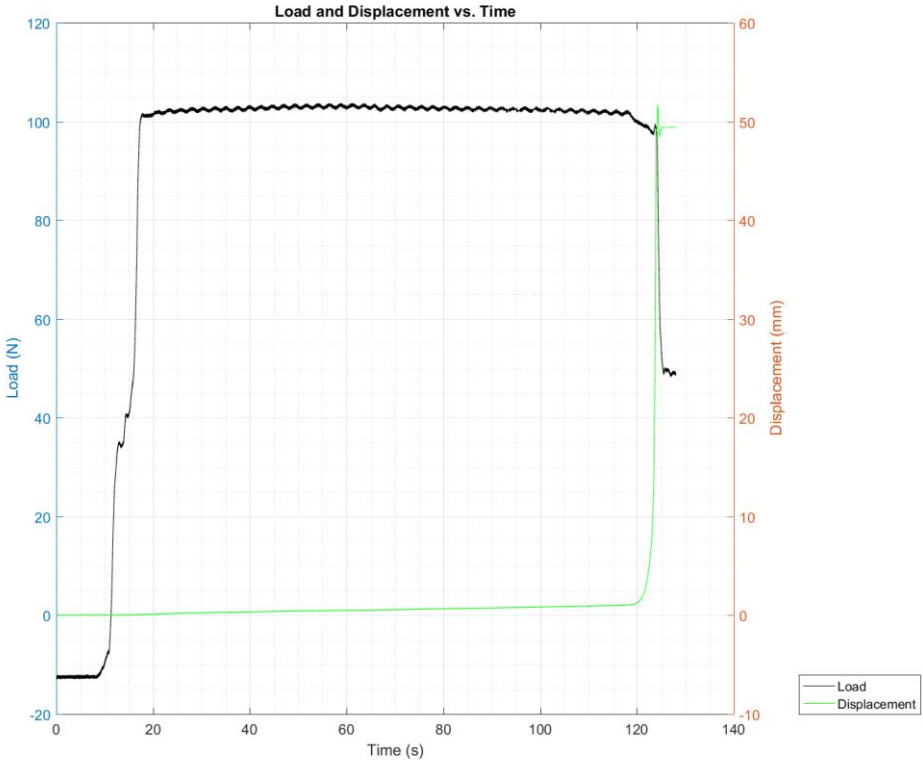
2D-S-130N -3



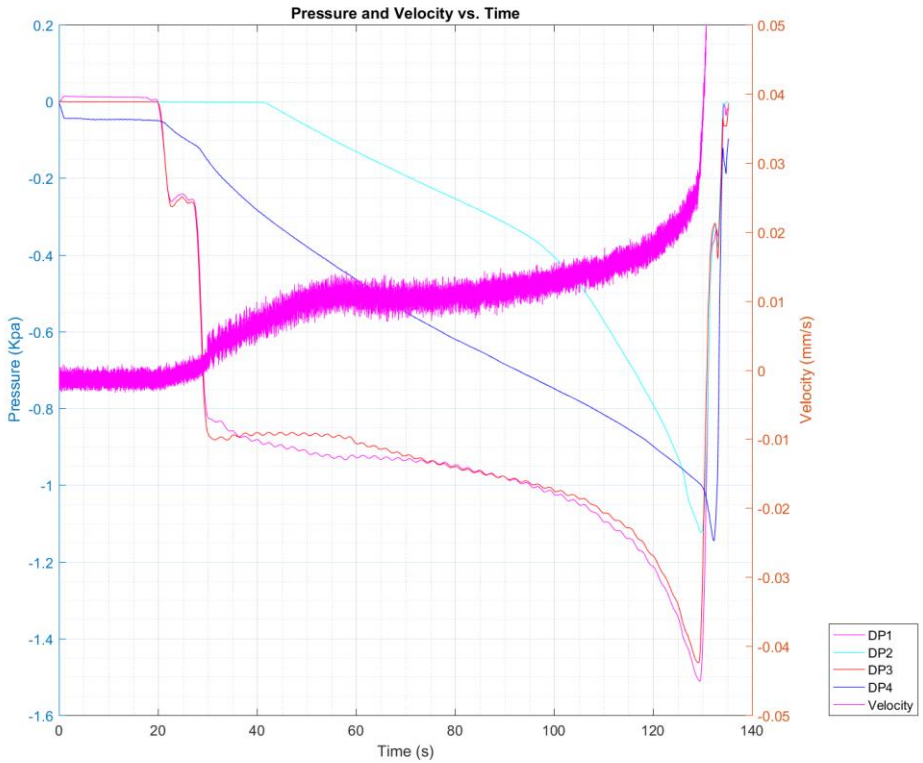
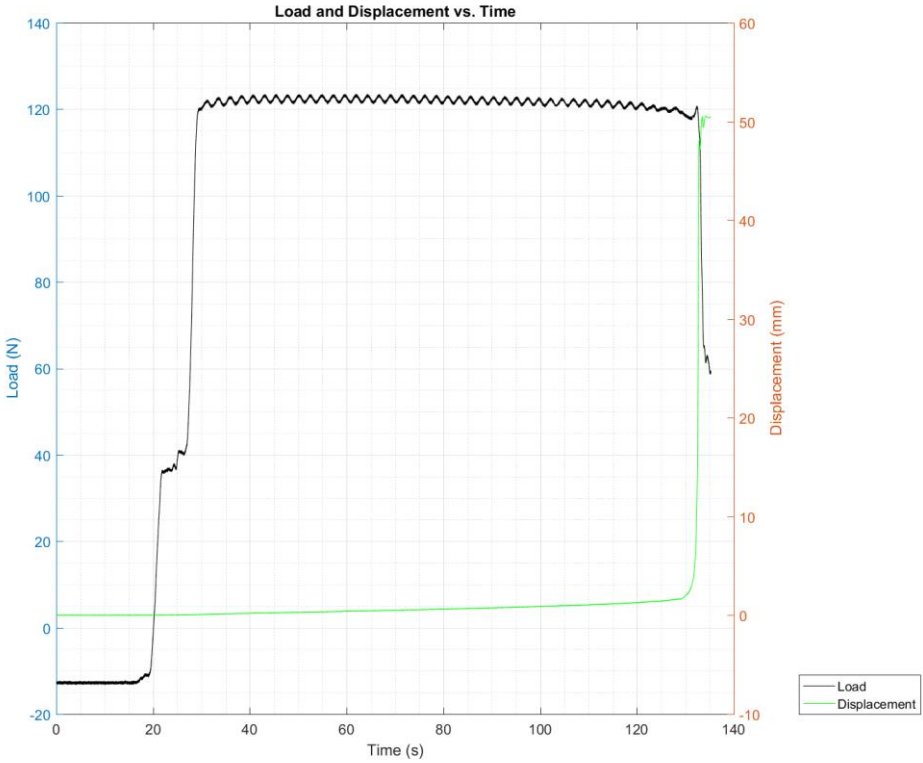
2D-S-150N -1



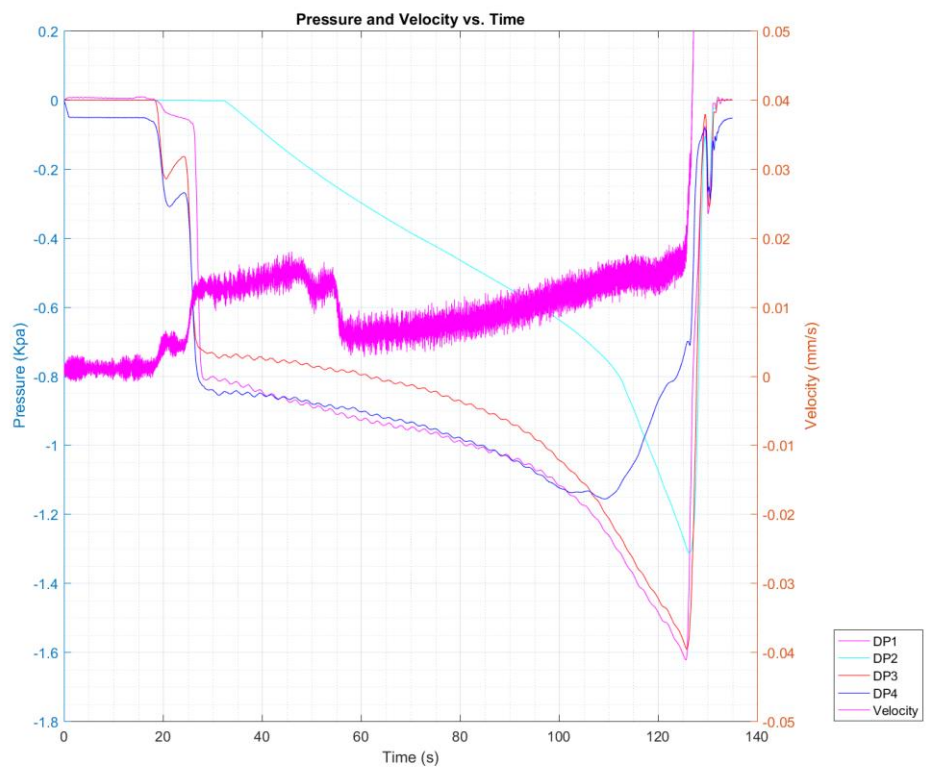
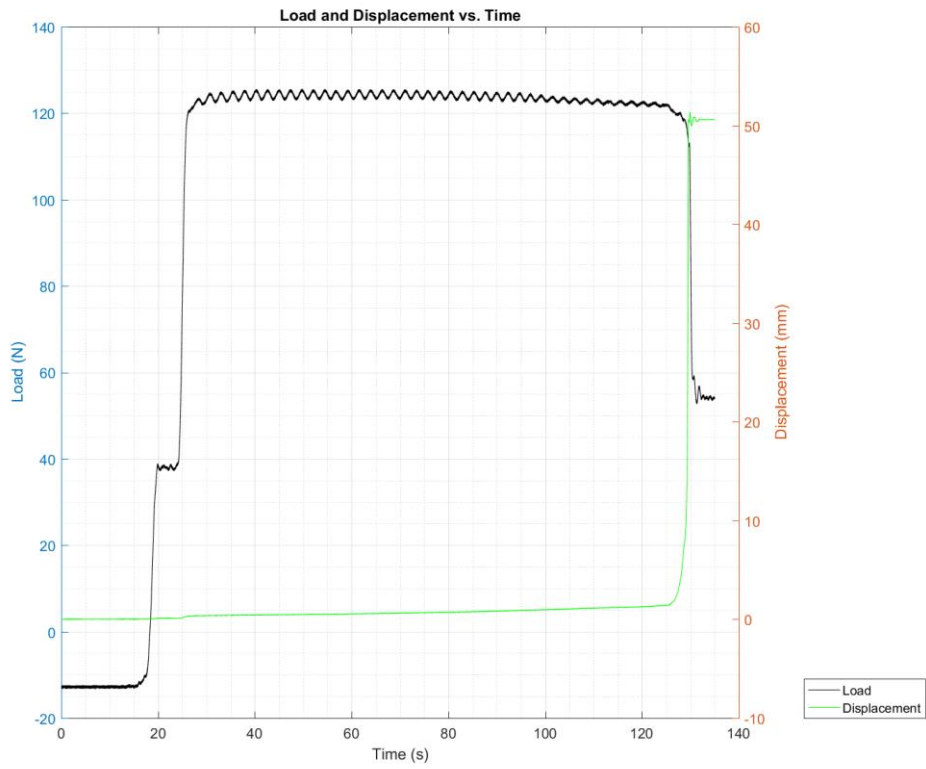
2D-S-150N -2



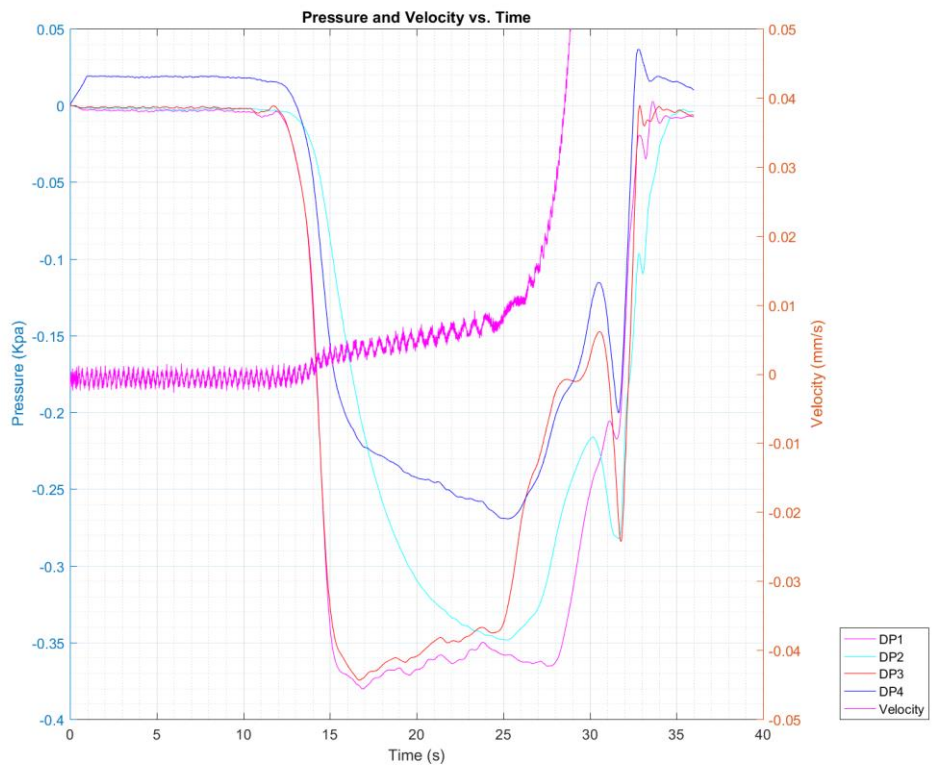
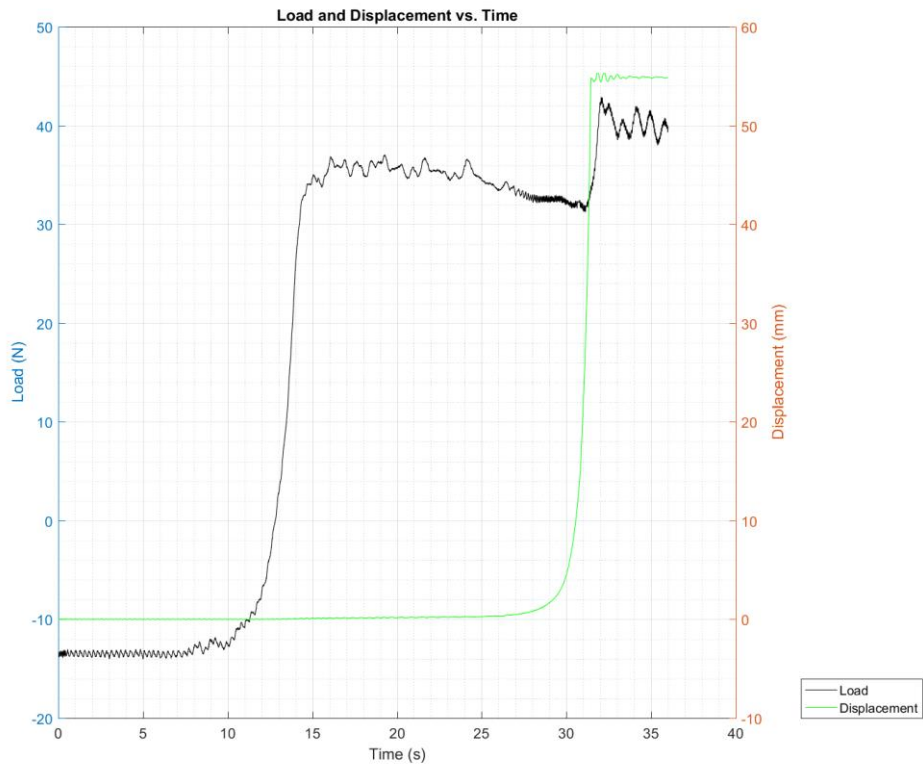
2D-S-170N -2



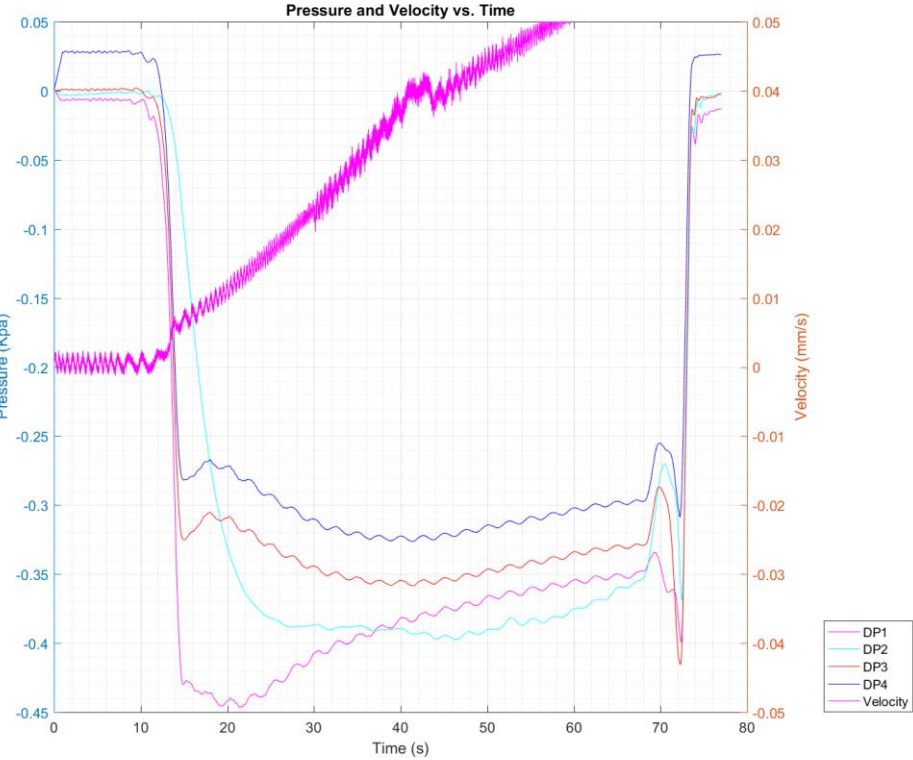
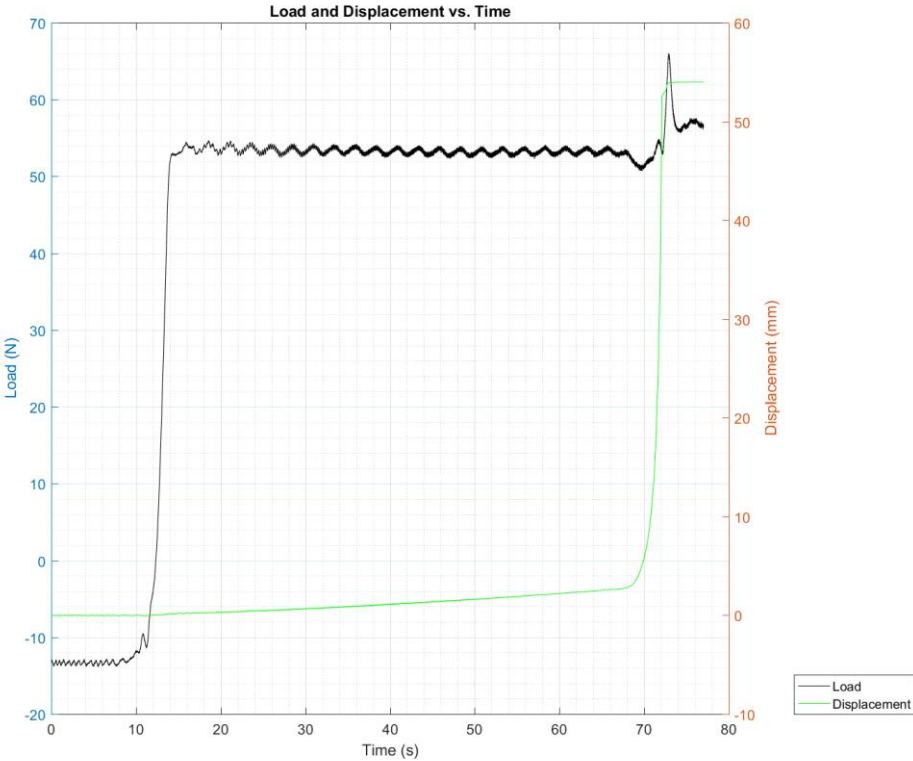
# 2D-S-170N -3



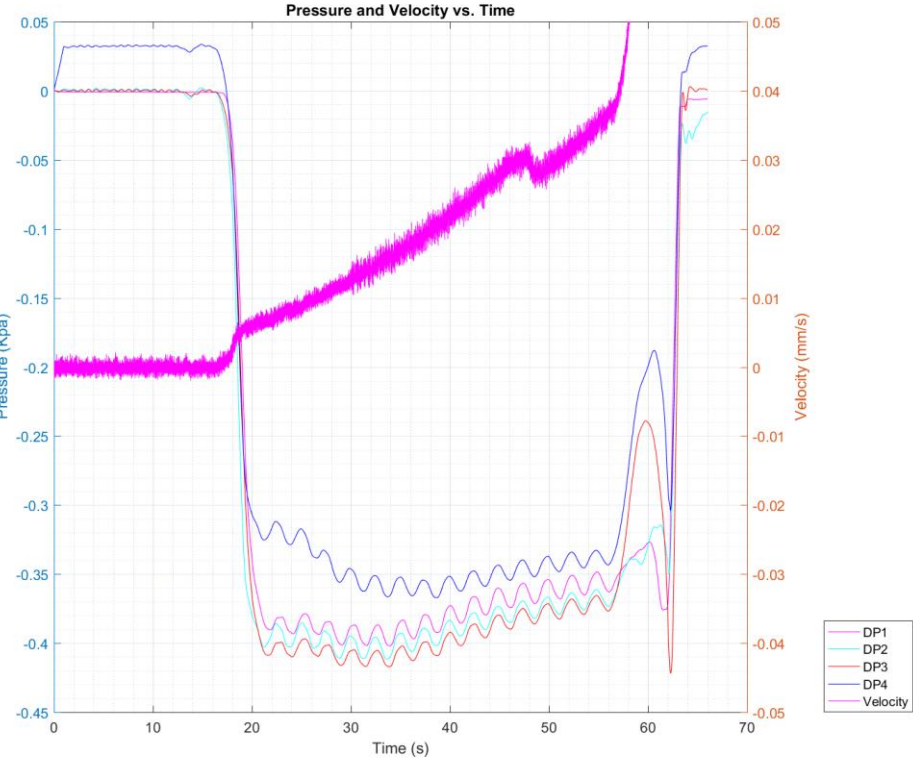
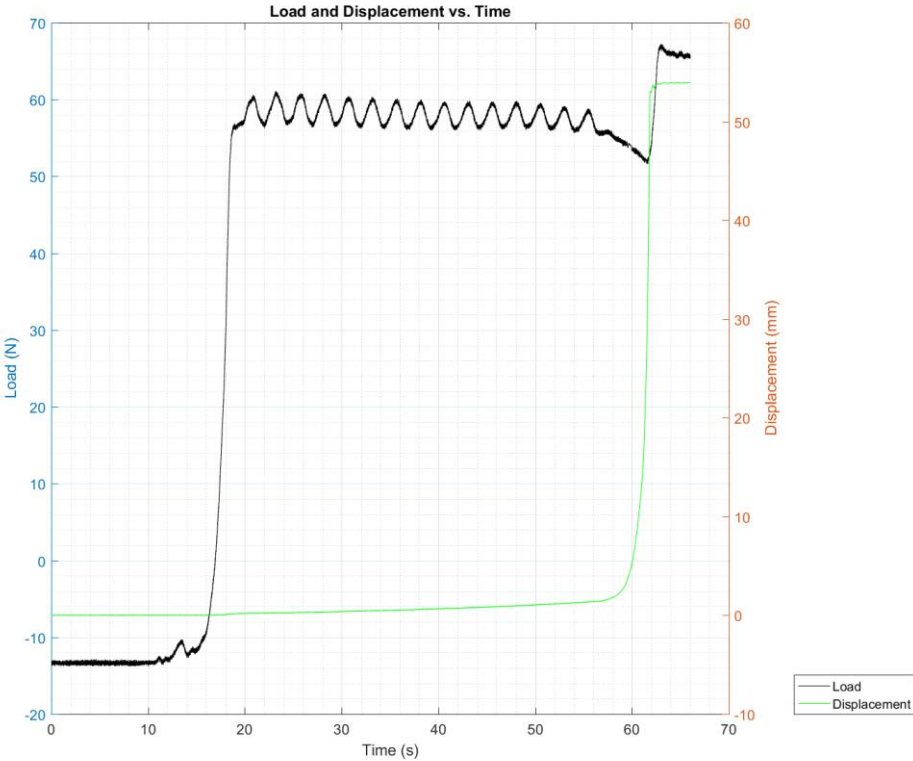
# 2D-G-90N -3



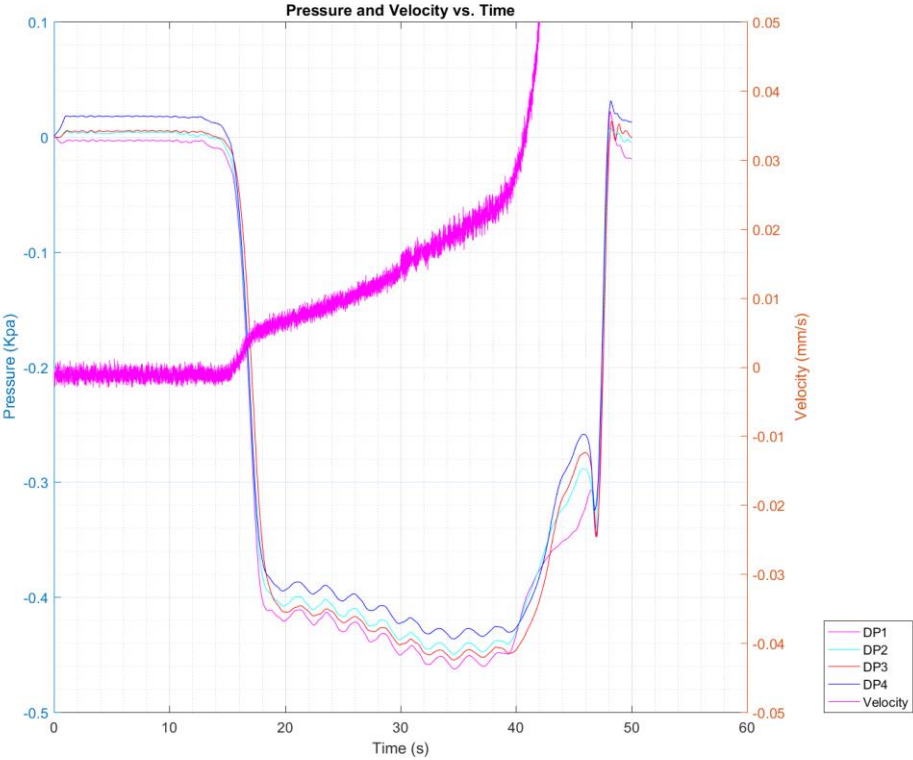
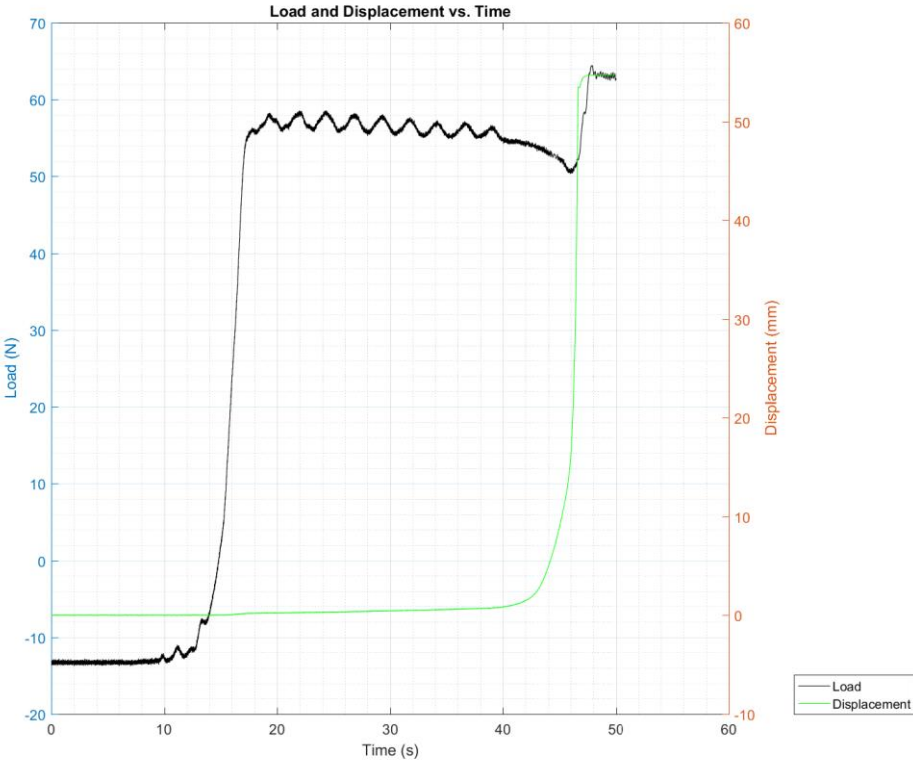
2D-G-110N -1



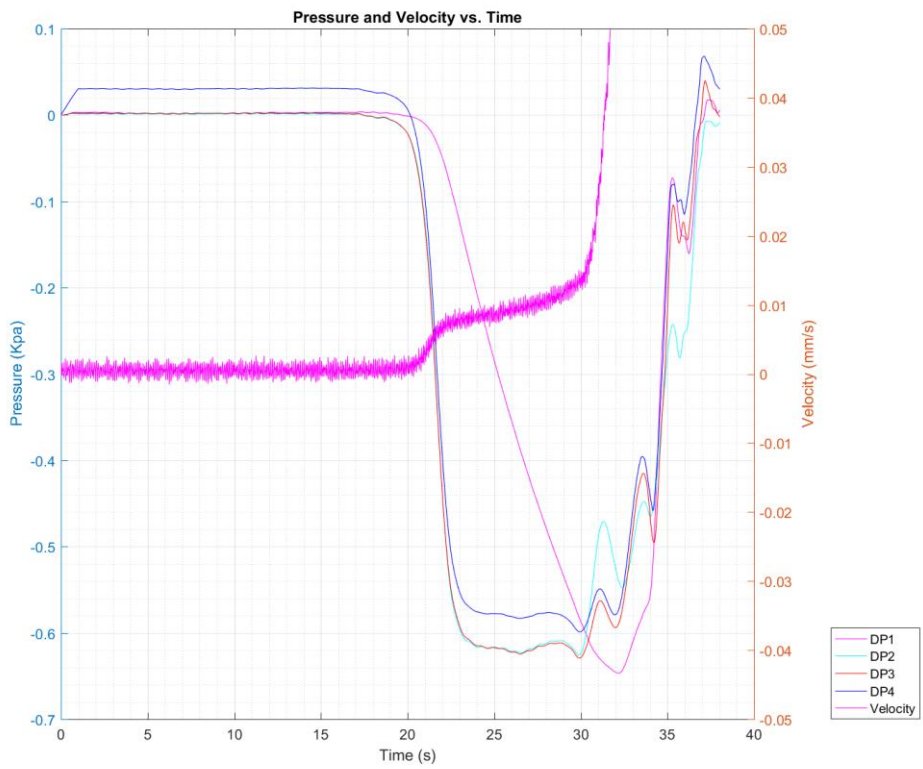
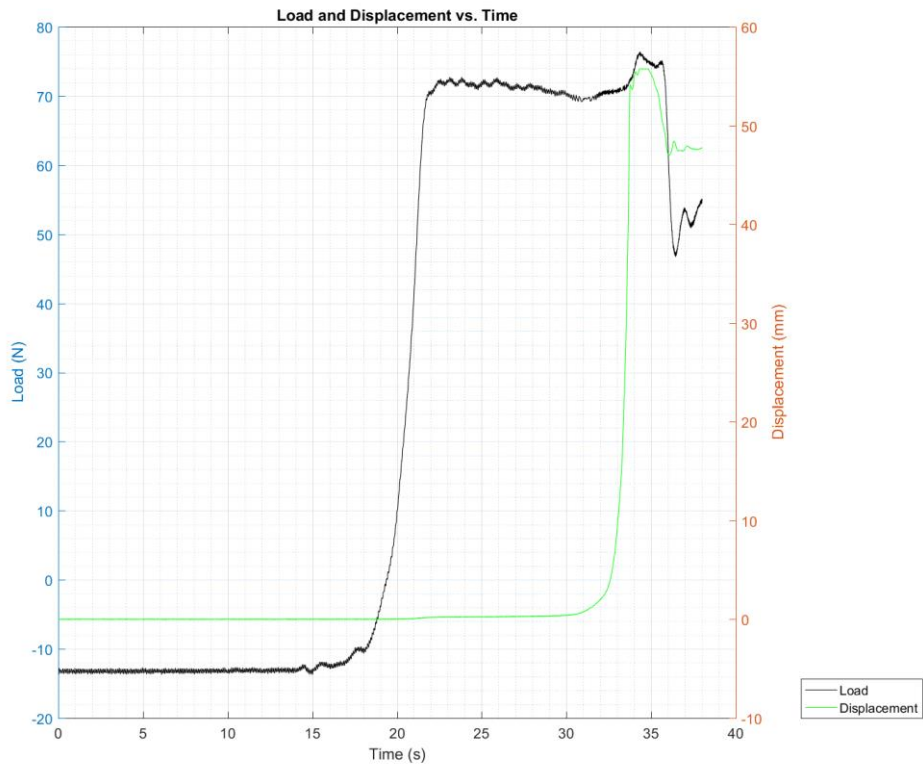
2D-G-110N -2



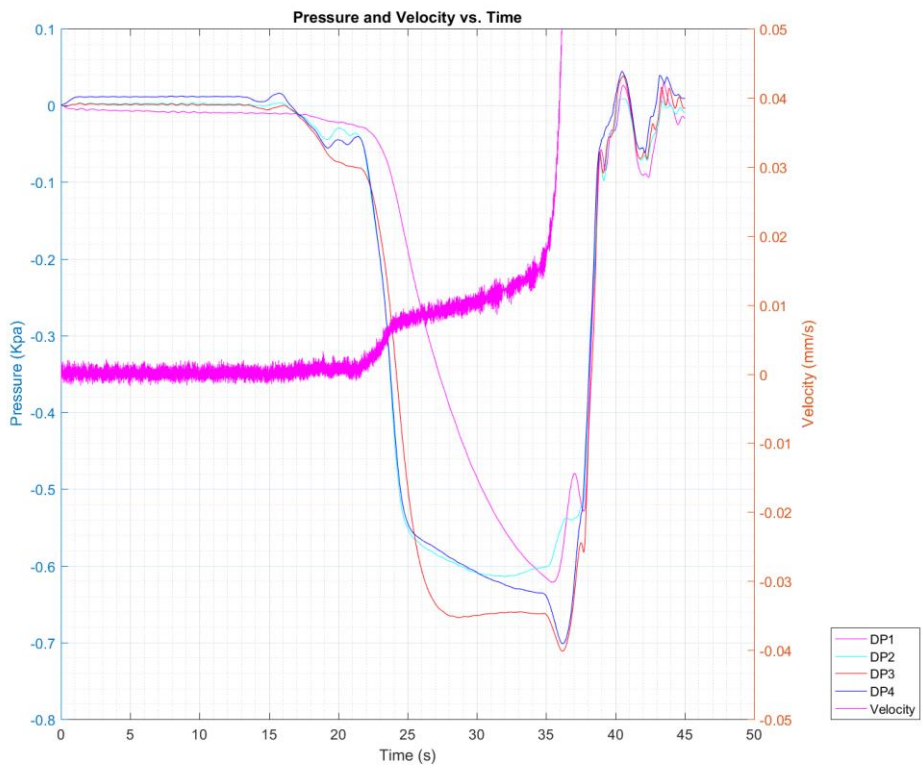
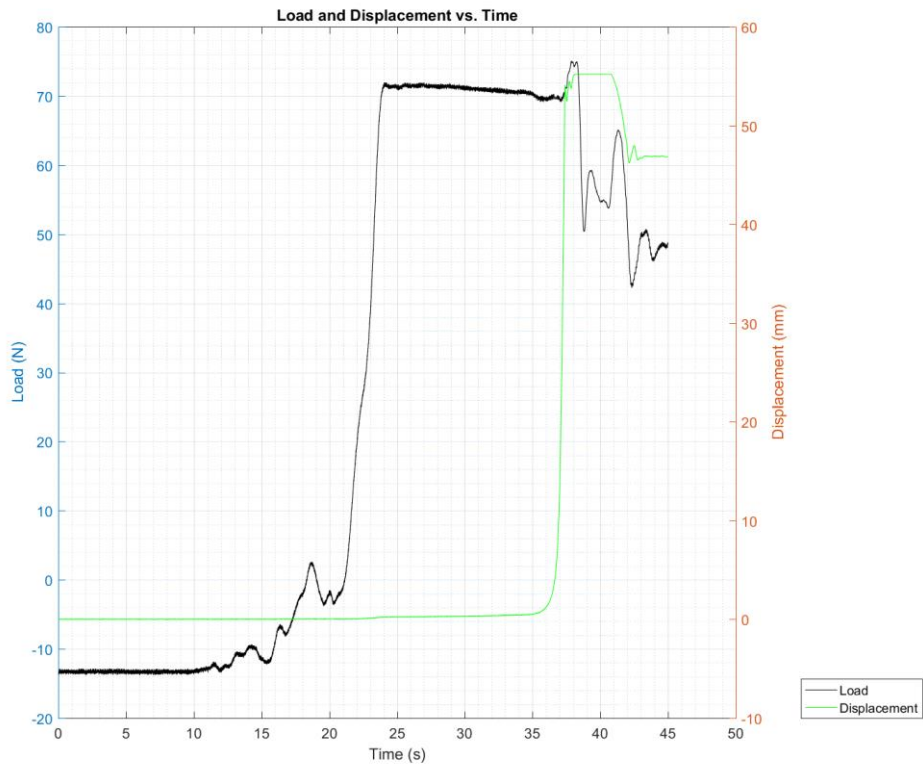
2D-G-110N -3



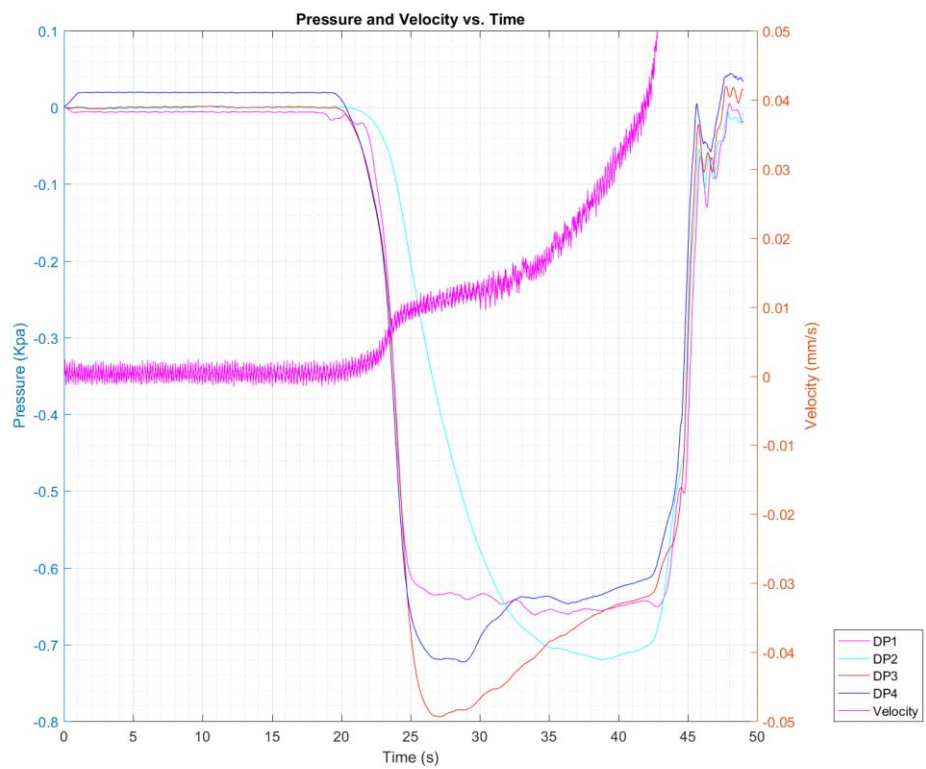
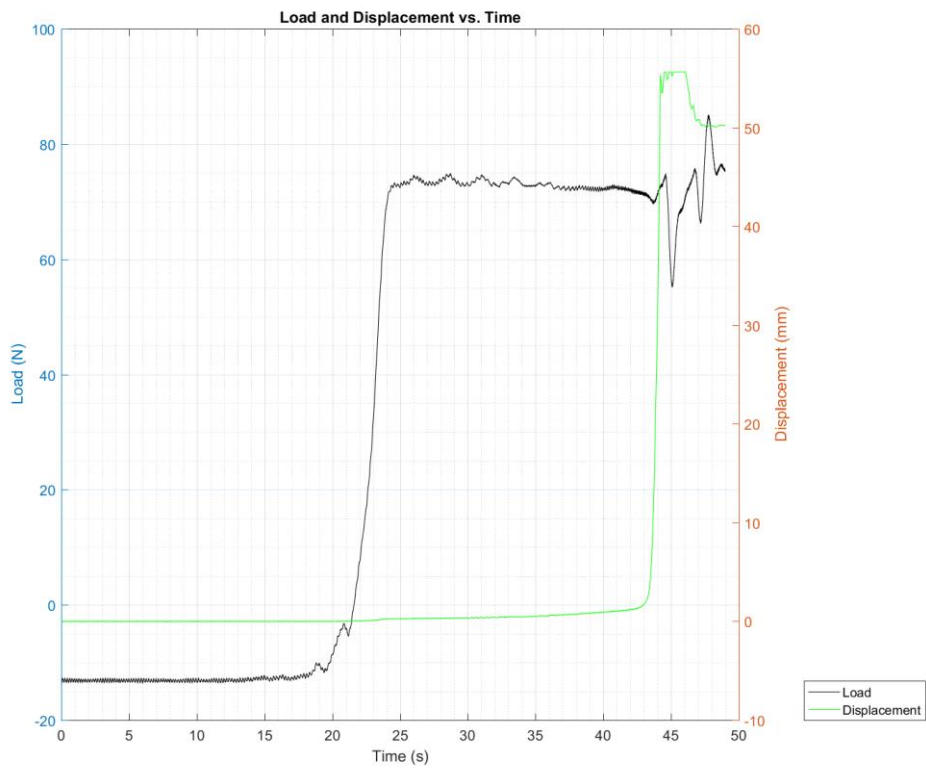
# 2D-G-130N -1



2D-G-130N -2

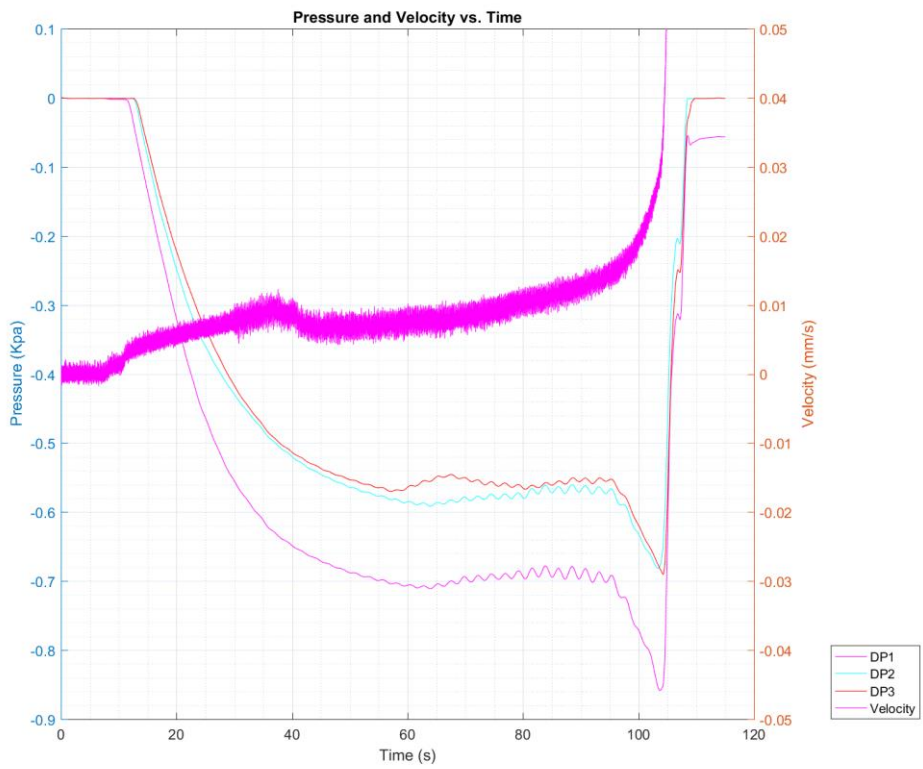
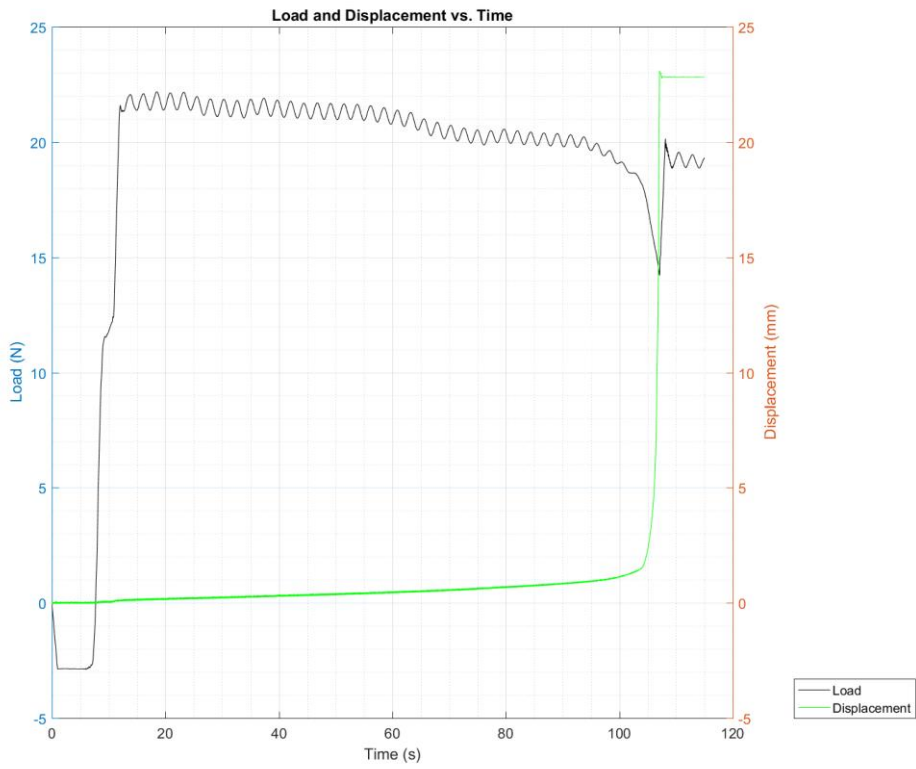


# 2D-G-130N -3

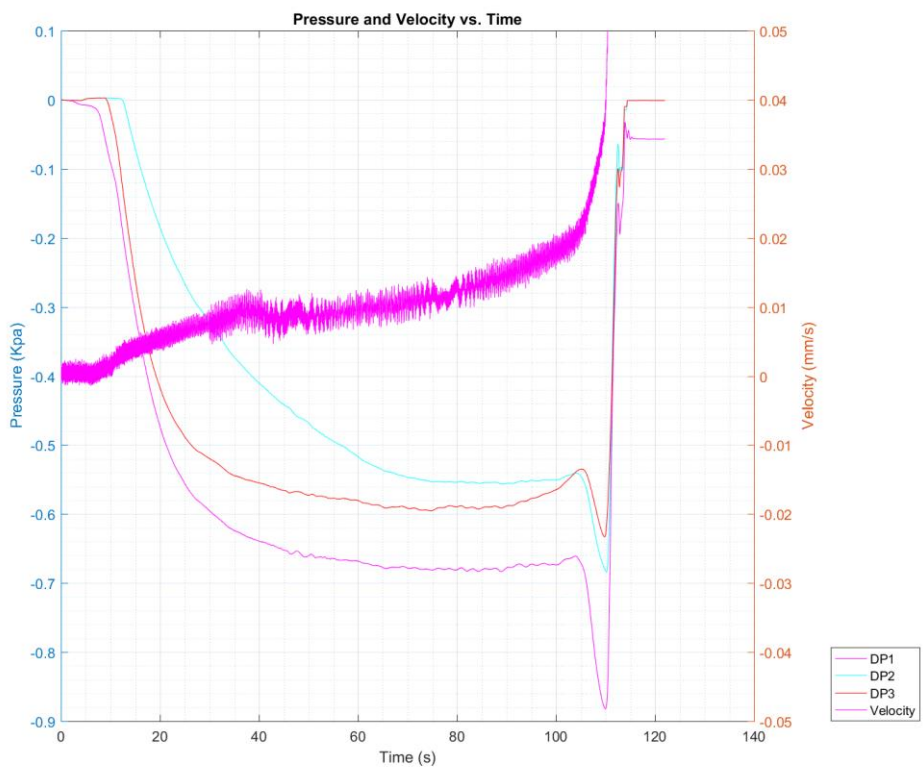
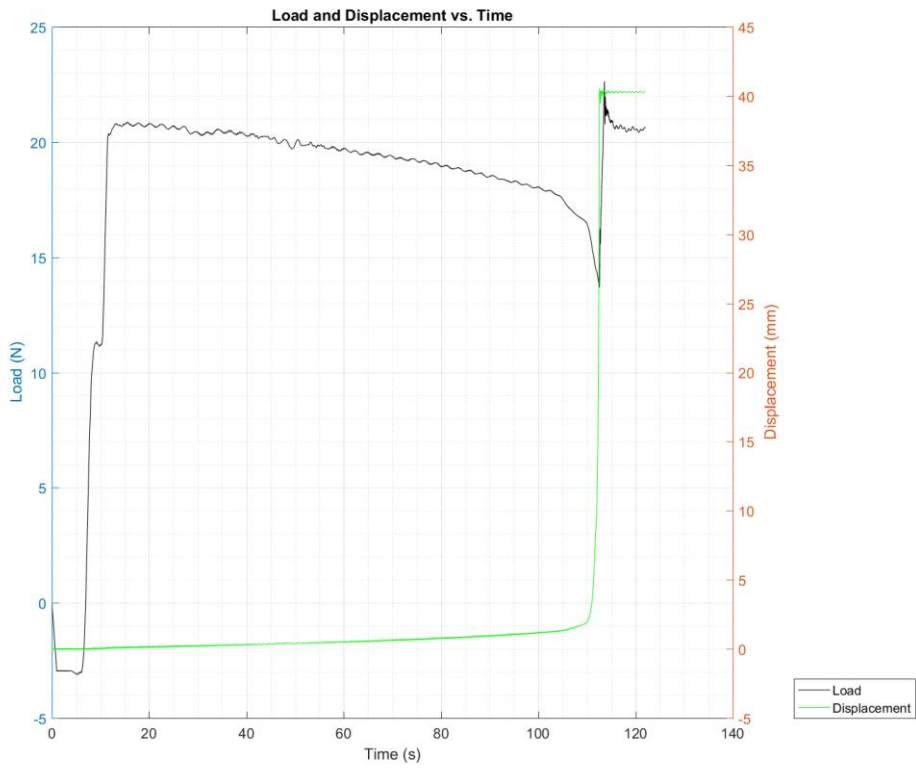


## **Appendix F      3-Dimensional Test Results**

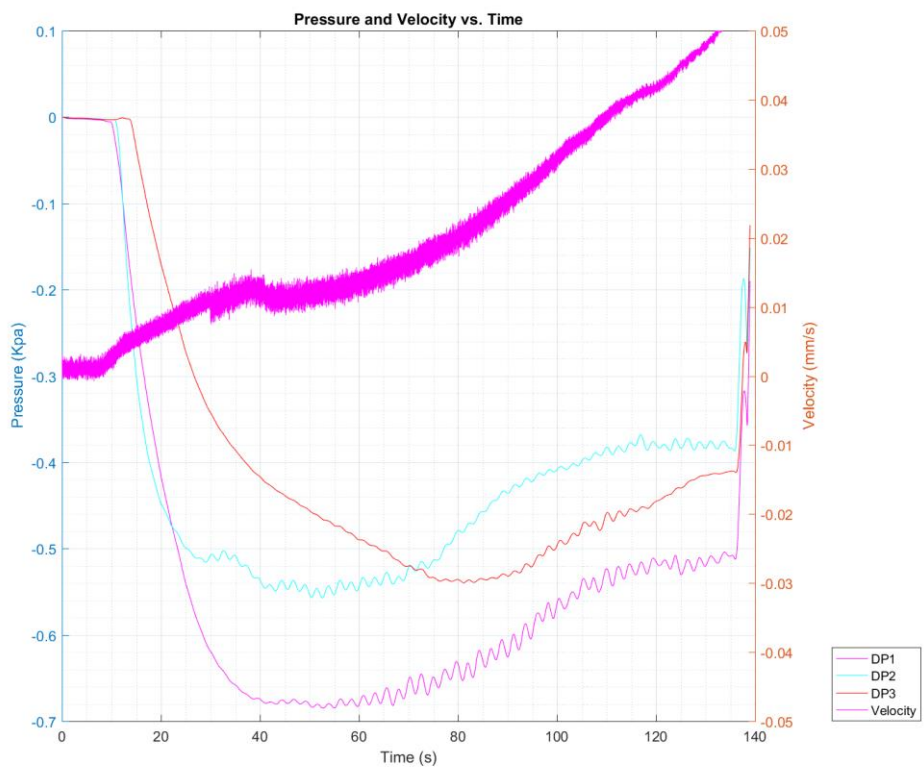
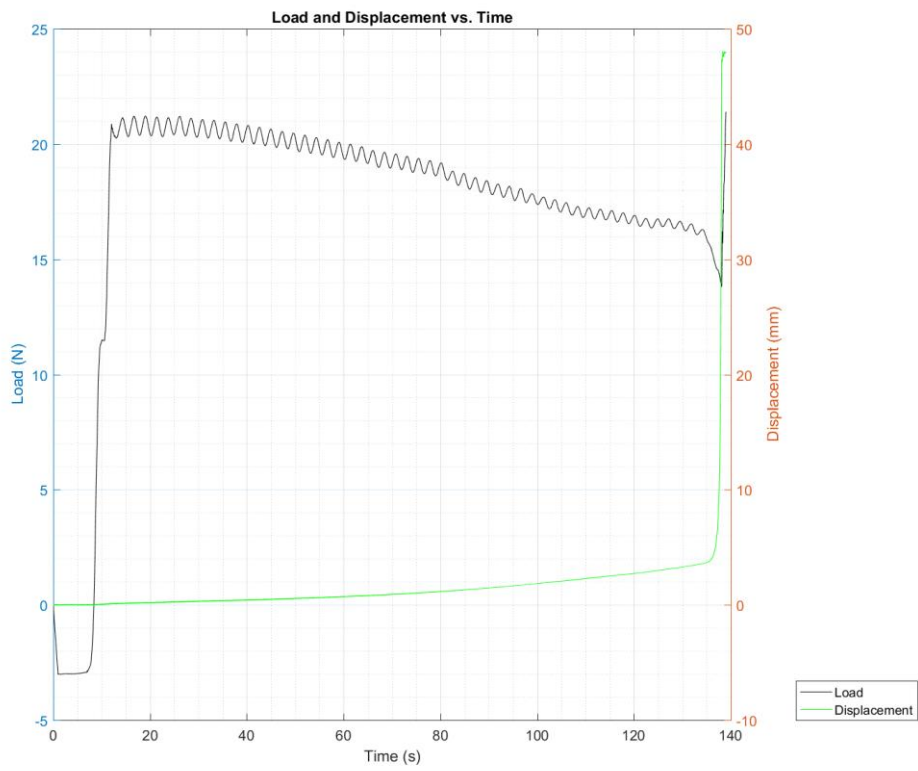
### 3D-S-65N -1



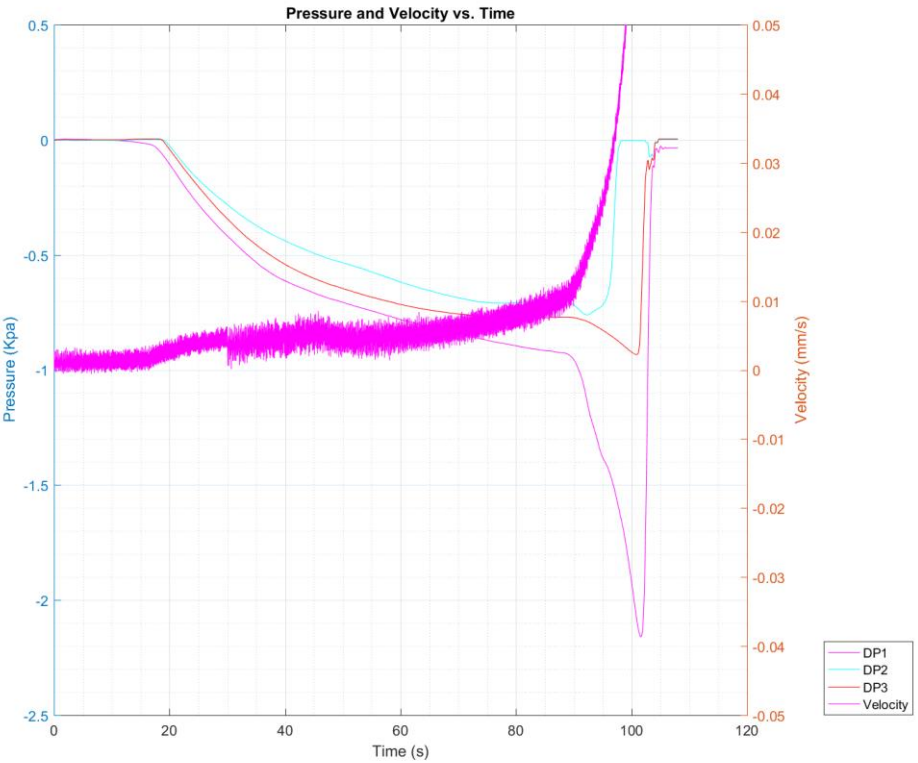
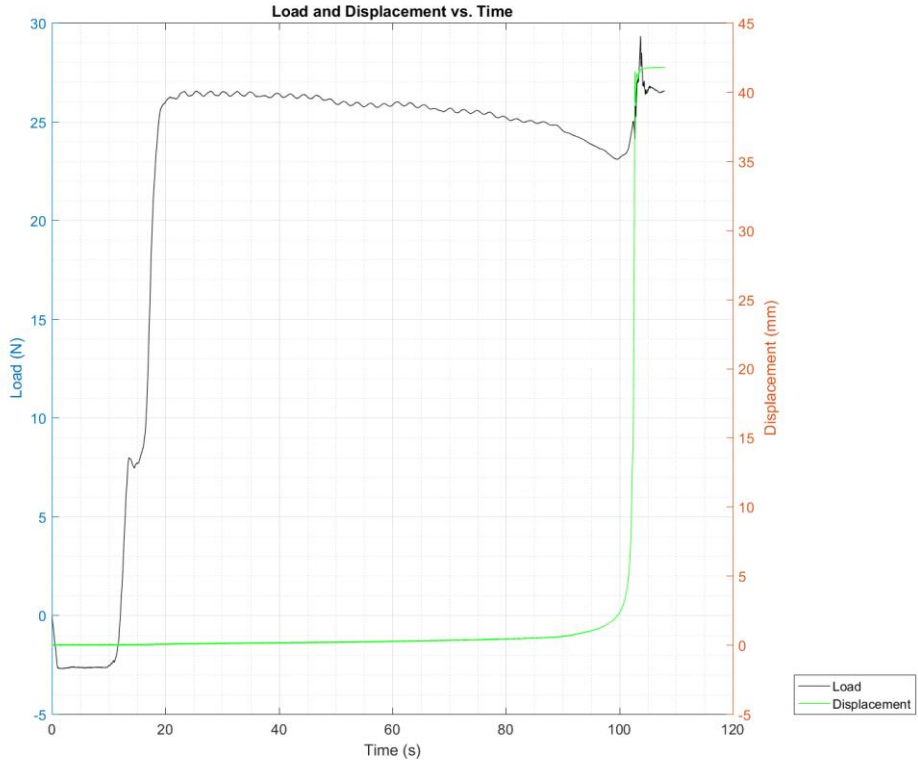
### 3D-S-65N -2



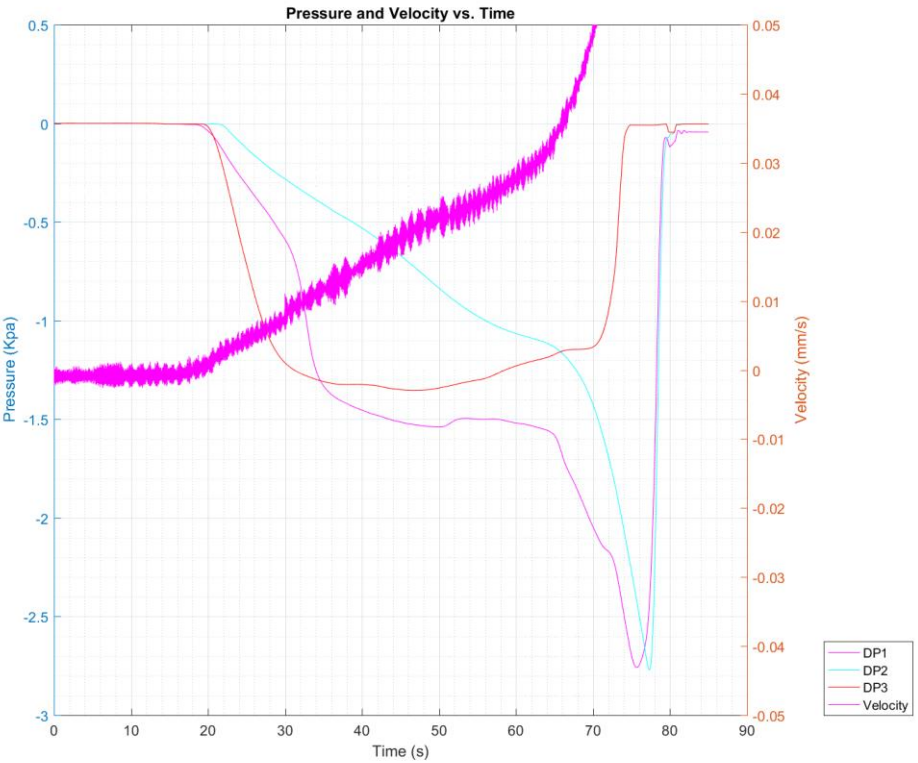
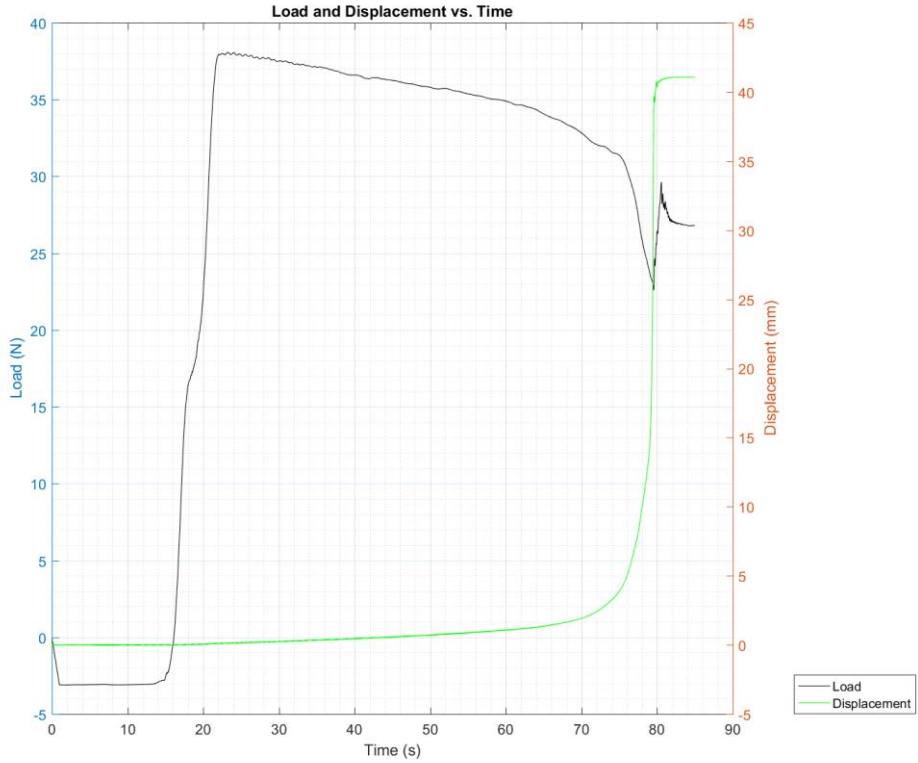
### 3D-S-65N -3



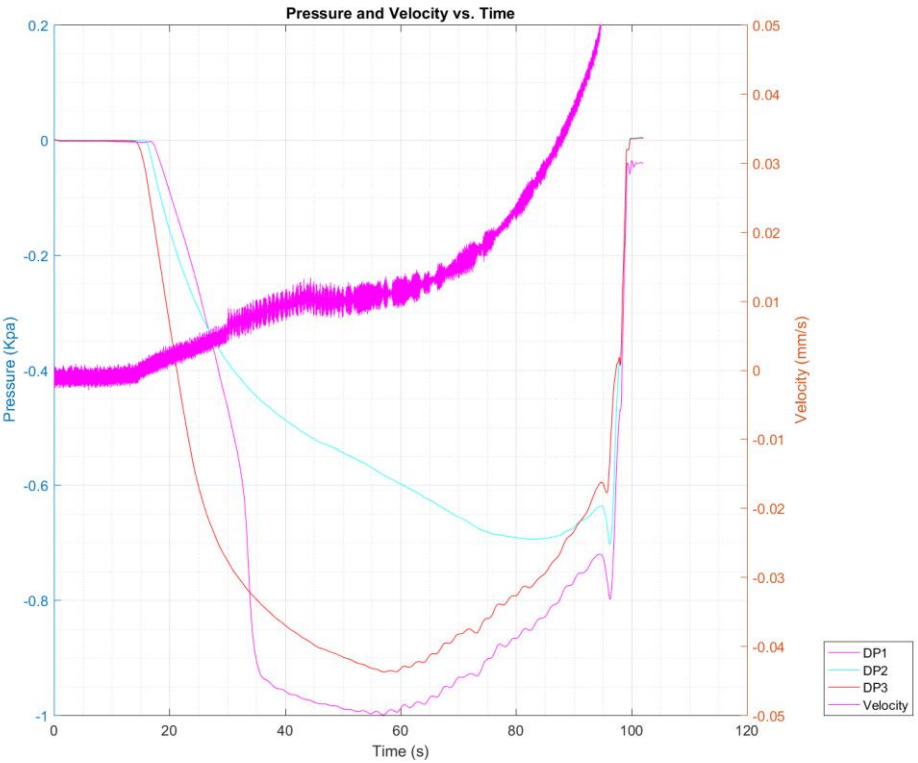
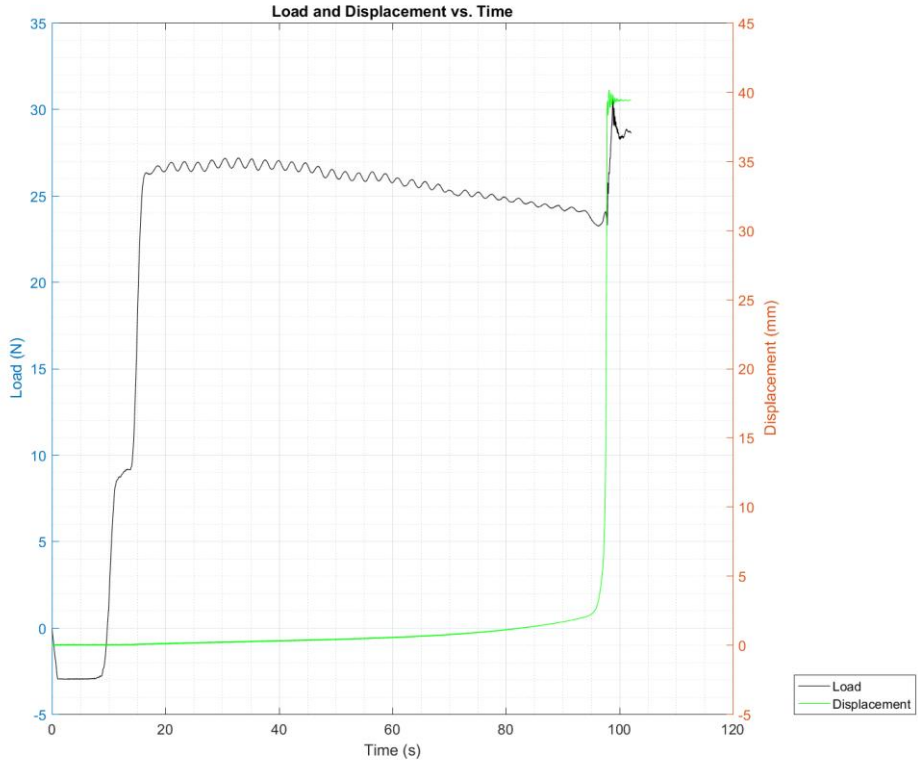
3D-S-70N -1



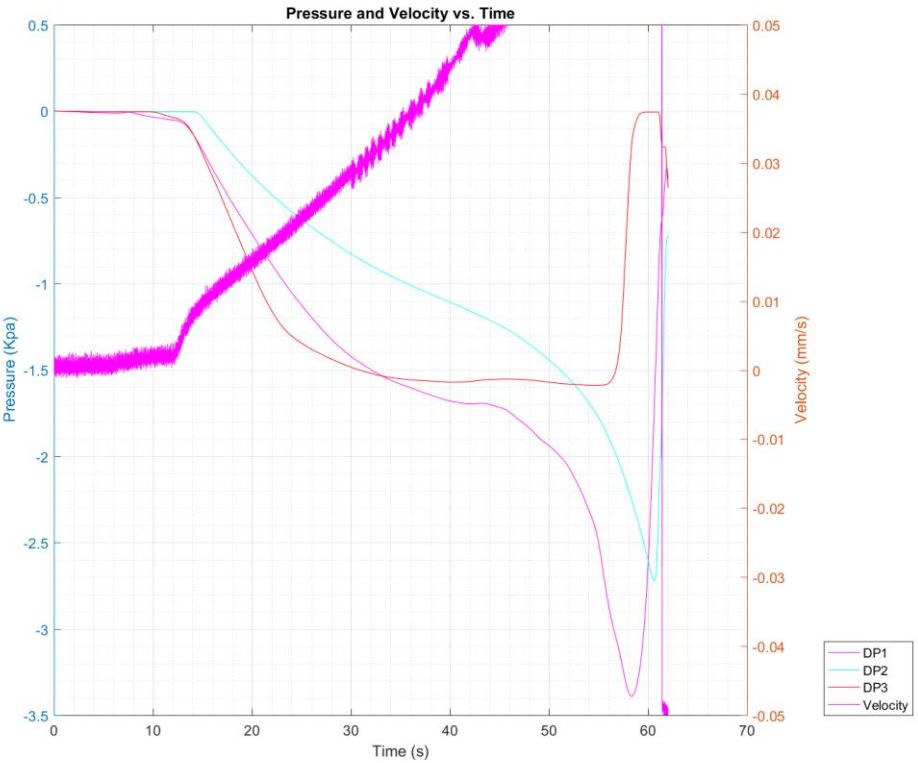
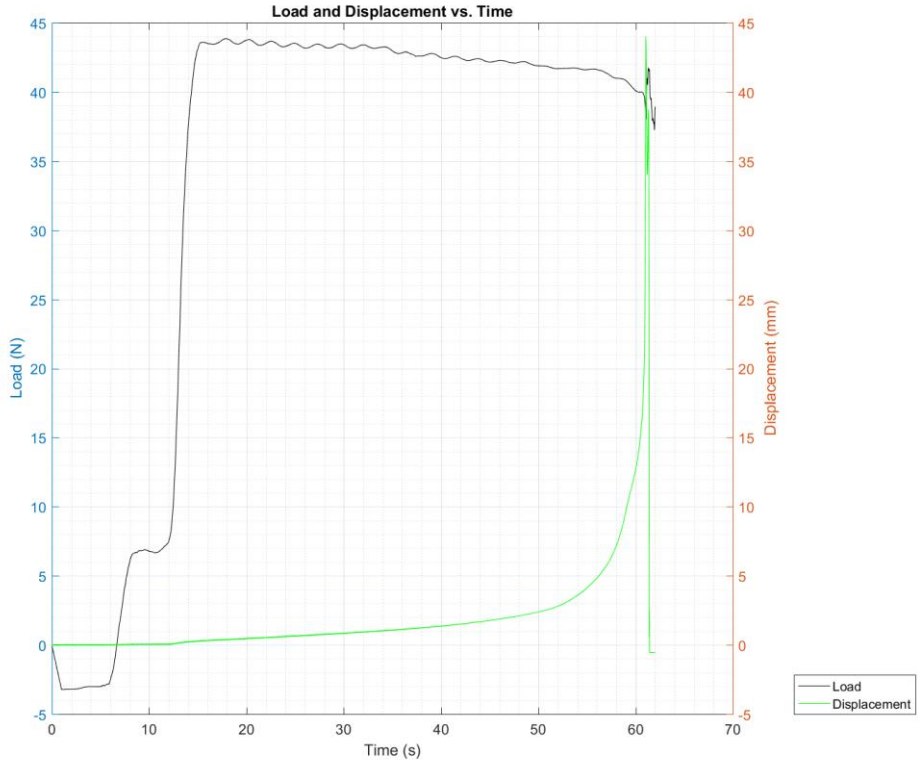
3D-S-70N -2



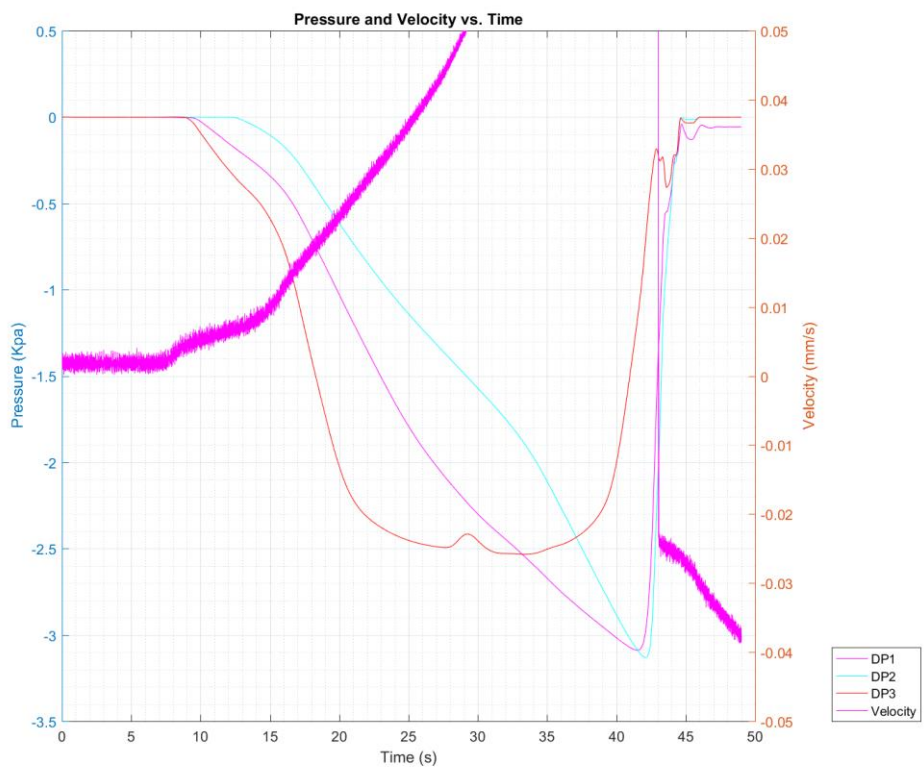
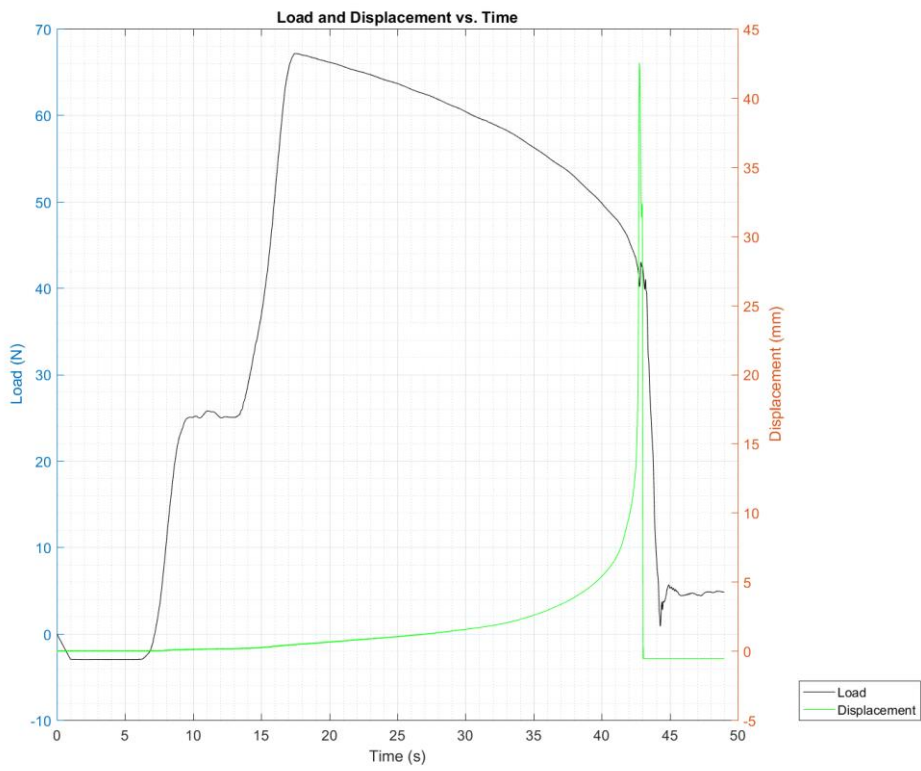
3D-S-70N -4



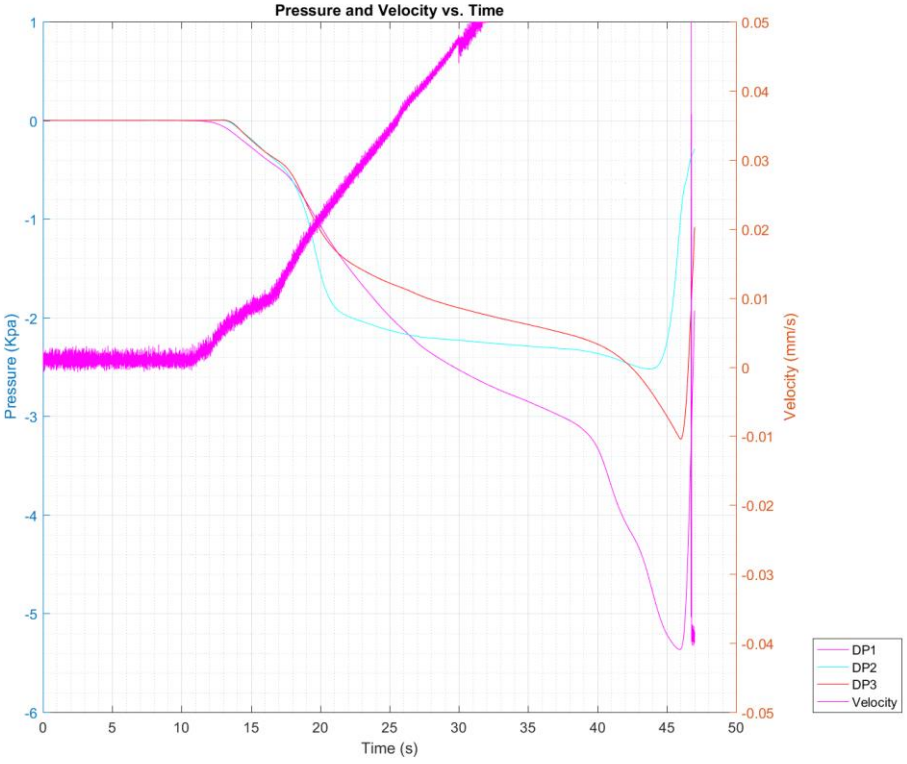
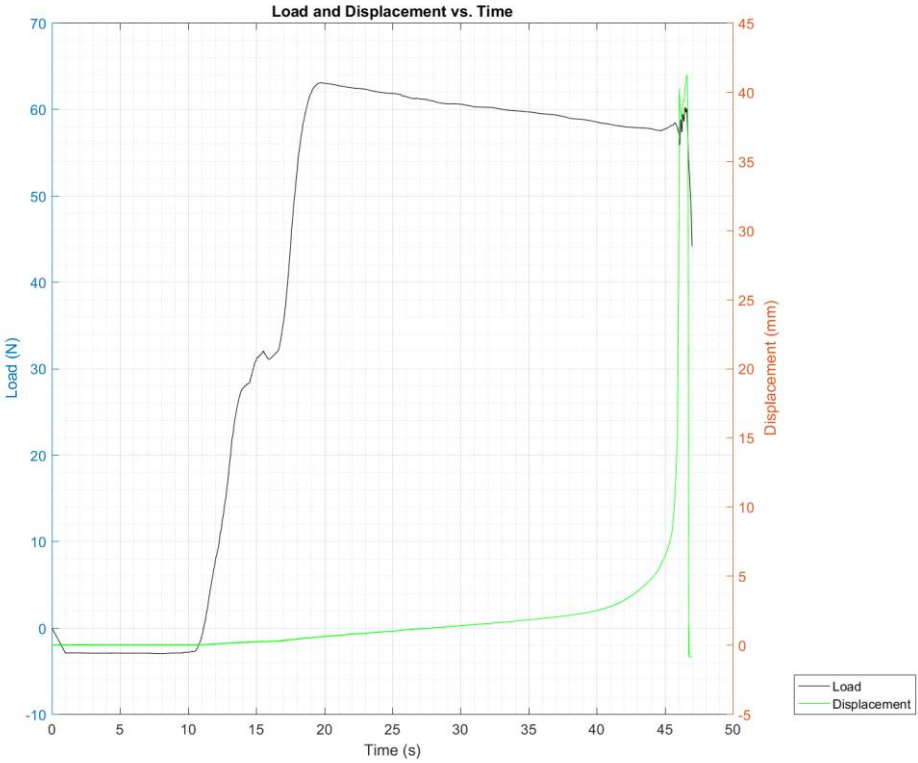
3D-S-90N -1



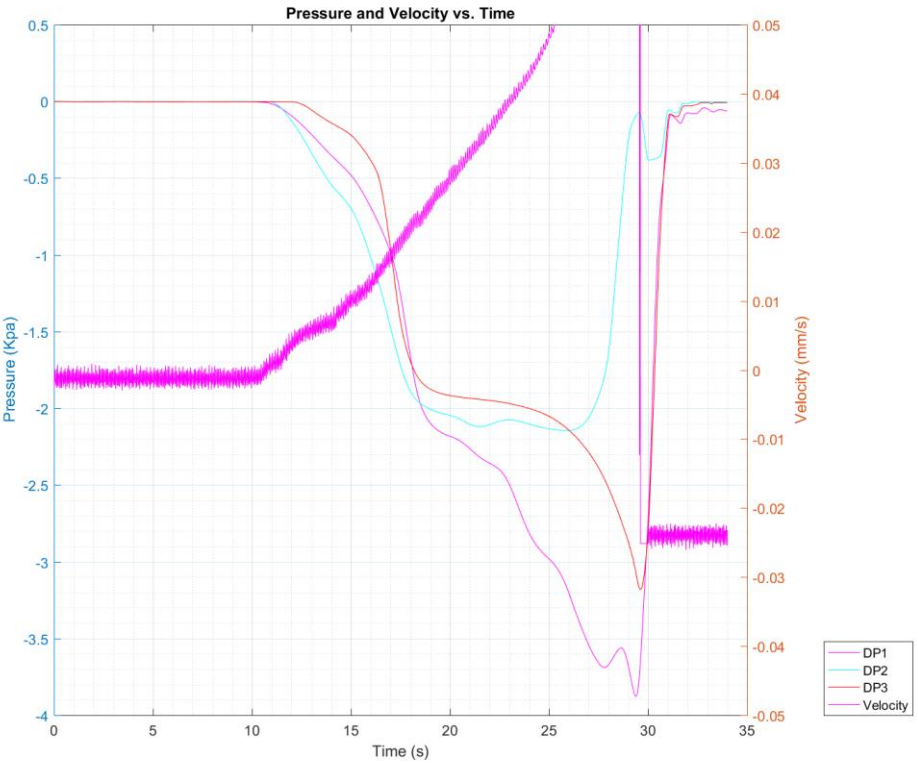
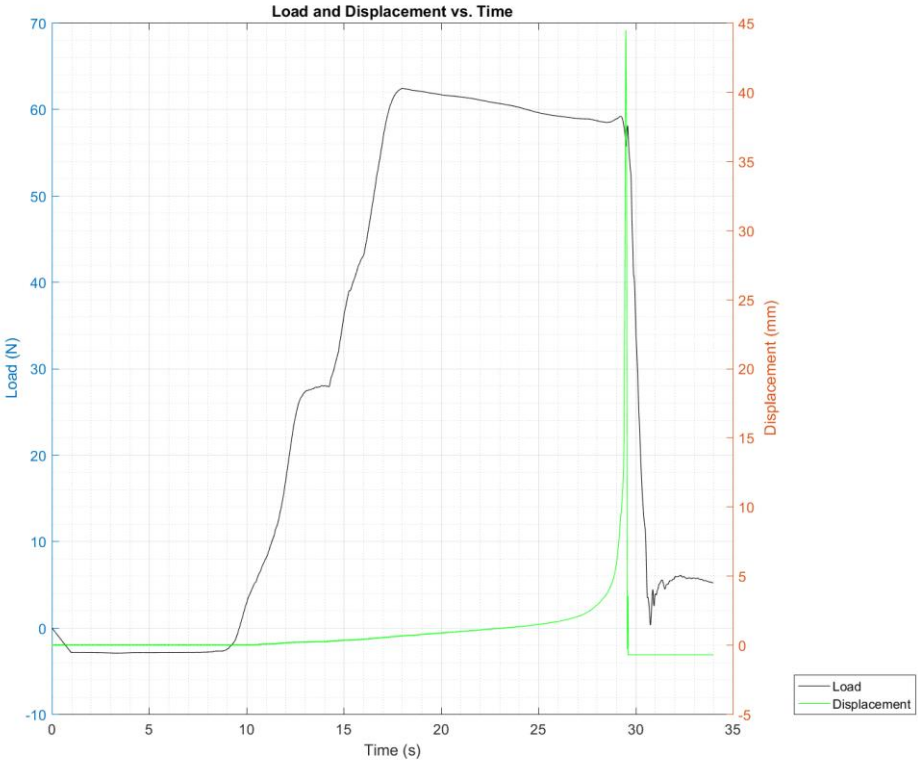
### 3D-S-90N -3



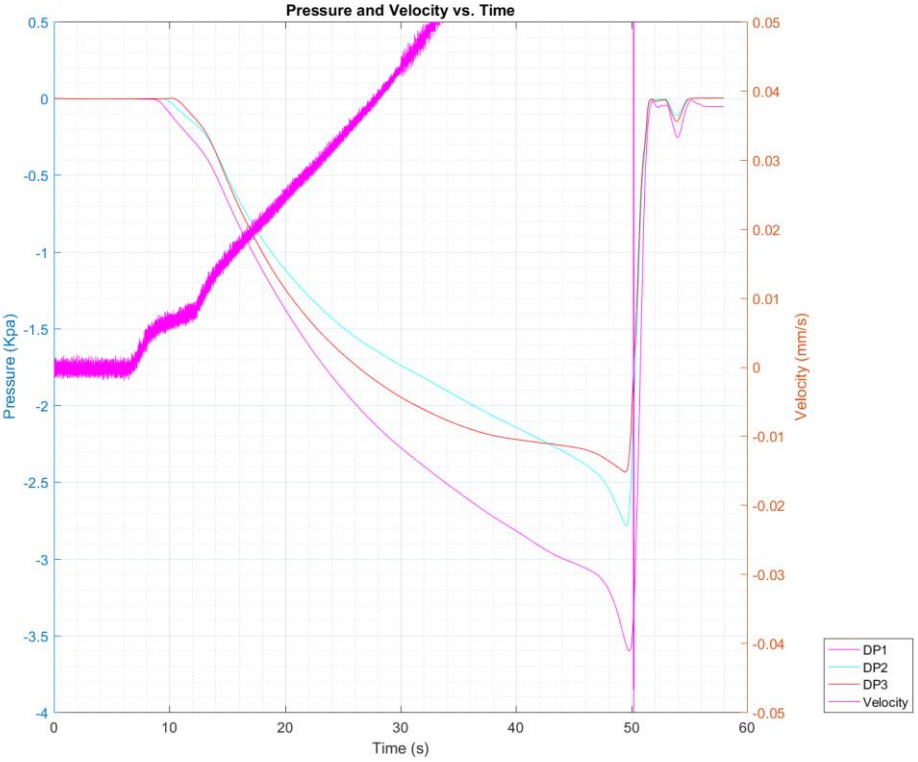
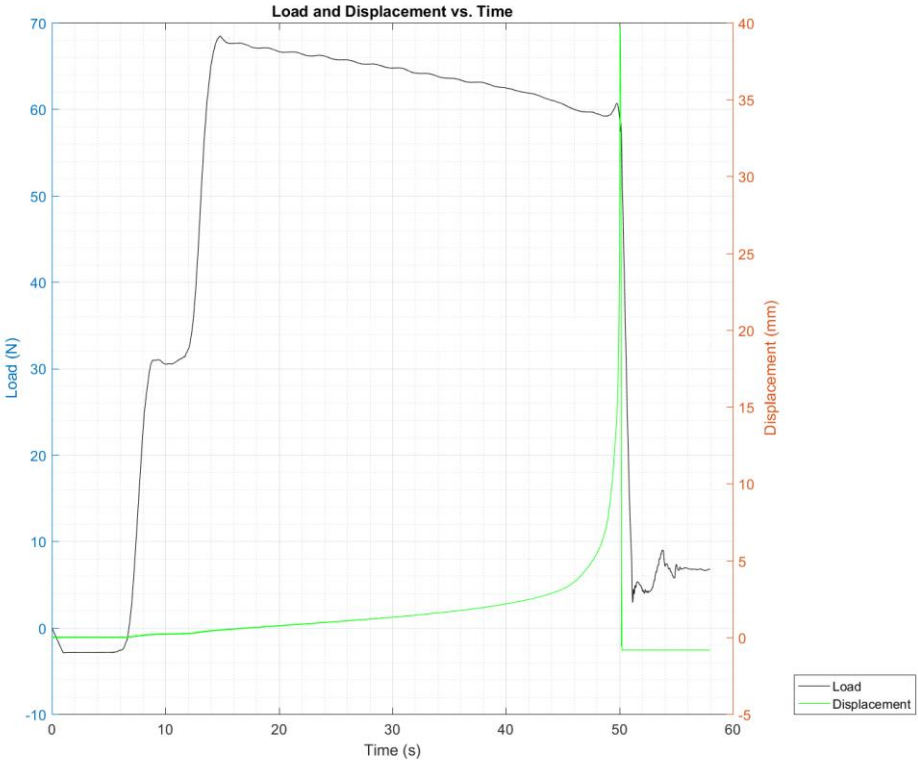
3D-S-110N -1



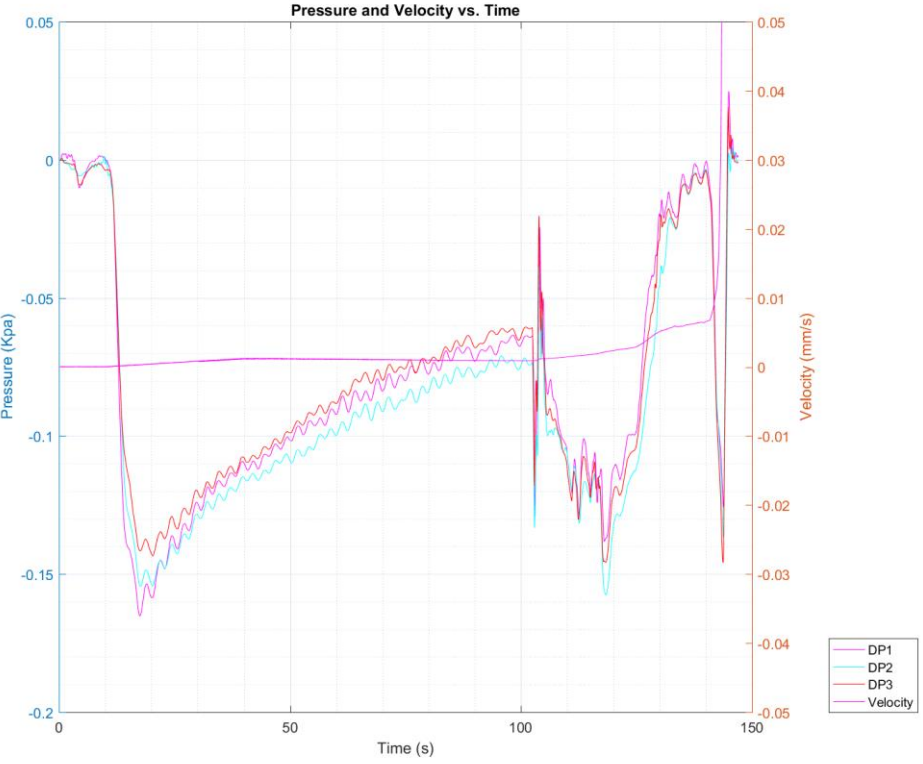
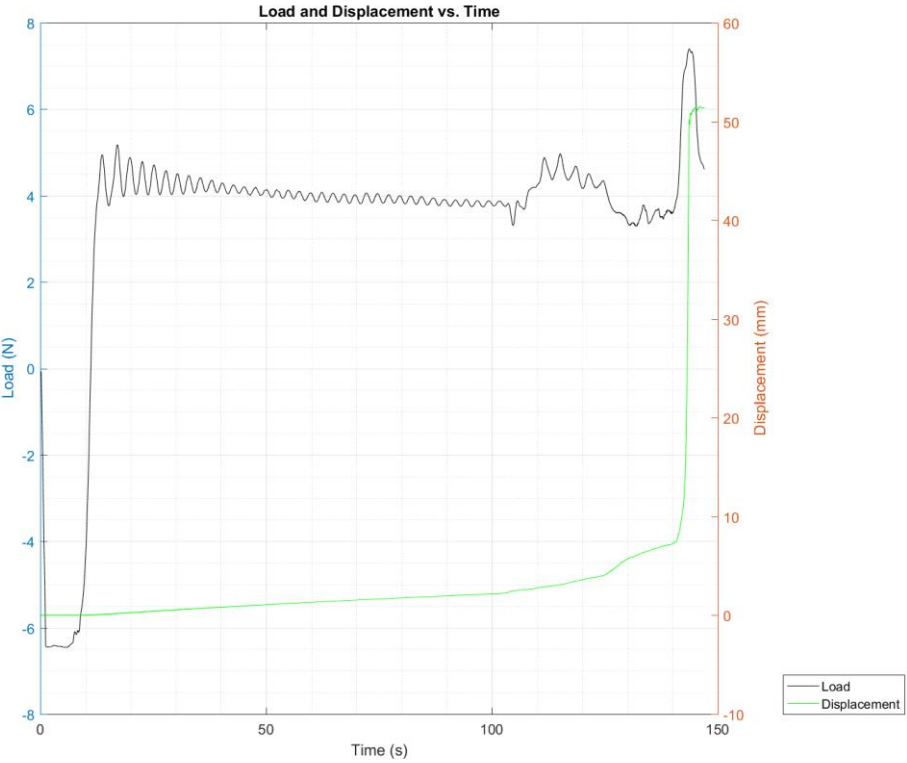
3D-S-110N -2



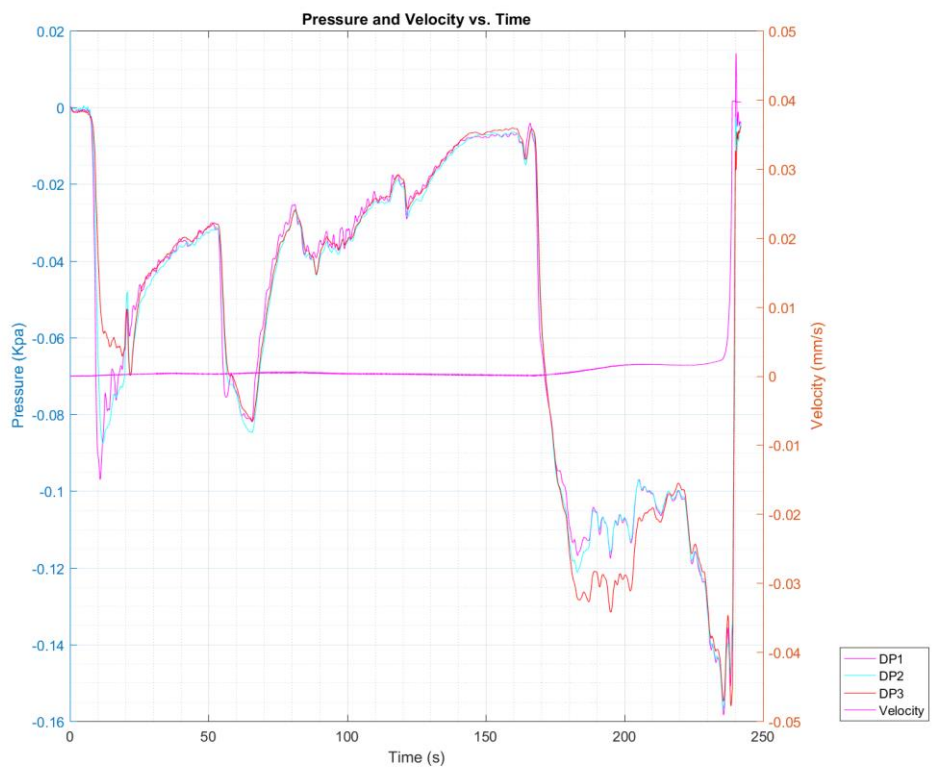
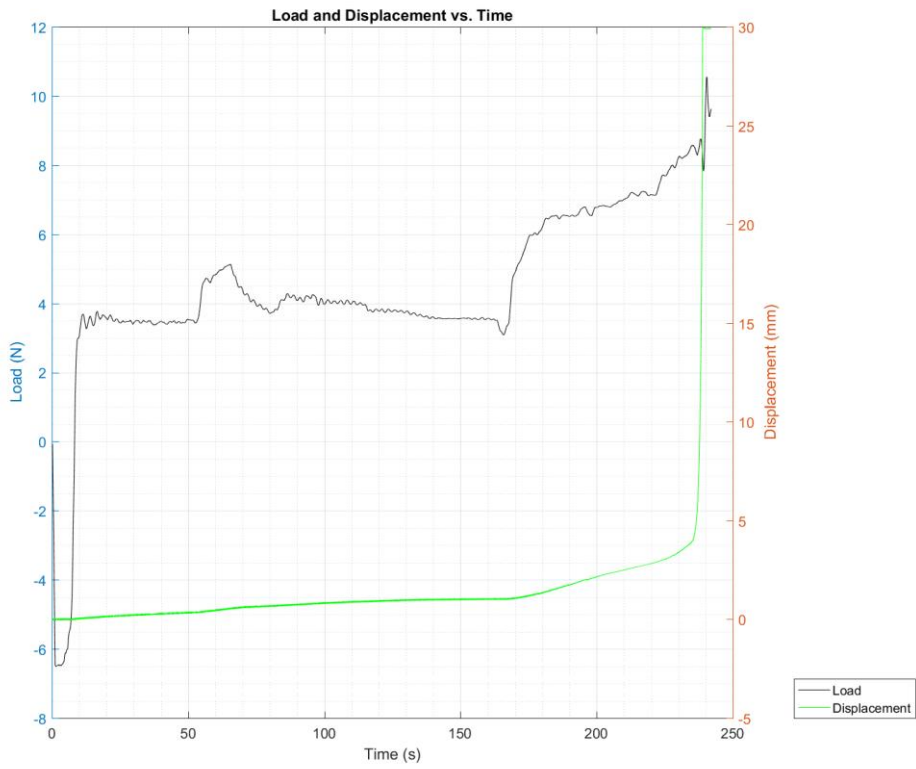
3D-S-110N -3



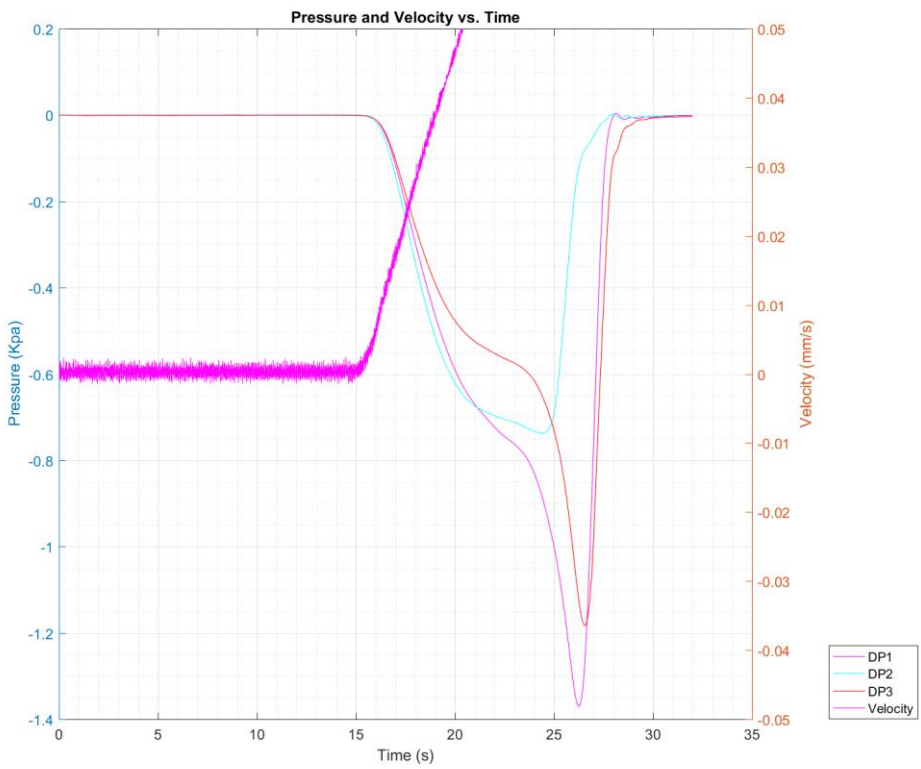
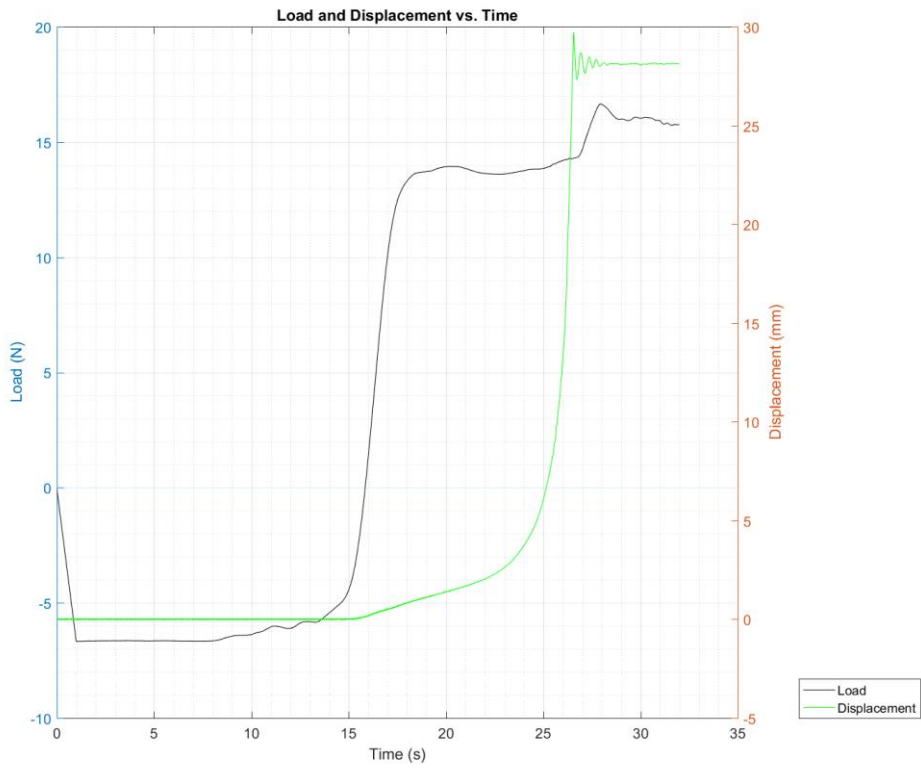
3D-G-50N -1



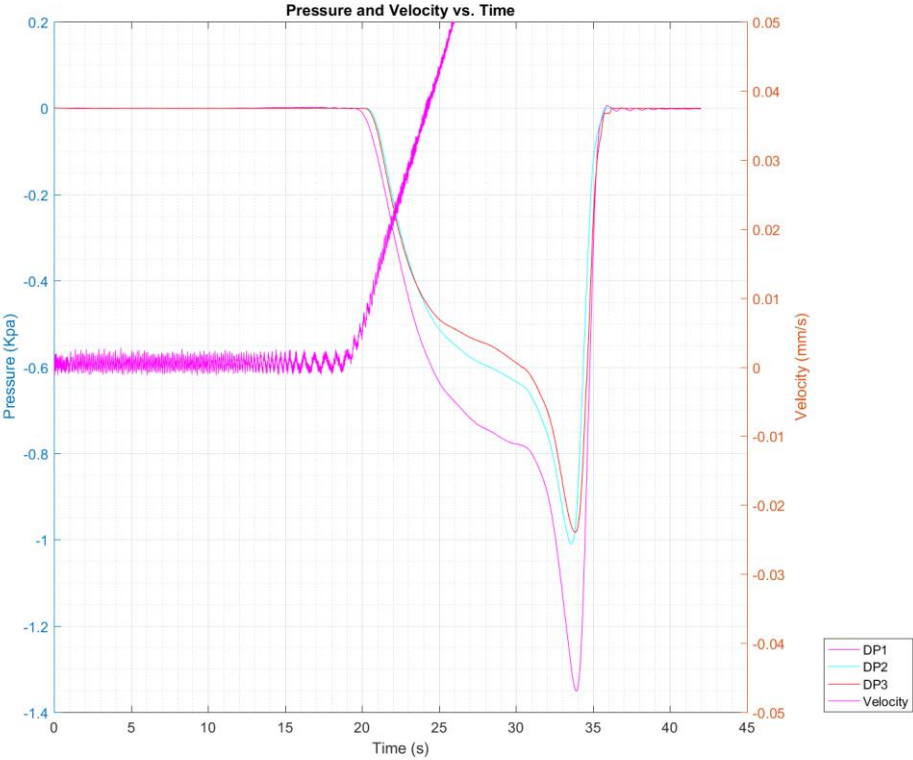
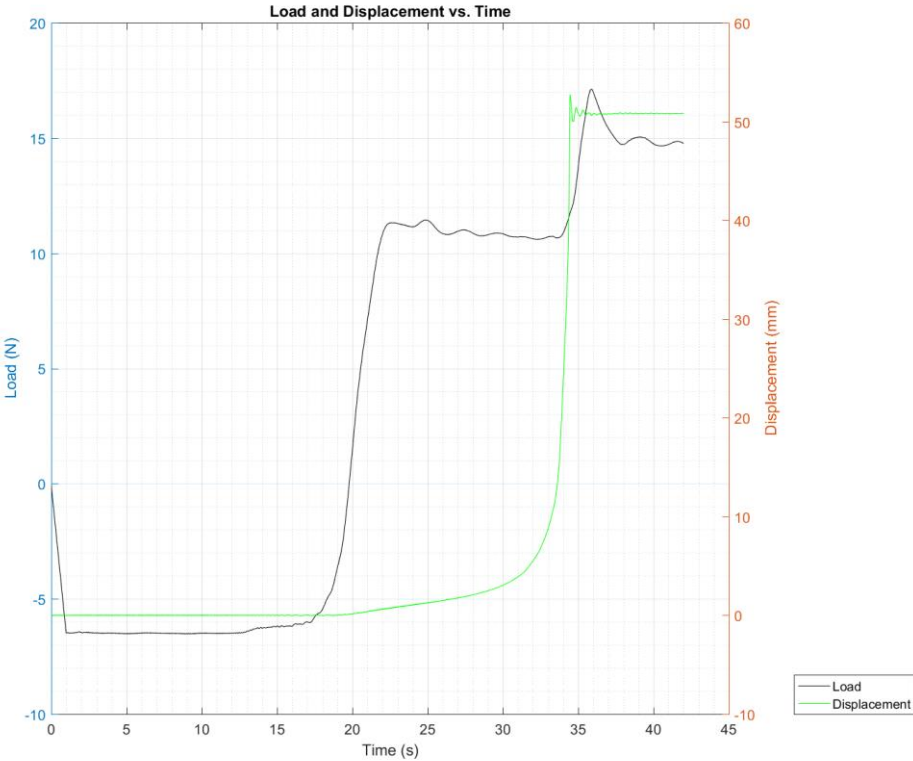
### 3D-G-50N -3



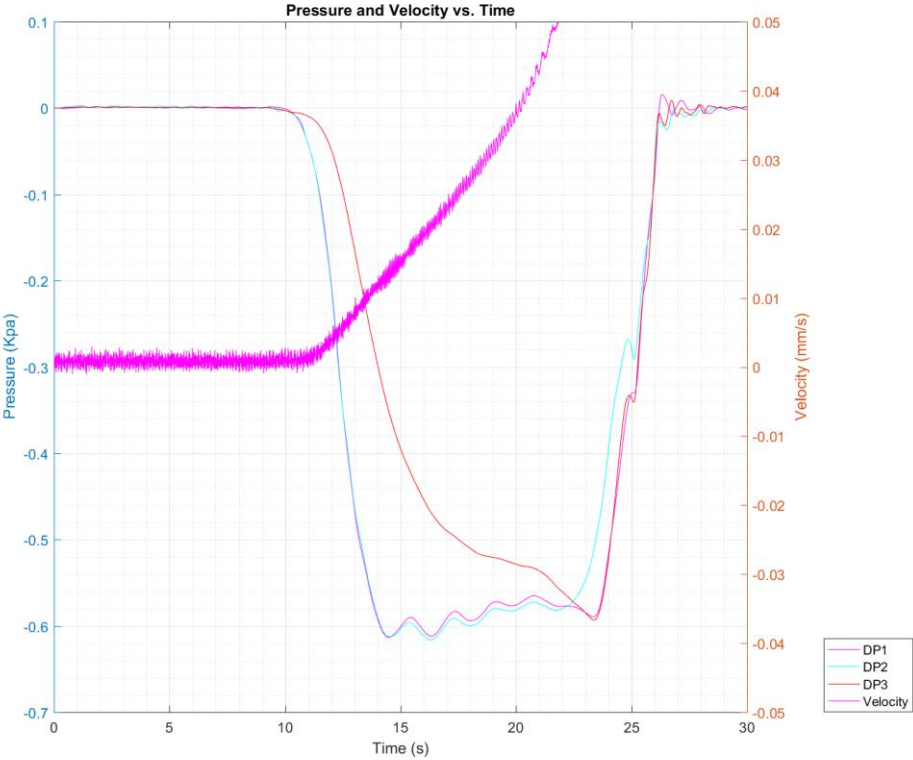
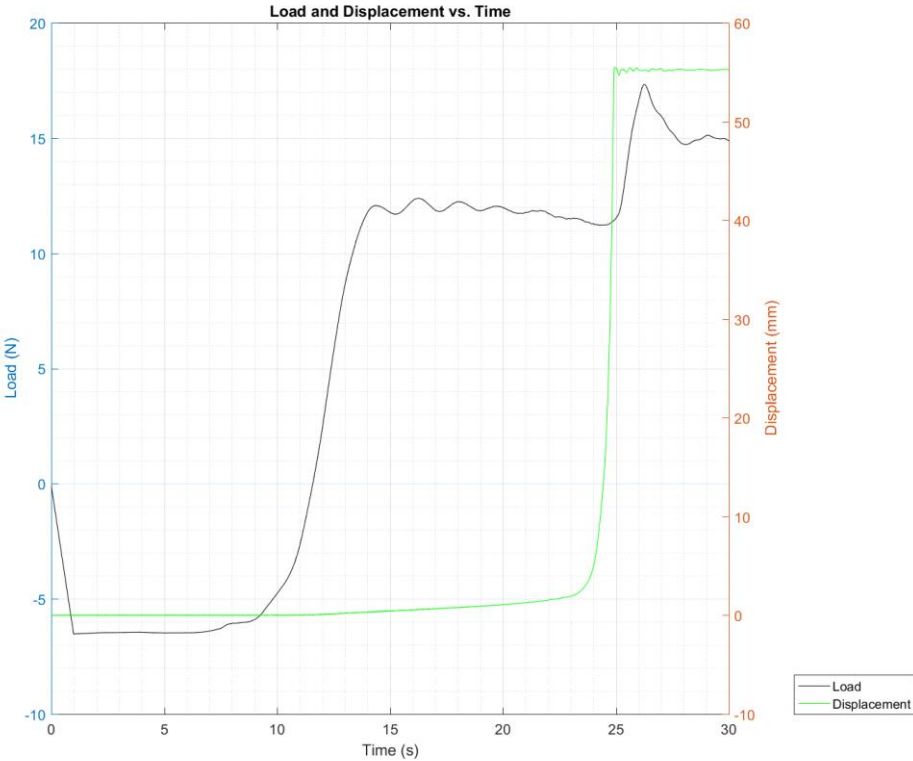
### 3D-G-60N -1



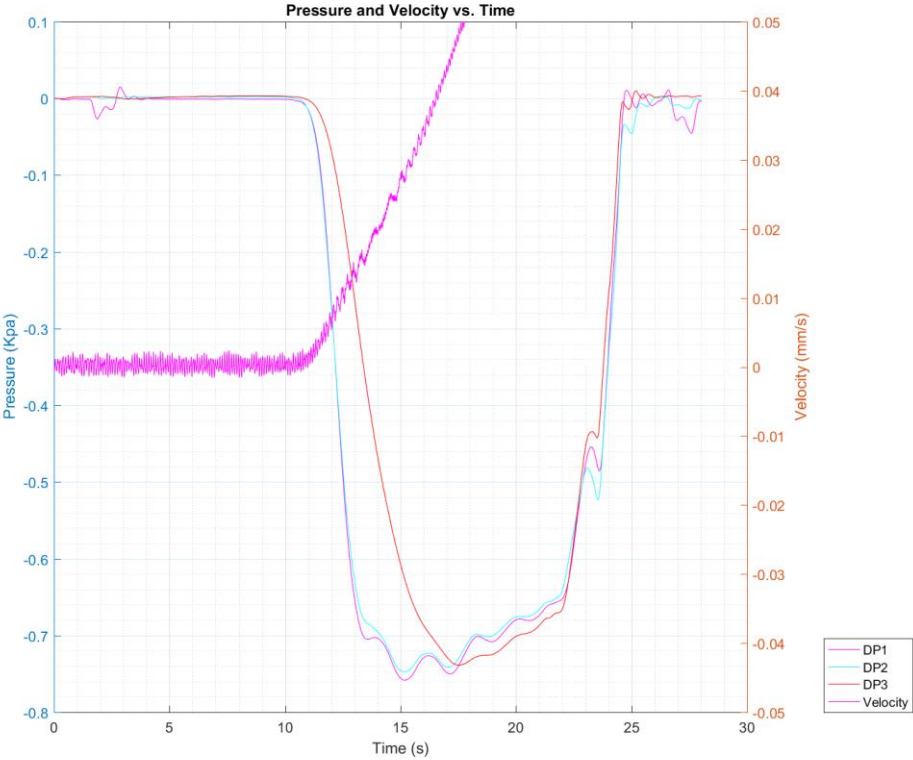
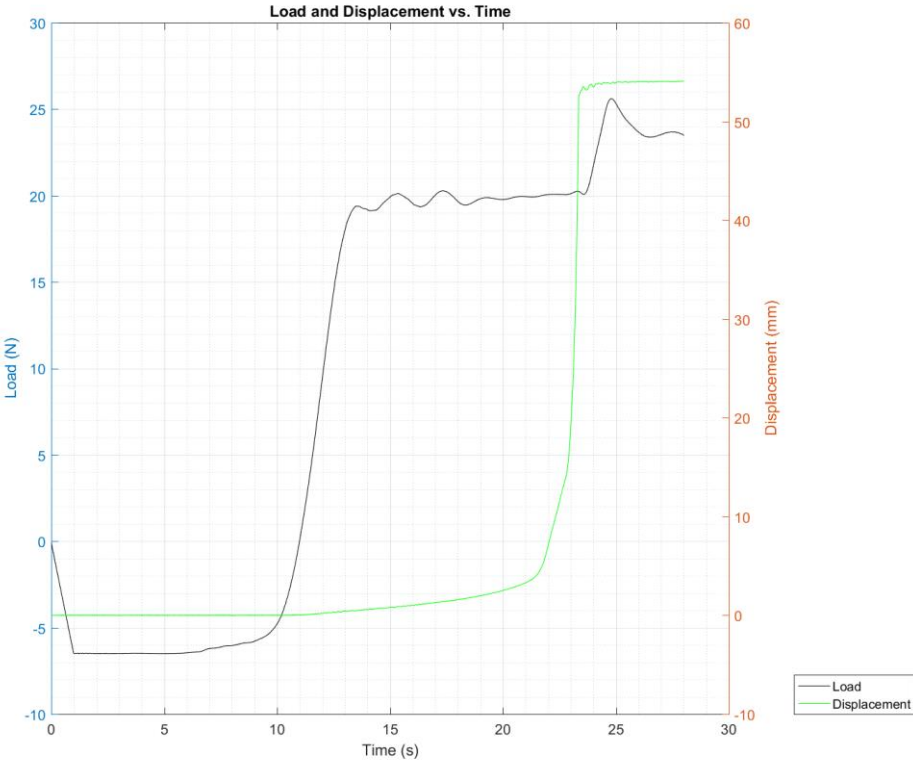
3D-G-60N -2



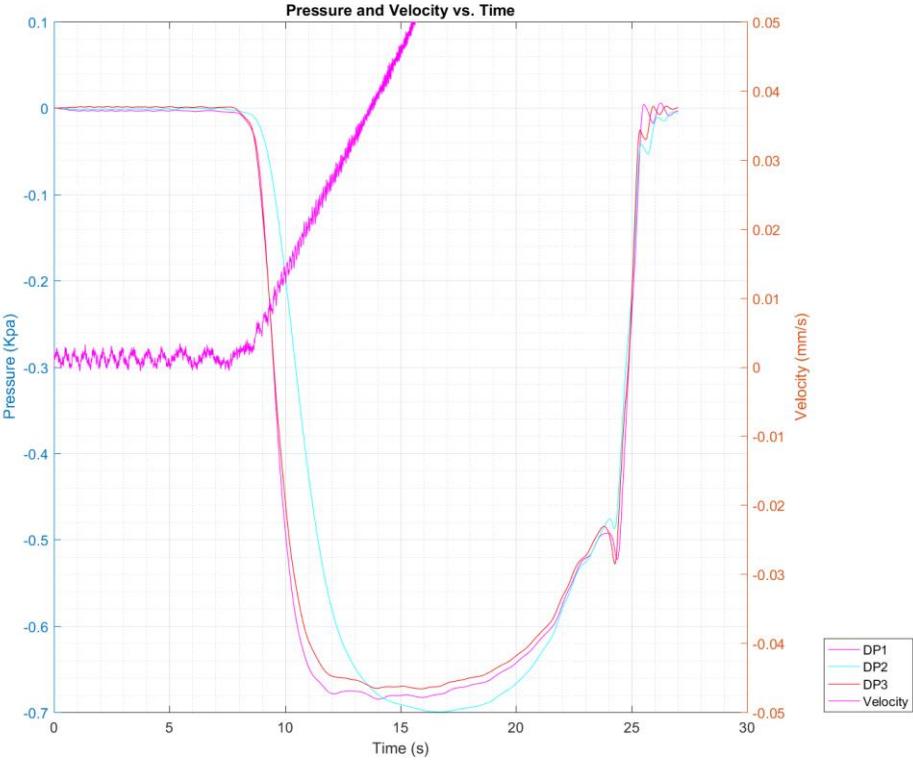
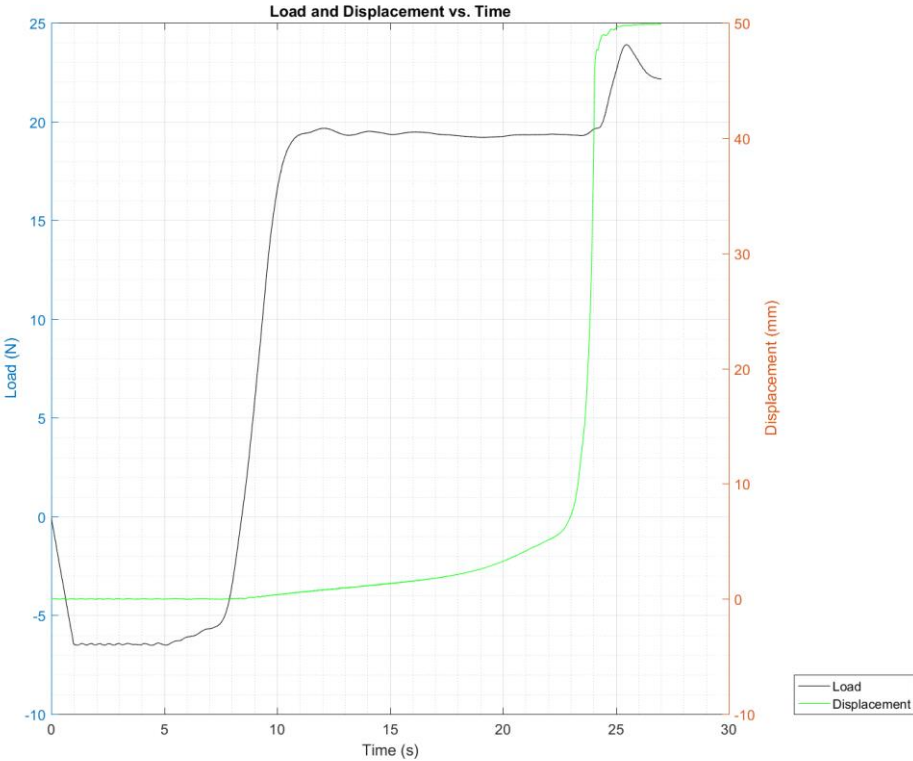
3D-G-60N -3



3D-G-70N -1



3D-G-70N -2



3D-G-70N -3

